

AD-A080 156

AIR FORCE INST OF TECH WRIGHT-PATTERSON AFB OH SCHOO--ETC F/G 12/1
SPECTRAL ANALYSIS OF SHORT RECORD TIME SERIES DATA.(U)

UNCLASSIFIED

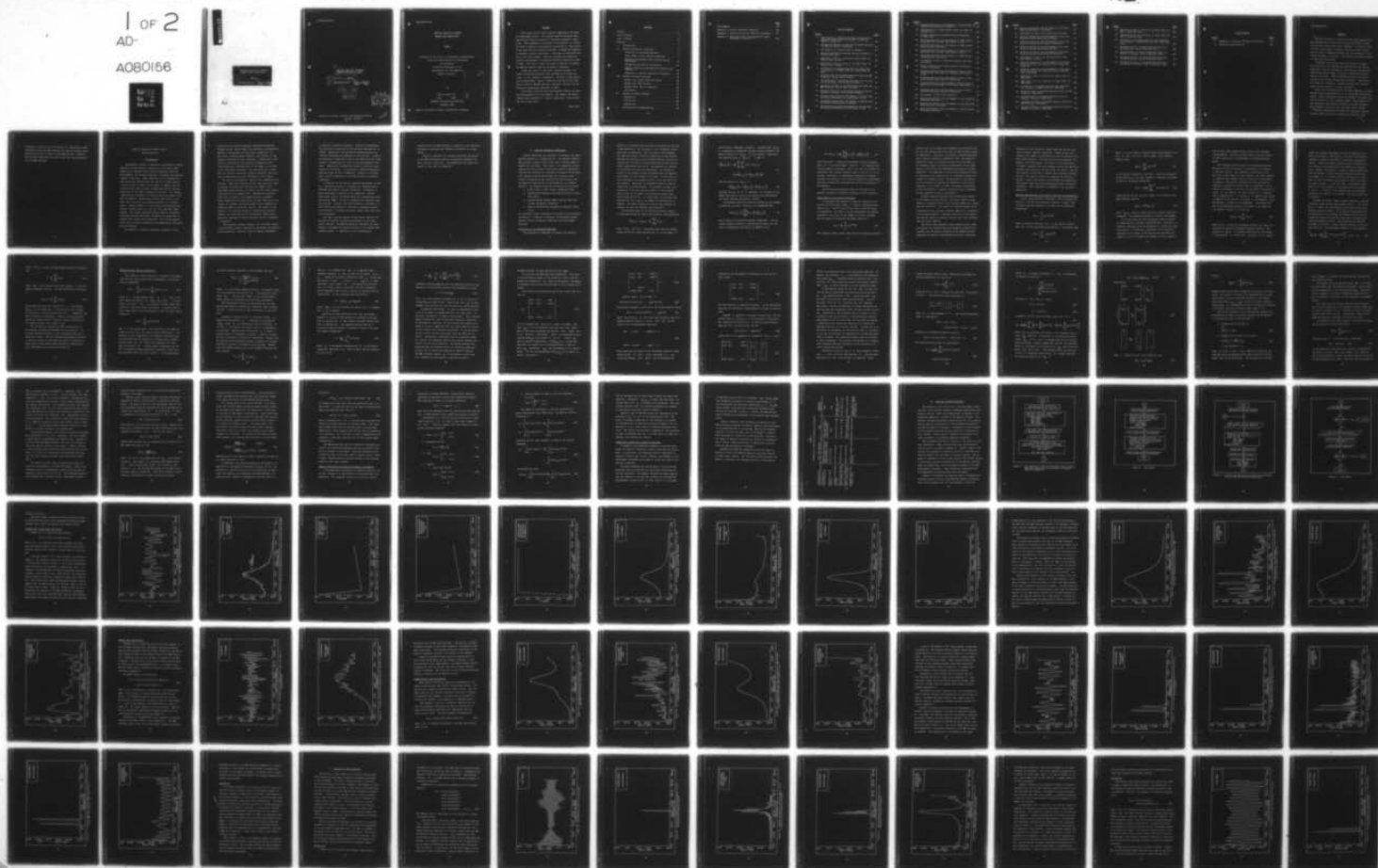
DEC 79 P B TERRY
AFIT/GE/EE/79-38

NL

1 OF 2

AD-

A080156



6
SPECTRAL ANALYSIS OF SHORT
RECORD TIME SERIES DATA ,

Master's THESIS,

AFIT/GE/EE/79-38

10

Paul B. Terry
Capt USAF

AFIT/GE/EE/79-38

6

SPECTRAL ANALYSIS OF SHORT
RECORD TIME SERIES DATA ,

9 Master's THESIS,

14 AFIT/GE/EE/79-38

10 Paul B. Terry
Capt USAF

11 Dec 79

12 148

DDC
RECEIVED
FEB 5 1980
A

Approved for public release; distribution unlimited

012 225

YB

**SPECTRAL ANALYSIS OF SHORT
RECORD TIME SERIES DATA**

THESIS

**Presented to the Faculty of the School of Engineering
of the Air Force Institute of Technology**

Air University

**in Partial Fulfillment of the
Requirements for the Degree of
Master of Science**

by

Paul B. Terry, B.S.

Capt USAF

Graduate Electrical Engineering

December 1979

| | |
|--------------------|--|
| Accession For | |
| NTIS GRLAI | <input checked="checked" type="checkbox"/> |
| DOC TAB | <input type="checkbox"/> |
| Unannounced | <input type="checkbox"/> |
| Justification | |
| By _____ | |
| Distribution/ | |
| Availability Codes | |
| Dist | Avail and/or special |
| A | |

Approved for public release; distribution unlimited

Preface

This thesis evolved from a problem suggested by the Rome Air Development Center. The original problem considered Maximum Entropy spectral analysis of Non-White Atmospheric Radio Noise. RADC suggested an extension of the analysis to include the work by Papoulis in bandlimited extrapolation. When actual noise tapes were not received from RADC, I changed the emphasis to analysis of short record data. Data that is extracted from only a few input samples. Specific problems were extracted from the proceedings of a Spectral Estimation Workshop at RADC in 1978. This report covers the areas of research to analyze the MEM and Papoulis spectral estimation techniques.

During the course of this work, valuable guidance, insight, and probing questions were provided by my thesis advisor, Lt. Col. Ronald J. Carpinella. His help is most gratefully acknowledged. Special thanks are also due to the readers Dr. Pater S. Maybeck and Capt. Stanley R. Robinson of the Electrical Engineering Department of AFIT.

This thesis could not have been possible without the help and encouragement of my wife Shauna. Her support and unselfishness have enabled me to achieve a major goal I have worked for for so many years.

Paul Terry

Contents

| | |
|--|----|
| Preface | 11 |
| List of Figures | v |
| List of Tables. | ix |
| Abstract. | x |
| I. Introduction. | 1 |
| II. Spectral Estimation Techniques. | 5 |
| Statistics of Estimated Spectrum. | 5 |
| Filter Banks or Fast Fourier Transforms | 8 |
| Smoothed Periodograms Using Discrete Fourier Transforms. | 10 |
| Maximum Entropy Spectral Estimation | 15 |
| Papoulis Bandlimited Extrapolation Spectral Es- timation. | 31 |
| Comparison of Spectral Estimation Techniques. . | 34 |
| III. Analysis of Known Processes | 37 |
| Example One: Second Order AR Process. | 42 |
| Example Two: ARMA Process | 57 |
| Example Three: Sum of Sinusoids | 60 |
| Conclusions | 72 |
| IV. Analysis of Radar Problems. | 73 |
| Problem One | 73 |
| Problem Two | 81 |
| Conclusions | 87 |
| V. Conclusions and Recommendations | 92 |

| | <u>Page</u> |
|---|-------------|
| Bibliography | 94 |
| Appendix A: Prolate Spheroidal Expansion | 98 |
| Appendix B: Subroutines Used for Spectral Estimation . | 101 |
| Appendix C: Additional Plots from Analysis of Known Processes in Section II. | 118 |

List of Figures

| <u>Figure</u> | | <u>Page</u> |
|---------------|---|-------------|
| 1. | Flow Diagram to Determine AR Model Order, Bartlett Spectrum, Sample Mean, and Variance of MEM and Papoulis Estimation | 38 |
| 2. | Interactive Routine to Calculate Estimated Spectrum for MEM and Papoulis Techniques | 40 |
| 3. | 128 Samples of a Second Order AR Sequence | 43 |
| 4. | Bartlett Smoothed Periodogram Spectral Estimate of Second Order Model. | 44 |
| 5. | Amplitude of FPE as a Function of Model Order for Second Order AR Model | 45 |
| 6. | Amplitude of AIC as a Function of Model Order for Second Order AR Model | 46 |
| 7. | Probability of Kolmogorov-Smirnov Two Sided Test as a Function of Model Order for Second Order AR Model | 47 |
| 8. | Estimated Mean of Estimated Spectrum Using the MEM Technique, Second Order AR Model. | 48 |
| 9. | Estimated Mean of Estimated Spectrum Using the Papoulis Technique, Second Order AR Model. | 49 |
| 10. | Estimated Variance of Estimated Spectrum Using the MEM technique, Second Order AR Model. | 50 |
| 11. | Estimated Variance of Estimated Spectrum Using the Papoulis Technique, Second Order AR Model | 51 |
| 12. | Estimated Spectrum from 128 Samples of Second Order AR Process Using MEM with Order Equal to Two. | 53 |
| 13. | Estimated Spectrum from 128 Samples of Second Order AR Process Using Papoulis Technique | 54 |
| 14. | Estimated Spectrum from 32 Samples of Second Order AR Process Using MEM with Order Equal to Two. | 55 |

| <u>Figure</u> | | <u>Page</u> |
|---------------|--|-------------|
| 15. | Estimated Spectrum from 32 Samples of Second Order AR Process Using Papoulis Technique | 56 |
| 16. | 128 Samples of an ARMA Sequence where the Input is Gaussian Noise | 58 |
| 17. | Bartlett Smoothed Periodogram Spectral Estimated of ARMA Input. | 59 |
| 18. | Estimated Spectrum from 128 Samples of ARMA Process Using MEM with AR Model Order Equal to Five. | 61 |
| 19. | Estimated Spectrum from 128 samples of ARMA Process Using Papoulis Technique | 62 |
| 20. | Estimated Spectrum from 32 Samples of ARMA Process Using MEM with AR Model Order Equal to Five. | 63 |
| 21. | Estimated Spectrum from 32 Samples of ARMA Process Using Papoulis Techniques. | 64 |
| 22. | 128 Samples of Sum of Sinusoids Sequence Plus Gaussian Noise | 66 |
| 23. | Bartlett Smoothed Periodogram Spectral Estimation of Sum of Sinusoids. | 67 |
| 24. | Estimated Spectrum from 128 Samples of Sum of Sinusoids Process Using MEM with AR Model Order Equal to 23. | 68 |
| 25. | Estimated Spectrum from 128 Samples of Sum of Sinusoids Process Using Papoulis Techniques. | 69 |
| 26. | Estimated Spectrum from 32 Samples of Sum of Sinusoids Process Using MEM with AR Model Order Equal to 17. | 70 |
| 27. | Estimated Spectrum from 32 Samples of Sum of Sinusoids Process Using Papoulis Techniques. | 71 |
| 28. | 128 Samples of Sum of Six Sinusoids. | 75 |
| 29. | Spectral Estimation from 128 Samples of Six Sinusoids Using MEM Techniques | 76 |
| 30. | Spectral Estimation from 128 Samples of Six Sinusoids Using Papoulis Techniques. | 77 |
| 31. | Spectral Estimation from 32 Samples of Six Sinusoids Using MEM Techniques | 78 |

| <u>Figure</u> | <u>Page</u> |
|--|-------------|
| 32. Spectral Estimation from 32 Samples of Six Sinu- soids Using Papoulis Techniques | 79 |
| 33. 128 Samples of Sum of Two Sinusoids Plus Noise. . . | 82 |
| 34. Spectral Estimation from 128 Samples of Two Sinu- soids Plus Noise Using MEM Techniques | 83 |
| 35. Spectral Estimation from 128 Samples of Two Sinu- soids Plus Noise Using Papoulis Techniques. | 84 |
| 36. Spectral Estimation from 32 Samples of Two Sinu- soids Plus Noise Using MEM Techniques | 85 |
| 37. Spectral Estimation from 32 Samples of Two Sinu- soids Plus Noise Using Papoulis Techniques. | 86 |
| 38. 128 Samples of Sum of Two Sinusoids Plus Noise Plus Impulsive Noise. | 88 |
| 39. Spectral Estimation from 128 Samples of Two Sinu- soids Plus Noise Plus Impulsive Noise Using MEM Technique | 89 |
| 40. Spectral Estimation from 128 Samples of Two Sinu- soids Plus Noise Plus Impulsive Noise Using Pap- oulis Techniques. | 90 |
| 41. Amplitude of FPE as a Function of Model Order for ARMA Model. | 119 |
| 42. Amplitude of AIC as a Function of Model Order for ARMA Model. | 120 |
| 43. Probability of Kolmogorov-Smirnov Two Sided Test as a function of Model Order for ARMA Model | 121 |
| 44. Estimated Mean of Estimated Spectrum Using the MEM Technique, ARMA Model | 122 |
| 45. Estimated Mean of Estimated Spectrum Using the Papoulis Technique, ARMA Model. | 123 |
| 46. Estimated Variance of Estimated Spectrum Using the MEM Technique, ARMA Model | 124 |
| 47. Estimated Variance of Estimated Spectrum Using the Papoulis Technique, ARMA Model. | 125 |

| <u>Figure</u> | <u>Page</u> |
|---|-------------|
| 48. Amplitude of FPE as a Function of Model Order for Sum of Sinusoids Input | 126 |
| 49. Amplitude of AIC as a Function of Model Order for Sum of Sinusoids Input | 127 |
| 50. Probability of Kolmogorov-Smirnov Two Sided Test as a Function of Model Order for Sum of Sinusoids Input. | 128 |
| 51. Estimated Mean of Estimated Spectrum Using the MEM Technique, Sum of Sinusoids Input. | 129 |
| 52. Estimated Mean of Estimated Spectrum Using the Papoulis Technique, Sum of Sinusoids Input . . . | 130 |
| 53. Estimated Variance of Estimated Spectrum Using the MEM Technique, Sum of Sinusoids Input. . . . | 131 |
| 54. Estimated Variance of Estimated Spectrum Using the Papoulis Technique, Sum of Sinusoids Input . | 132 |

List of Tables

| <u>TABLE</u> | | <u>PAGE</u> |
|--------------|--|-------------|
| I | Comparison of Spectral Estimation Techniques | 36 |
| II | Subroutine Identification | 102 |

Abstract

↓
Spectral estimation of data from some radar applications and seismological events is not accurate when short records are evaluated using traditional techniques. A record of data is short if the number of samples from the process is more than an order of magnitude smaller than the reciprocal of the lowest frequency of interest. This analysis considers records of fewer than 128 samples.

Techniques that produce improved frequency and amplitude resolution over smoothed periodograms and Fast Fourier Transforms (FFT) are considered. Specifically, the Burg Maximum Entropy Method (MEM) and Papoulis Bandlimited Extrapolation are derived. These techniques are shown to produce estimates that become unbiased and consistent. Additionally, the effects of windowing, a problem inherent with periodograms, are not observed in these techniques.

Model order determination for the MEM technique is accomplished through implementation of two techniques developed by Akaike. These techniques are derived through the maximum likelihood estimation of the estimated power. Using Akaike's order techniques, MEM spectral estimation provides extremely good frequency resolution from very short input records.

→ Papoulis bandlimited extrapolation techniques provided accurate results when short records are evaluated. The

technique is limited, in this research, to computational times commensurate with the MEM technique and does not produce resolution accuracy that is observed from MEM analysis. However, the estimated amplitudes are much closer than those generated from the MEM technique.

Spectral Analysis of Short Record Time Series Data

I. Introduction

Considerable interest is generated by government research agencies in power spectral estimation of time series data. Traditional techniques (Fast Fourier Transforms (FFT) and Periodograms) are typically employed to determine the spectral content of the data. These techniques are not adequate for time series data samples that are limited in number (short). A record of data is short if the number of samples from the process is more than an order of magnitude smaller than the reciprocal of the lowest frequency of interest. For example, a short period recording of a seismic event may produce less than 100 samples. Seismological events often occur at the lower end of the very low frequency spectrum (1 to 30,000 Hertz). Another example is a set of data indicating doppler frequency shifts based on a very few (less than 100) radar returns. This thesis considers several spectral estimation techniques and determines what techniques are applicable to analyze short record time series data. The criteria measured are the statistical properties and computational efficiency of each technique.

The spectral estimation techniques considered in this

thesis are Fast Fourier Transform, smoothed periodograms, Maximum Entropy Method (MEM), and bandlimited extrapolation. Methods of determining the statistical properties, i.e. mean value, autocorrelation function, and variance, of the spectral estimates are also considered. Additionally, evaluation of the bias in the statistical estimates is provided along with a determination of the impact of the bias on the statistical estimates. The time required to implement the analysis algorithms (computer execution time) and ease of application are also considered in this thesis.

To carryout the analysis, several basic assumptions are required. Since the statistics of the input data are totally unknown, we assume that the data are samples from a stationary random process, the result of some linear system being driven by an unknown noise. Through this research, equal spaced samples of the random process is assumed. These assumptions are justified by the fact that many of the signals of interest are characterized by the foregoing assumptions (Refs 2,7,24,25,28, and 39). The intent of this research is to provide a means of estimating the spectral density, not identification of the spectral density data. Therefore, hypothesis testing techniques are not considered or attempted.

The following sections provide a mix of current theoretical knowledge, general application techniques, and specific problem analysis. Section II lays the general groundwork

in spectral estimation techniques. Methods of determining the statistical properties of the estimated spectrum are included. Traditional and smoothed periodogram spectral estimation techniques are discussed in this section. A detailed theoretical background of MEM is included along with three methods of determining the order of the autoregressive (AR) model. Bandlimited extrapolation spectral estimation techniques are introduced. In particular, a method developed by Papoulis using the FFT is suggested. Section II concludes with a tabular comparison of the above spectral estimation techniques.

In Section III the Bartlett smoothed periodogram is used as a "calibration factor" to evaluate the averaged results from MEM and Papoulis spectral estimation. Confidence in these techniques is derived by the comparison. Several known input signals, including simple AR, autoregressive moving average (ARMA), and sum of sinusoids plus Gaussian noise, are analyzed. Finally, each input process is evaluated as a short record (128 samples or less with a sampling interval of one second) to determine analysis results under near realistic conditions.

The final analysis section of this thesis (Section IV) provides the results of spectral estimation of two "real world" problems. The MEM and Papoulis techniques are implemented to determine the spectral content of the unknown time sampled signals. A comparison of the resulting data

indicates that the MEM technique is superior to the constrained Papoulis technique when frequency resolution is a prime factor.

Section V concludes the research indicating the utility of the MEM and Papoulis spectral estimation techniques for short record of input data. Recommendations for future research in this area are suggested.

II. Spectral Estimation Techniques

Several approaches are available to determine the power spectral density of a random process. The methods selected must provide accurate results when only a limited number of samples are available. Additionally, the complexity of the spectral analysis hardware and software must be considered. This section outlines the techniques considered for the spectral analysis problem and provides the rationale used to select the maximum entropy spectral estimation method and the Papoulis algorithm as the techniques for the problem analysis. The methods initially considered are as follows:

1. Filter banks or Fast Fourier Transforms (FFT).
2. Smoothed Periodograms using discrete Fourier Transforms (DFT).
3. Maximum Entropy Method (MEM) using the Burg coefficient estimation techniques.
4. Papoulis Bandlimited Extrapolation Spectral Estimation.

An overview of these techniques is provided in the following subsections. A measure of accuracy is developed through analysis of the statistical properties of the estimated spectrum.

Statistics of the Estimated Spectrum

The appropriate techniques to estimate the spectral

density of an unknown input process are developed in the following subsection. The accuracy of the estimation techniques must be determined. Just how good is the estimate? Two important values provide an indication of the accuracy. The mean and variance of the estimated spectral density indicates the true value of the spectrum and how well the estimate approximates this value. Two measures for accuracy of an estimate are bias and consistency. An estimate is biased if the parameter being estimated minus the expected value (mean) of the estimate is not zero. If the result is zero (unbiased), the estimated value is the true value (on the average). Therefore, an unbiased estimate is more accurate than a biased estimate. An estimator is said to be consistent if the bias and the variance of the estimate tend to zero as the number of observations become large (Refs 29:536 and 41:71). In other words, the estimator approaches the true value as the number of observations increases. The ideal estimator is the one that produces estimates that are both unbiased and consistent.

The estimated mean of the estimated spectral density is calculated using the sample mean equation (Ref29:536-537).

$$E\{\hat{p}(\omega_n)\} = \hat{m}_p(\omega_n) = \frac{1}{N} \sum_{i=0}^{N-1} \hat{p}_i(\omega_n) \quad (1)$$

where $\hat{p}_i(\omega_n)$ are the n estimated power spectral density values for the i th input sequence and N is the number of

statistically independent sequences. Assuming that $\hat{m}_p(\omega_n)$ is a sequence of independent Gaussian random variables, the density function of $\hat{m}_p(\omega_n)$ is also Gaussian. Therefore, the expected value of $[\hat{m}_p(\omega_n)]^2$ is equal to

$$\begin{aligned} E\{[\hat{m}_p(\omega_n)]^2\} &= \frac{1}{N^2} \sum_{i=0}^{N-1} \sum_{j=0}^{N-1} E\{\hat{p}_i(\omega_n)\hat{p}_j(\omega_n)\} \\ &= \frac{1}{N} E\{[\hat{p}_i(\omega_n)]^2\} + [\hat{m}_p(\omega_n)]^2 \frac{N-1}{N} \end{aligned} \quad (2)$$

and the variance of $\hat{m}_p(\omega_n)$ is

$$\text{Var}[\hat{m}_p(\omega_n)] = E\{[\hat{m}_p(\omega_n)]^2\} - [E\{\hat{m}_p(\omega_n)\}]^2 \quad (3)$$

From Eqs (2) and (3), as N increases, the variance of the sample mean goes to zero and the sample mean approximates the actual spectrum arbitrarily closely.

The maximum likelihood variance estimate of the estimated spectrum is called $\text{Var}\{\hat{p}(\omega_n)\}$ by (Ref29:536-537)

$$\text{Var}\{\hat{p}(\omega_n)\} = \frac{1}{N} \sum_{i=0}^{N-1} [\hat{p}_i(\omega_n)]^2 - [\hat{m}_p(\omega_n)]^2 \quad (4)$$

and is shown to be biased by Maybeck (Ref27:398). The unbiased variance estimate is derived and is shown, for the case of independent observation, by Maybeck to be

$$\text{Var}'\{\hat{P}(\omega_n)\} = \frac{1}{N-1} \sum_{i=0}^{N-1} \left[\hat{P}_i(\omega_n) \right]^2 - \frac{N}{N-1} \left[\hat{m}_p(\omega_n) \right]^2 \quad (5)$$

where the prime (') denotes the unbiased variance estimator. Thus, if N is large enough, $N/(N-1) \approx 1$, the maximum likelihood estimate is unbiased. Also, note that the estimate is consistent, the variance estimate tends to zero as N is increased. Therefore, if independent sequences are assumed, the mean and variance of the estimated spectrum is determined, providing information concerning the bias and consistency of the estimate.

The following paragraphs provide an overview of the spectral estimation techniques considered in this research.

Filter Bank or Fast Fourier Transform

A straightforward approach to spectral analysis is to present the time domain signal to a bank of narrowband band-pass filters. Each filter will only pass a specific range of frequencies. The bank of filters approximate the Fourier Transform in the limit as the number of filters increases and the range of frequencies decreases (Ref 20:4).

$$X(\omega) = \frac{1}{2\pi} \int_{-\infty}^{\infty} x(t) e^{-j\omega t} dt \quad (6)$$

The technique offers almost ideal spectral estimation analysis,

limited only by the number and bandwidth of the filters and the roll off characteristics of the non ideal filters actually implemented. Typically, the system is realized digitally and is usually limited by computation time. The amount of computation time to transform a given set of time data to the frequency domain is inversely proportional to the bandwidth of each filter [the Heisenberg Uncertainty Principle (Ref20:5)]. The bandwidth of the filters determine frequency resolution (the concentration of a spectral estimate expressed in frequency units), indicating that finer resolution is achieved by reducing the bandwidth of each filter. Therefore, if the input is finite, and short as described in the introduction, frequency resolution may be jeopardized when computation time is constrained.

Another inherent difficulty with filter bank analysis is the window function effects. The finite data is interpreted as a multiplication of the original signal by a window function (Ref 20:5). The result is a spectrum which is the convolution of the original, desired, spectra by a transform of the window function. Incorrect selection of the window function may result in analysis that is truly very different than the actual spectra.

The filter bank approach is thus limited by the trade-off between time measured data and frequency resolution obtainable, and the proper selection of the window function. Oppenheim and Schafer (Ref29:549-553) provide an excellent

discussion of the effects of window functions and the relation to correct spectral estimation. Simply stated, windowing is the result of convolving the data of interest with some window function. The function may be rectangular, triangular, and other shapes. The result of the convolution, in effect, truncates the input sequence outside the period of interest and conditions the data inside the period. The window function is selected to insure a more accurate representation of the spectral density by negating the effects of the FFT. Close relationships exist between the windowing of the original input data and periodogram spectral estimation techniques. This technique is discussed in the following subsection.

Smoothed Periodograms Using Discrete Fourier Transforms(DFT).

If the input process is stationary (initial assumptions Section I) and the autocorrelation function is known, then the power spectral density of the input can be determined (Ref30:338).

$$P(\omega) = \int_{-\infty}^{\infty} \phi(t)e^{-j\omega t} dt \quad (7)$$

where the Fourier Transform $P(\omega)$ is the spectral density and $\phi(t)$ is the autocorrelation function. In discrete form,

$$P(\omega) = \sum_{k=-\infty}^{\infty} \phi_N(k)e^{-j\omega k} \quad (8)$$

where N is the number of nonzero input autocorrelation values. If $x(k)$ is a real, finite length, input sequence $0 \leq k \leq N-1$ then,

$$X_N(\omega) = \sum_{k=0}^{N-1} x(k)e^{-j\omega k} \quad (9)$$

is the Fourier Transform of the input. Since the autocorrelation function of the input sequence is unknown, an estimated value is introduced (Ref29:542).

$$\hat{\phi}_n(k) \equiv \frac{1}{N-|n|} \sum_{k=0}^{N-|n|-1} |x(k)x(k-n)| \quad (10)$$

Combining Eqs (8),(9), and (10) leads to an estimate of the power spectral density.

$$\hat{P}_p(\omega_n) = \frac{1}{N} |X_N(\omega_n)|^2 \quad (11)$$

where $\hat{P}_p(\omega_n)$ denotes a power spectral estimate using Periodograms. This spectrum estimate is called a periodogram.

It can be shown that the periodogram spectral density is biased and not consistent (Ref29:540-545). Therefore, alternative techniques must be considered to estimate the spectral density. Of particular importance in the estimation technique is the length of the lag for each estimate with respect to the total sample size (Number of total samples)

and the particular window function used in the frequency transformation. Bartlett and Welch (Refs 8 and 44) consider these problems in the development of smoothed periodograms.

One technique used to modify the periodogram spectral estimator so that the estimate is consistent is attributed to Bartlett (Ref 8). The technique is particularly useful with a large number of input samples. The input sequence is segmented into several sections each with a fixed number of samples. The spectral estimated from all sections are averaged to produce an estimate that is consistent. The estimate is consistent if and only if the number of sections is large. If, for example, the input consists of N samples and is separated into K sections of M samples each, Eq(11) is applied to each section to produce K periodograms. Each periodogram is assumed to be independent. An average over all the periodograms produces an estimate of the spectrum. The spectral estimator is written as:

$$\hat{P}_B(\omega_n) = \frac{1}{K} \sum_{i=1}^K \hat{P}_i(\omega_n) \quad (12)$$

where $\hat{P}_i(\omega)$ is the i th periodogram estimate and $\hat{P}_B(\omega_n)$ is the Bartlett smoothed periodogram spectral estimate. The variance of $\hat{P}_B(\omega_n)$ is inversely proportional to the number of periodograms, K (Ref29:548). Therefore, as K becomes

large, the variance approaches zero and the Bartlett estimate is consistent. Additionally, the bias of the Bartlett estimator is greater than that of the simple periodogram (Ref 8). These two results indicate that the reduction of the variance is accomplished at the expense of increased bias. However, increasing K results in fewer samples for each periodogram, thereby decreasing frequency resolution. For example, if it is known that the spectrum has a narrow peak, M must be chosen large enough to resolve the peak. For small variance, K must be large. The number of samples of the input sequence is determined by the variables K and M . Clearly, if low variance and fine frequency resolution are implicit, an extremely long input record may be required.

Blackman and Turkey suggest another approach to spectral estimation using smoothed periodograms (Ref 9). The technique is to smooth the periodogram by convolution with an appropriate spectral window. Welch applied the Blackman-Turkey hypothesis to the averaged periodogram solution and developed the spectrum estimation technique of averaging modified periodograms (Ref 44). Welch modifies the Bartlett procedure by applying a window function directly to the data input sections. The periodogram (Eq(11)) is thus modified

to

$$\hat{P}_{pw}(\omega_n) = \frac{1}{MU} \left| \sum_{n=0}^M x^{(i)}(n)W(n)e^{-j\omega n} \right|^2, \quad i=1,2,\dots,k \quad (13)$$

where $x^{(i)}(n)$ is the n th input sample from the i th section, and

$$U = \frac{1}{M} \sum_{n=0}^{M-1} W^2(n) \quad (14)$$

where $W(n)$ is the desired window and $\hat{P}_{pw}(\omega_n)$ is the windowed periodogram function. The smoothed spectral estimator is

$$\hat{P}_w(\omega_n) = \frac{1}{K} \sum_{i=1}^K \hat{P}_{pw}(\omega_n) \quad (15)$$

Welch shows that with the inclusion of U , the estimate $\hat{P}_w(\omega_n)$ is not biased and, if the sections do not overlap, the variance is inversely proportional to K . Therefore, the Welch estimator is consistent. Clearly, the Bartlett procedure is a simplification (subset) of Welch's method with the window function $W(n)$ equal to one.

For the specific application under consideration in this thesis, smoothed periodograms are not practical. For accurate spectral estimation, these procedures must have a large data record. Bartlett smoothed periodogram techniques do provide a means of verifying the results of analysis on known signals under known conditions when the MEM and Papoulis techniques are verified in Section III.

Maximum Entropy Spectral Estimation

The concept of linear prediction is based on the assumption that any linear system can be represented in discrete-time by (Ref25:562)

$$x(n) = - \sum_{k=1}^M \beta_k x(n-k) + A \sum_{j=0}^P \gamma_j y(n-j), \gamma_0=1 \quad (16)$$

where $y(\cdot)$ is some unknown input, β_k , γ_j , and A are some unknown parameters, and $1 \leq k \leq M$ and $1 \leq j \leq P$. In other words, the output, $x(n)$, is predicted by some linear combination of previous outputs and inputs. A special case of this linear model is the autoregressive (AR) (all-pole) model defined by

$$x(n) \equiv \sum_{k=1}^M \beta_k x(n-k) + y(n) \quad (17)$$

and M is the system order. This equation is the model assumed to be valid for the analysis under consideration. The equation can be interpreted as a stochastic difference equation and describes the samples of a sequence from a random process where $y(n)$ is a white noise sequence with zero mean and variance σ_y^2 . Finite order AR processes are useful in representing many physically significant linear random processes (Ref 1,11,12,24, and 25). J.P. Burg provides

the power spectral equation for this AR Model (Ref 12).

$$\hat{P}(\omega_m) = \frac{P_{M+1}\Delta t}{\left| 1 - \sum_{n=1}^M \hat{\beta}_n e^{-j\omega_m n \Delta t} \right|^2} \quad (18)$$

where Δt is the input sampling interval. The proper values for the prediction coefficients $\hat{\beta}_n$, the prediction error power P_{M+1} , and the model order M must be determined. These values are discussed in the following paragraphs.

The relationship between the AR process and the maximum Entropy Method is extensively researched (Refs 13,38,39 and 40). A brief overview of the relationship is provided here.

Consider a situation where M different things, m_i , happen with probability P_i . Information is defined as $-\log_a P_i$ where P_i is a particular event (Ref 47:428). If all the P_i are known to be equal a priori, no Information is available. However, when a particular P_i is known, a certain amount of Information is gained. Clearly, the probability of occurrence is related to Information. Shannon (Ref 36) explored this Information Theory to measure the average Information required to transmit a given message. Shannon calls the measure entropy and is the average Information per time interval.

$$H = -k \sum_{i=1}^M P_i \log_r P_i \quad (19)$$

where k is a constant and \log_r is a logarithm base r . Consider a process x_t that can take on the values x_1, x_2, \dots, x_n . Assume the available Information about x_t is the average values $\langle f_1(x_t) \rangle$, $\langle f_2(x_t) \rangle$, \dots , $\langle f_m(x_t) \rangle$ of some functions $f_i(x_t)$, where $m \leq n$. The probability distribution $P_t = F(x_t)$ that is consistent with the Information and is maximally free of other limitations maximizes the entropy Eq(19). In the continuum case (Ref 38:413),

$$H = - \int f(\underline{z}_N) \ln \{cf(\underline{z}_N)\} d\underline{z} \quad (20)$$

where $f(\underline{z}_N)$ is a joint probability density for N elements, and C is a constant.

Smylie et al (Ref 38:410-414) show that the entropy measure H is not a valid measure for frequencies and suggest an entropy rate h that relates the power spectral density to entropy rate. The suggested entropy rate for a stationary Gaussian process is defined in terms of the spectral density (Ref38:414)

$$h \equiv \frac{1}{4f_N} \int_{-f_N}^{f_N} \ln P(\omega) d\omega \quad (21)$$

where f_N is the Nyquist frequency and \ln is the natural logarithm. Replacing $P(\omega)$ with the power spectral density, Eq (8), yields

$$h = \frac{1}{4f_N} \int_{-f_N}^{f_N} \ln \left[\sum_{k=-\infty}^{\infty} \phi(k) e^{-j\omega k} \right] d\omega \quad (22)$$

assuming a uniform sampling rate and sampling interval of one. Smylie et al (Ref 38:414) continued the derivation to yield

$$h = \frac{1}{2} \ln \{ \det [\Phi_M] \} \quad (23)$$

where Φ_M is the positive semidefinite M by M matrix of autocorrelation coefficients. Smylie shows that Φ_M is equi-diagonal and indicates that such matrices are named Toeplitz.

To maximize the entropy, Φ_M must be determined in such a way as to impart no assumptions about the input data. No erroneous information is added to the analysis. This restraint departs extensively from the previous estimation techniques. In the Bartlett technique, the data outside the window is assumed to be zero, suggesting that the autocorrelation function is zero outside some limiting time period. If the autocorrelation is zero, periodic extensions used with FFTs are implicit. Consequently, additional data is erroneously added. As a result, the estimated spectral data may be somewhat different than the actual spectrum. The Maximum Entropy technique provides an alternate choice for selecting autocorrelations, one in which no Information is added or implied. The MEM technique implies Φ_M is calculated in such a way as to maximize the uncertainty or entropy and make no

assumptions about the data outside the time sample.

To calculate the MEM power spectrum[Eq(18)] , the order of the AR process (length of the prediction filter) and the prediction coefficients (β_n) must be determined. Procedures to determine these values are discussed in the following paragraphs.

The toeplitz autocorrelation matrix for an Mth order process is

$$\Phi_M = \begin{bmatrix} \phi(0) & \phi(1) & . & . & . & \phi(M) \\ \phi(1) & \phi(0) & . & . & . & \phi(M-1) \\ . & . & . & . & . & . \\ . & . & . & . & . & . \\ . & . & . & . & . & . \\ \phi(M) & \phi(M-1) & . & . & . & \phi(0) \end{bmatrix} \quad (24)$$

if it is assumed that $\phi(0), \phi(1), \dots, \phi(M)$ are known. Suppose ϕ_{M+1} is to be estimated from this data, then $\phi(M+1)$ must be selected to maximize the entropy. Also, $\phi(M+2)$ and so on. Therefore, from Eq(23), $\phi(M+1)$ is determined by maximizing $\det[\Phi_{M+1}]$ with respect to $\phi(M+1)$. Since Φ_{M+1} must be positive semidefinite, $\det[\Phi_{M+1}]$ has a single maximum when the product rule of differentiation is applied. With ϕ_{M+1} determined, ϕ_{M+2} can be determined in a similar manner. For the case maximizing $\det[\Phi_{M+1}]$ with respect to $\phi(M+1)$ the result is

$$\begin{vmatrix}
 \phi(1) & \phi(0) & \dots & \phi(M-1) \\
 \phi(2) & \phi(1) & \dots & \phi(M-2) \\
 \cdot & \cdot & \cdot & \cdot \\
 \cdot & \cdot & \cdot & \cdot \\
 \cdot & \phi(M-1) & \dots & \cdot \\
 \phi(M+1) & \phi(M) & \dots & \phi(1)
 \end{vmatrix} = 0 \quad (25)$$

Solving Eq(17) for AR order M ,

$$x(n) = \beta_1 x(n-1) + \beta_2 x(n-2) + \dots + \beta_M x(n-M) + y(n) \quad (26)$$

Multiplying through by $x(n-k)$, $k \leq 0$, and taking expected values,

$$\phi(k) = \beta_1 \phi(k-1) + \beta_2 \phi(k-2) + \dots + \beta_M \phi(k-M) \quad (27)$$

where $E\{x(n-k)y(n)\} = 0$ for a zero mean Gaussian input $y(n)$.

Substituting the values of $k=1, 2, \dots, M+1$ into Eq (27) yields a set of simultaneous equations.

$$\begin{array}{rcl}
 \phi(1) & -\beta_1 \phi(0) - \dots - \beta_M \phi(M-1) & = 0 \\
 \cdot & \cdot & \cdot \\
 \cdot & \cdot & \cdot \\
 \cdot & \cdot & \cdot \\
 \phi(M+1) & - \beta_1 \phi(M) - \dots - \beta_M \phi(1) & = 0
 \end{array} \quad (28)$$

These equations are known as the Yule-Walker equations (Refs 25, 43, and 46). If $\phi(0), \dots, \phi(M)$ are known, β_1, \dots, β_M can be determined. Also, $\phi(M+1)$ can be determined by

solving for the determinant of the matrix of all the $\phi(i)$ set to zero.

$$\begin{vmatrix} \phi(1) & \phi(0) & . & . & . & \phi(M-1) \\ \phi(2) & \phi(1) & . & . & . & \phi(M-2) \\ . & . & . & . & . & . \\ . & . & . & . & . & . \\ . & . & . & . & . & . \\ \phi(M+1) & \phi(M) & . & . & . & \phi(1) \end{vmatrix} = 0 \quad (29)$$

but this equation is identical to Eq(25). So the Yule-Walker equations are identical to maximizing the entropy of the process.

Suppose k [Eq(27)] is allowed to equal zero. The expected value of $x(n-k)y(n)$ is $E\{x(n-k)y(n)\} = E\{x(n)y(n)\}$, but $E\{x(n)y(n)\} = E\{y^2(n)\} = \sigma_y^2$ for the zero mean Gaussian model Eq (17). Eq (27) is now, for $k=0$,

$$\phi(0) - \beta_1 \phi(1) - \dots - \beta_M \phi(M) = \sigma_y^2 \quad (30)$$

and Eq (28) can be augmented to include all $k=0,1,\dots,M$ as,

$$\begin{bmatrix} \phi(0) & \phi(1) & . & . & . & \phi(M) \\ \phi(1) & \phi(0) & . & . & . & \phi(M-1) \\ . & . & . & . & . & . \\ . & . & . & . & . & . \\ . & . & . & . & . & . \\ \phi(M) & \phi(M-1) & . & . & . & \phi(0) \end{bmatrix} \begin{bmatrix} 1 \\ -\beta_1 \\ . \\ . \\ . \\ -\beta_M \end{bmatrix} = \begin{bmatrix} \sigma_y^2 \\ 0 \\ . \\ . \\ . \\ 0 \end{bmatrix} \quad (31)$$

which is an alternate form of the Yule-Walker equations. In general, the variance, σ_y^2 , is estimated as the prediction error power P_{M+1} , resulting from the convolution of $x(n)$ with the $M+1$ point prediction error filter Eq(17) (Ref39: 187). P_{M+1} is often referred to as the innovations power.

If the data are known for the $M-1$ case, the data for the M th case is determined by calculating the coefficients β_1, \dots, β_M , autocorrelation $\phi(M)$, innovations power P_{M+1} , and then calculating the power spectrum Eq(18). For the $M+1$ case, there are $M+1$ equations and $M+2$ unknowns. Burg (Refs 11,12 and 13) develops an elegant procedure that does not make any assumptions about the data outside the sample. Additionally, the technique does not require a prior estimate of the autocovariance or autocorrelation function. Burg suggests that the error power be calculated by running a prediction error filter over the data in a forward and backward direction, but not off the data. As each set of coefficients is estimated, the error filter order is increased by one and the procedure is repeated until the desired model order is reached. The appropriate model order is discussed in later paragraphs. The recursion corresponds to an approximate maximum likelihood estimation of the AR coefficients (Refs 10:46-84 and 13:375).

Consider the case of a set of N input samples of data, $x(1), \dots, x(N)$, all with equal spacing Δt , and the power spectrum of an M th order AR model is required. First,

assume the model order is zero. Therefore, an estimate of the autocorrelation for lag one is

$$\hat{\phi}_0(1) = \frac{1}{N} \sum_{n=1}^N x^2(n) \quad (32)$$

where the (1) in $\hat{\phi}_0(1)$ denotes the first lag. From Eq(31), $P_1 = \phi_0(0)$. The system for model order one is

$$\begin{bmatrix} P_1 & \hat{\phi}_0(1) \\ \hat{\phi}_0(1) & P_1 \end{bmatrix} \begin{bmatrix} 1 \\ \hat{\beta}_{11} \end{bmatrix} = \begin{bmatrix} P_2 \\ 0 \end{bmatrix} \quad (33)$$

where $\hat{\beta}_{11}$ is the estimate of β_1 . The forward prediction error is, from Eq(17)

$$\begin{aligned} e_1^f(n) &= x(n) - \hat{x}(n) \\ &= x(n) - \beta_{11}x(n-1) \quad ; n=2,3,\dots,N \end{aligned} \quad (34)$$

Similarly, the backward prediction error is

$$e_1^b(n) = x(n) - \hat{\beta}_{11}x(n+1) \quad ; n=N-1, N-2, \dots, 1 \quad (35)$$

The prediction error power is calculated by

$$\begin{aligned} P_1 &= \frac{1}{2(N-1)} \sum_{n=1}^{N-1} \{ [x(n+1) - \hat{\beta}_{11}x(n)]^2 \\ &\quad + [x(n) - \hat{\beta}_{11}x(n+1)]^2 \} \end{aligned} \quad (36)$$

where $\hat{\beta}_{11}$ is chosen to minimize P_1 . $\hat{\beta}_{11}$ is calculated by (Refs 5:70 and 11:5)

$$\hat{\beta}_{11} = \frac{2 \sum_{n=1}^{N-1} x(n)x(n+1)}{\sum_{n=1}^{N-1} [x^2(n) + x^2(n+1)]} \quad (37)$$

Solving for $\hat{\phi}(1)$ and P_2 yields

$$\hat{\phi}_1(1) = \hat{\beta}_{11}\phi(0) \quad (38)$$

$$P_2 = P_1(1 - \hat{\beta}_{11}^2) \quad (39)$$

In general, for the step from model order $M-1$ to M , (40)

$$P_M = \frac{1}{2(N-M)} \sum_{n=1}^{N-M} \left\{ \left[x(n) - \sum_{j=1}^M \hat{\beta}_{Mj} x(n-j) \right]^2 + \left[x(n+M) - \sum_{j=1}^M \hat{\beta}_{Mj} x(n+M-j) \right]^2 \right\}$$

where P_M is minimized with respect to the estimated coefficient $\hat{\beta}_{MM}$ (Ref5:71). Calculation of the prediction coefficients $\hat{\beta}_{Mk}$; $j=1,2,\dots,M-1$ is accomplished by the Levinson-Durbin procedure. Makhoul (Ref25:566) outlines the procedure which is a technique for solving for the $\hat{\beta}_{Mj}$ data with estimated $\hat{\phi}(j)$ and Eq(31). The procedure solves for the data in only M^2 operations and requires $2M$ storage locations. The recursion equation for $\hat{\beta}_{Mj}$ is

$$\hat{\beta}_{Mj} = \hat{\beta}_{M-1j} - \hat{\beta}_{MM} \hat{\beta}_{M-1M-j} \quad ; 1 \leq j < M \quad (41)$$

From Eq(31),

$$\begin{vmatrix} \phi_M(0) & . & . & . & \phi_M(M) \\ . & . & & & . \\ . & & . & & . \\ . & & & . & . \\ \phi_M(M) & . & . & . & \phi_M(0) \end{vmatrix} \begin{vmatrix} 1 \\ -\hat{\beta}_{M1} \\ . \\ . \\ -\hat{\beta}_{MM} \end{vmatrix}$$

$$= \left\{ \begin{vmatrix} 1 \\ -\hat{\beta}_{M-1|i|} \\ . \\ . \\ -\hat{\beta}_{M-1M-1} \end{vmatrix} - \hat{\beta}_{MM} \begin{vmatrix} 0 \\ \hat{\beta}_{M-1M-1} \\ . \\ . \\ \beta_{M-1} \ 1 \\ 1 \end{vmatrix} \right\} \quad (42)$$

$$= \begin{vmatrix} P_M \\ 0 \\ . \\ . \\ . \\ x \end{vmatrix} - \hat{\beta}_{MM} \begin{vmatrix} x \\ 0 \\ . \\ . \\ . \\ P_M \end{vmatrix} = \begin{vmatrix} P_{M+1} \\ 0 \\ . \\ . \\ . \\ 0 \end{vmatrix}$$

where x indicates a don't care condition, and

$$P_{M+1} = P_M (1 - \hat{\beta}_{MM}^2) \quad (43)$$

Finally,

$$\hat{\phi}_M(M) = - \sum_{j=1}^M \hat{\phi}_M(M-j) \hat{\beta}_{Mj} \quad (44)$$

Anderson (Ref 5) provides an algorithm to carryout the recursions. The routine is suitable for implementation on a computer and is used in the analysis sections of this report. The coefficients $\beta_{M1}, \dots, \beta_{MM}$ and the error power (innovations power) are implemented in Eq(18) to produce an estimate of the power spectrum of AR model order equal to M .

Statistical properties of the MEM spectral estimate are investigated by Makhoul and Kromer (Refs 23 and 25:568-569). It is determined that the MEM estimate is:

1. Asymptotically unbiased, as

$$M \rightarrow \infty,$$

$$E\{\hat{P}(\omega_n)\} = P(\omega) \quad (45)$$

2. Asymptotically Normal with variance

$$\text{Var}\{\hat{P}(\omega_n)\} = \frac{2M}{N} \{P^2(\omega_n)\} \quad (46)$$

at each frequency ω_n .

Thus, for large M and N and a smooth true spectrum, any spectrum can be approximated arbitrarily closely by the AR model (Refs 39:192 and 25:569). Fuller makes this statement

even stronger in a theorem for any continuous spectral density (Ref18:147-149).

To estimate the power spectrum using MEM , the order of the AR model must be correctly determined. Three techniques are suggested in the following paragraphs. Selection of the technique to be used in analyzing unknown data inputs is primarily contingent on the simplicity of implementation.

One order selection method considers the well-known statistical analysis tool, the Kolmogorov-Smirnov single sample test for goodness of fit. The test is found in several sources (Refs 10,15, and 37). Additionally, computer programs are generally available in program libraries.

An estimate of the input sequence is generated by applying the prediction coefficients Eq(41)

$$\hat{x}(n) = \sum_{j=1}^M \beta_{Mj} x(n-j) \quad (47)$$

for model order M , and the error is determined

$$e(n) = \hat{x}(n) - x(n) ; 1 \leq n \leq N \quad (48)$$

If the prediction coefficients are correctly estimated and the order is correct, then $e(n)$ equals $y(n)$ [Eq(17)]. The initial assumption is that the system [Eq(17)] is driven by white-Gaussian noise (WGN). The power spectral density of

WGN is constant over all frequencies. Therefore, $E(\omega)$, the power spectral density of $e(n)$, will be constant over some bandwidth if $\hat{x}(n)$ is a correct estimate. Integrating $E(\omega)$ over this bandwidth will produce a ramp function approximating the uniform distribution. The Kolmogorov-Smirnov test compares the integrated $E(\omega)$ with an actual uniform distribution function, and generates an output that represents a probability estimate of how well the integrated $E(\omega)$ approximates the uniform distribution. This probability output for order equal to M is compared to previous values from similar test on orders up to M . The maximum Kolmogorov-Smirnov probability corresponds to the best estimate of the system order.

The Kolmogorov-Smirnov test clearly necessitates considerable manipulation of the data. Therefore, the test requires a large amount of programming and computer time. Because of these factors, Kolmogorov-Smirnov tests are not included in the final analysis section of this paper. However, because of the confidence many statistical practitioners have in this test, it is used as a verification and confidence building tool for the following two model order determining techniques.

The problem of model order determination has been extensively investigated in the past few decades. Many of the techniques result in considerable computations and many assumptions (Refs 6,16,17,34, and 45). Two techniques developed by Akaike (Refs 1,2,3, and 4) show considerable promise

and are used as analysis tools to evaluate the problem considered in this paper.

Akaike's first technique adopts a decision theoretical approach in which a value of merit is defined for each AR model. The figure of merit is the mean-square error of the one-step-ahead prediction determined by using the MEM to estimate the coefficients, $\hat{\beta}_1$. In other words, if $\hat{x}(n)$ is defined as the estimated prediction of $x(n)$, then

$$\text{FPE} = E\{[x(n) - \hat{x}(n)]^2\} \quad (49)$$

where FPE is called the final predictor error. Another estimate ($\hat{y}(n)$) is generated from the same coefficients and an independent realization $y(n)$. FPE for this case is

$$\text{FPE} = E\{[y(n) - \hat{y}(n)]^2\} \quad (50)$$

Akaike (Ref 1) shows that the expression for the FPE of the Mth order AR process is then

$$(\text{FPE})_M = \frac{N+M+1}{N-M-1} P_{M+1} \quad (51)$$

where N is the total sample size and P_{M+1} is as defined by Eq(31). The scheme is to determine some maximum order $L < N$. Then calculate FPE, Eq(51), for successive order $M(M=1,2,\dots,L)$. The minimum FPE yields the estimate of the AR model order for prediction. FPE order estimation techniques are investigated by several authors and provide

excellent results (Refs 3,22,39,and 40). This technique is simply implemented and requires only one subjective assumption, namely selection of the maximum possible order L .

In a recent paper by R.H. Jones (Ref 22), it is determined that the FPE scheme outlined by Akaike becomes biased as the model order approaches the sample size. This result is verified by experimental investigation. Jones shows that if the input data is white noise, the estimated one step prediction variance remains constant as model order increases to $N/2$ (for an N -sample input) . For orders above $N/2$, the variance decreases linearly as model order increases. With white noise as an input, the variance should remain constant for all models. To off-set the decreased variance, Jones suggests the following modifications to the FPE Eq(51)

$$(FPE)_M = \begin{cases} \frac{N+M+1}{N-M-1} P_{M+1} & 0 \leq M \leq N/2 \\ \frac{N+M+1}{N-M-1} P_{M+1} / (1.5 - M/N) & N/2 < M \leq N-1 \end{cases} \quad (52)$$

Applying this new FPE equation yields a constant variance for all model orders up to $N-1$.

In subsequent work Akaike extended the FPE scheme to be applicable to any maximum likelihood situation (Ref 1). He describes an information criterion for estimating the model order that employs the \ln -maximum likelihood estimate of a given process. Akaike's A-information criterion (AIC) is

defined by

$$(AIC)_M = -2 \ln (\text{maximum likelihood}) + 2M \quad (53)$$

"A" denotes the first case, with the expectation that B,C,... may follow. It turns out that for the case of univariate AR model with Gaussian input (Ref 21),

$$(AIC)_M = N \ln (P_{M+1}) + 2(1+M) \quad (54)$$

Again, a maximum order $L < N$ is selected and the minimum AIC denotes the proper estimate of the model order. R.H. Jones (Ref 21:895) shows that AIC and FPE select the same order. Additionally, Jones suggests that FPE and AIC are asymptotically equivalent. AIC, like FPE, is easily implemented and is therefore, a desirable analysis tool for the problem under consideration.

The Maximum Entropy spectral estimation techniques outlined in the preceding paragraphs provide an excellent tool for the research in this paper. Since the problems are described for short record data, MEM is ideally suited. Additionally, MEM provides an unbiased estimate of the spectral density of the input sequence.

Papoulis Bandlimited Extrapolation Spectral Estimation

A new algorithm, developed by A. Papoulis (Refs 31, 32, and 33) appears to be applicable to the problem under consideration. The technique involves an iterative routine

using only a discrete FFT/IFFT. Specifically, Papoulis' algorithm is applicable to stationary bandlimited signals. The algorithm is based on one simple assumption

$$P(\omega) = 0 \text{ whenever } |\omega| > \sigma \quad (55)$$

Note that this assumption does not restrict the time function $x(n)$ to some specific value outside the period of interest.

The problem is to find the Fourier Transform of a band-limited function $x(t)$ in terms of some simple segment of $x(t)$, $x(n)$. Papoulis suggests that the solution is found by the following iteration:

$$1. \text{ Form } x_1(t) = \begin{cases} x(t) & |t| < T \\ 0 & |t| > T \end{cases} \quad (56)$$

2. Determine the FFT

$$X_1(\omega) = \mathcal{F} [x_1(t)] \quad (57)$$

$$3. \text{ Form } P_1(\omega) = \begin{cases} X_1(\omega) & |\omega| < \sigma \\ 0 & |\omega| > \sigma \end{cases} \quad (58)$$

4. Compute

$$x_2(t) = \mathcal{F}^{-1} \{P_1(\omega)\}$$

$$x'_2(t) = \begin{cases} x(t) & |t| < T \\ x_2(t) & |t| > T \end{cases} \quad (59)$$

5. Continue steps 2,3, and 4 to the nth iteration to yield

$$P_n(\omega) = \begin{cases} X_n(\omega) & |\omega| < \sigma \\ 0 & |\omega| > \sigma \end{cases} \quad (60)$$

The number of iterations ,n, can be controlled by a preset mean-square error (MSE) value. The MSE for the nth iteration is

$$e_n = \int_{-\infty}^{\infty} [x(t) - x_n(t)]^2 dt \leftrightarrow \frac{1}{2\pi} \int_{-\sigma}^{\sigma} [P(\omega) - P_n(\omega)]^2 d\omega \quad (61)$$

$$e_n = \int_{|t| < T} [x(t) - x_n(t)]^2 dt + \int_{|t| > T} [x(t) - x_n(t)]^2 dt$$

rewriting the far right integral in terms of the Fourier Transform

$$e_n = \int_{|t| < T} [X(t) - x_n(t)]^2 dt + \frac{1}{2\pi} \int_{|\omega| > \sigma} |P(\omega) - X_{n+1}(\omega)|^2 d\omega \quad (62)$$

$$+ \int_{-\sigma}^{\sigma} |P(\omega) - P_{n+1}(\omega)|^2 d\omega$$

From Eqs(61) and (62),

$$e_n - e_{n+1} = \int_{|t| < T} [x(t) - x_n(t)]^2 dt + \frac{1}{2\pi} \int_{|\omega| > \sigma} |P(\omega) - X_{n+1}(\omega)|^2 d\omega \quad (63)$$

The two integrals on the right side of Eq(63) are never less than zero. Therefore, $e_n - e_{n+1}$ is never less than zero. It follows then, that e_n is monotone non-increasing. This conclusion indicates that the iteration procedure can continue to some value to satisfy a preset condition.

Papoulis (Ref 31:738-740) proves the convergence of the technique, $e_n \rightarrow 0$ as $n \rightarrow \infty$ in the deterministic case. The proof is through a comparison of the technique to a method for extrapolation of band-limited functions based on the expansion of $x_1(t)$ into a series of prolate spheroidal functions. The results are provided in Appendix A. The algorithm is used by Gerchberg (Ref 19), in a 1974 report on image processing, with satisfactory results.

Comparison of Spectral Estimation Techniques

To complete the background information concerning techniques for spectral estimation, several areas must be considered. In particular, the techniques must be applicable to analysis of short input record. However, some aspects of the traditional techniques can be used to verify the newer or unfamiliar techniques.

Articles by Burnard and LaCoss (Refs 7 and 24) provide additional data and solidify the conclusions concerning the various techniques. For example, Burnard and LaCoss suggest that the variance of the spectral estimate for both MEM and Periodograms is proportional to $2L/N$, where L is the number

of sections from the total of N samples. Also, LaCoss shows that frequency resolution is inversely proportional to N for Periodograms and inversely proportional to N^2 for MEM. These results, along with the conclusions derived in this section are provided in Table I. Clearly, the MEM and Papoulis techniques are applicable to the problem under consideration.

Several different input sequences are applied to both MEM and Papoulis spectral estimation computer coded algorithms. It is determined that on the average, MEM routines complete execution in about the same time as the Papoulis' routine when the number of iterations is less than 100. Therefore, the number of Papoulis iterations is limited to a maximum of 100 to allow a rough equivalence in computational time between the MEM and Papoulis techniques.

Smoothed periodogram techniques provide the basis of analysis to verify the MEM and Papoulis techniques applied to known signal samples. The following section provides the results of applying the techniques derived in this section.

TABLE I

Comparison of Spectral Estimation Techniques

| Characteristic | Trad./Periodogram | MEM | Papoulis Technique |
|--|---|--|--|
| Estimation of Autocorrelation | Weights lag values with some function, introducing window effects | Uses lag values to estimate unknown lags optimally | None |
| Spectral window effects | Always present | None | None |
| Variance of spectral estimate | $2 L/N$ for Bartlett | Proportional to $2 \frac{L}{N}$ | Dependent on number of iterations |
| Resolution (closely spaced spectral lines) | Proportional to $\frac{1}{N}$ | Proportional to $\frac{1}{N^2}$ | Proportional to $\frac{1}{N}$ |
| Spectral estimate of short input records | Reduced resolution | Method designed for short record analysis | extremely acceptable |
| Computational time, N sample input | Several N sample windows required | Single sample group | Single sample group, dependent on number of iterations |

III. Analysis of Known Processes

The purpose of this section is to provide graphic illustrations of the spectral analysis techniques developed in the previous section. Known time sampled data is applied to the estimation equations to determine the spectral content. The Bartlett smoothed periodogram technique provides true spectral density data for verification of the estimates developed by the MEM and Papoulis techniques. Calculation of the variance of the estimated spectrum provides additional information about accuracy. Three specific examples are evaluated to develop confidence in the MEM and Papoulis techniques.

The techniques developed in Section II are applied in several subroutines. These routines have been coded using Fortran IV and are provided in Appendix B. Figure 1 shows a simplified flow diagram of an analysis routine to determine the spectral density and statistics of an input process. The sequence is assumed to be very large (greater than 30,000 points), to facilitate accurate determination of the Bartlett periodogram, the sample mean, and the estimated variance of the MEM and Papoulis techniques. These values are calculated from 64 independent realizations each with 128 samples.

Figure 2 illustrates the algorithm used to determine the estimated spectral density using MEM and Papoulis techniques. This routine assumes that the input sequence is short as

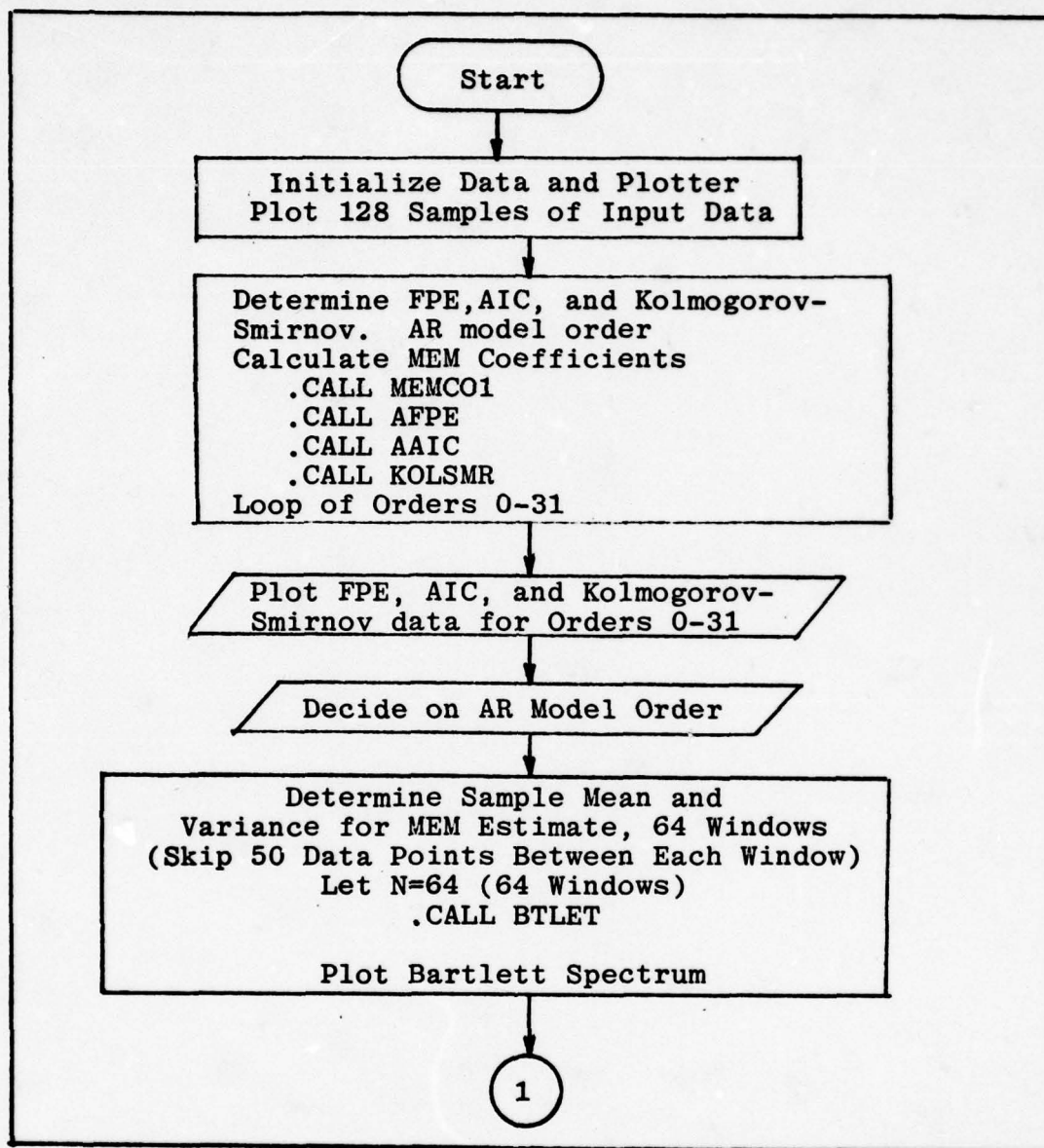


Figure 1. Flow Diagram to Determine AR Model Order, Bartlett Spectrum, Sample Mean, and Variance of MEM and Papoulis Estimation

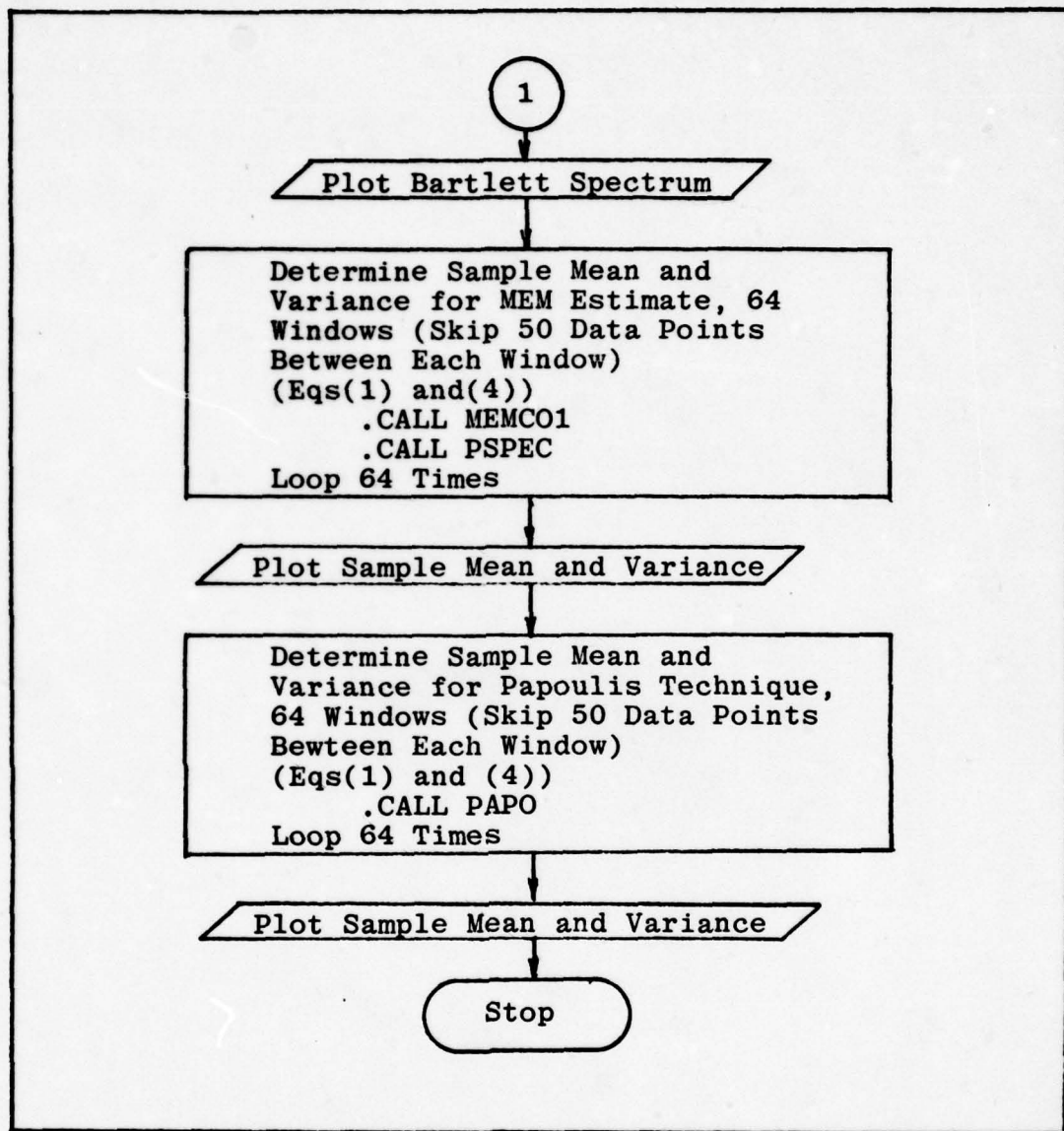


Figure 1. (Continued)

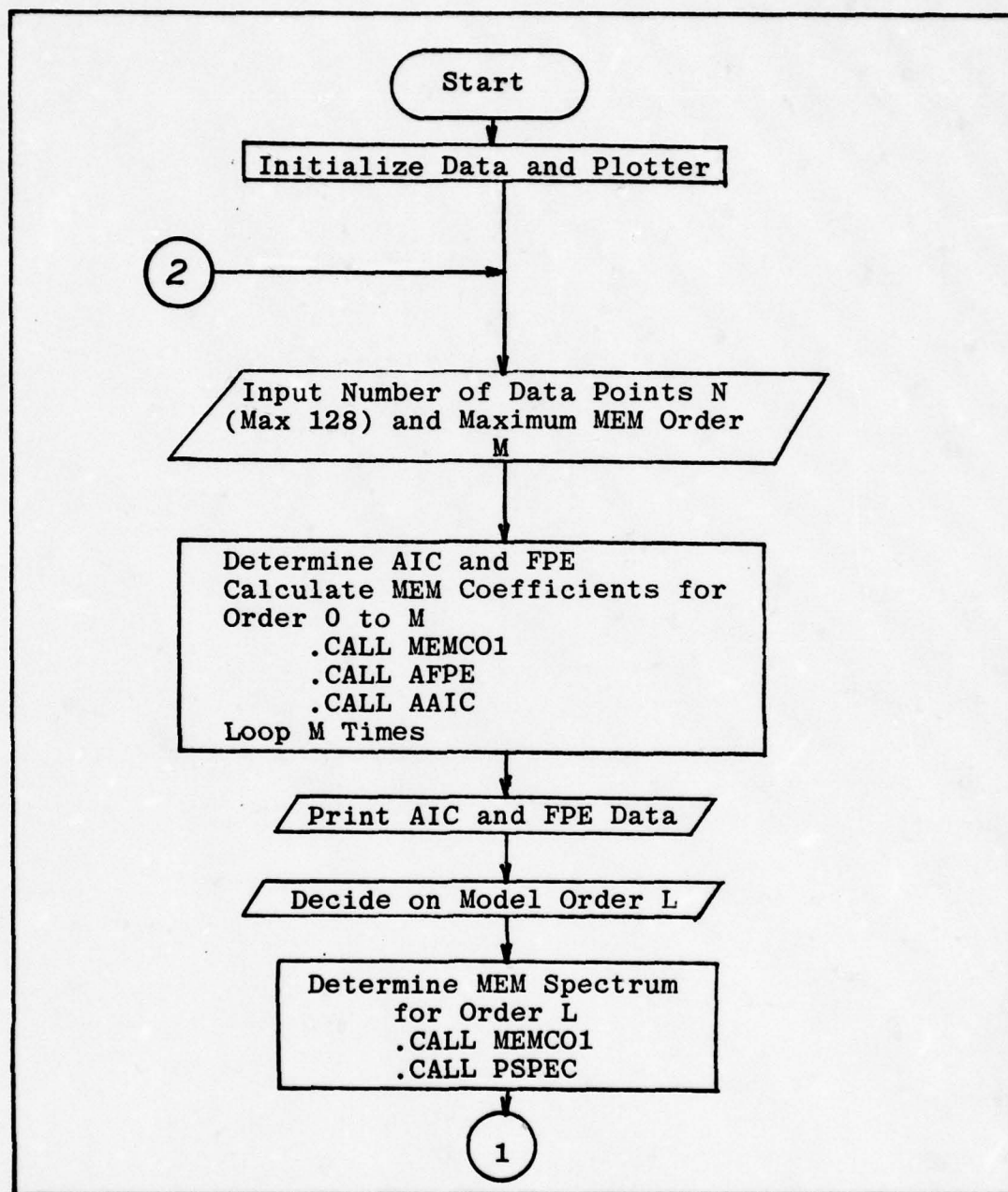


Figure 2. Interactive Routine to Calculate Estimated Spectrum for MEM and Papoulis Techniques.

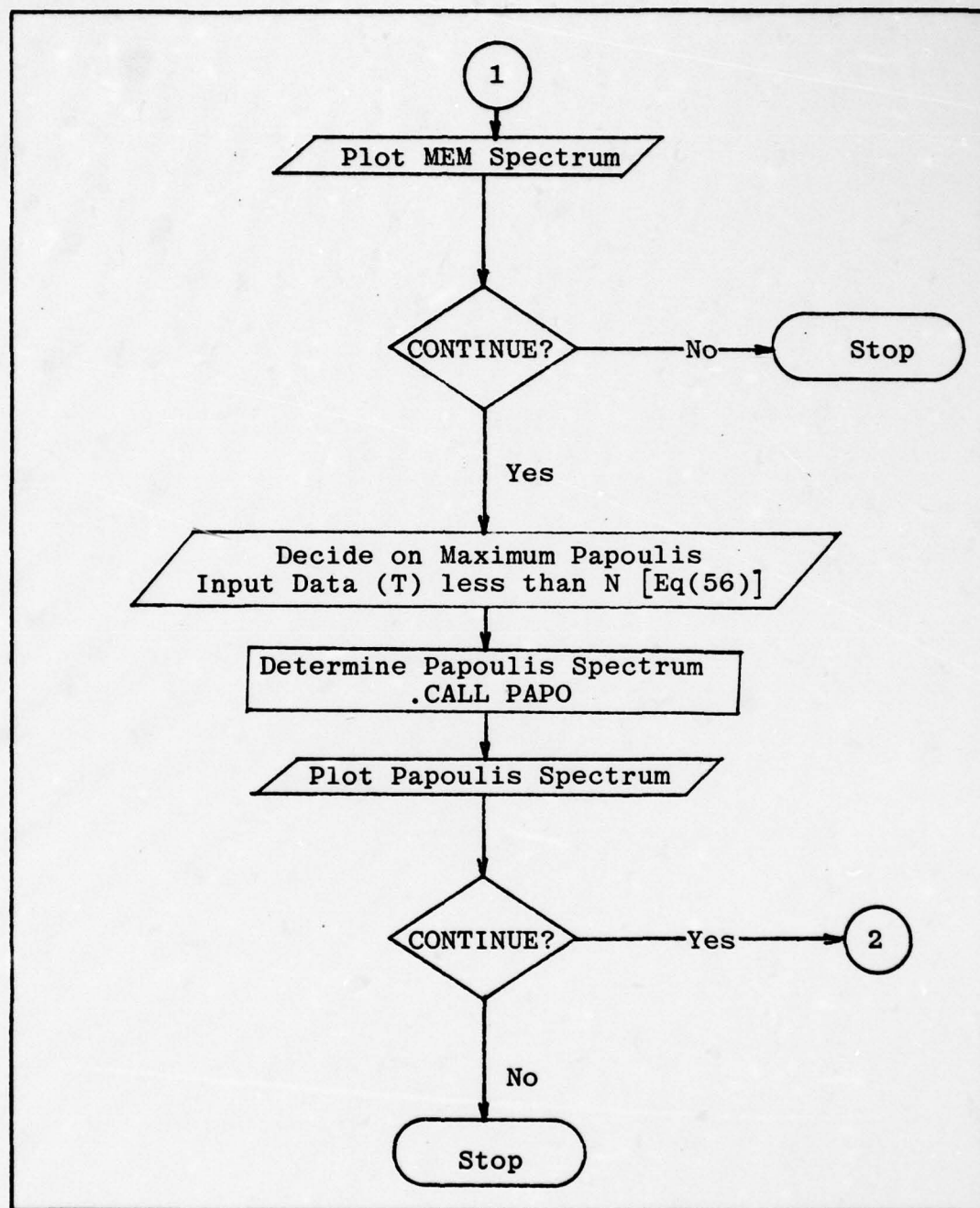


Figure 2. (Continued)

defined in Section I.

The three signals evaluated in this section are a simple 2nd order AR process, and autoregressive-moving average process, and a sum of two cosines plus Gaussian noise.

Example One: Second Order AR Process

Example one is a simple AR input sequence

$$x(n) = 0.75x(n-1) - 0.5x(n-2) + \eta(n) \quad (64)$$

where $\eta(n)$ is a Gaussian distributed sequence with zero mean and variance equal to one. This sequence should have a spectral density that resembles a second order low pass system.

A 128 point sample of the input sequence is provided in Figure 3. The expected results are verified by the results of the Bartlett estimate, Figure 4. Data from the MEM model order calculations are provided in Figures 5, 6, and 7. As expected, AIC and FPE model estimation techniques indicate a minimum at order equal to two. Additionally, the Kolmogorov-Smirnov analysis indicates a maximum at model order equal to two. These three model order determining techniques clearly suggest that the MEM technique with AR order equal to two is the most correct model. Figures 8 through 11 show the estimated mean and variance of the MEM and Papoulis techniques. Notice how closely the estimated mean from the MEM technique approximates the expected results from the Bartlett technique

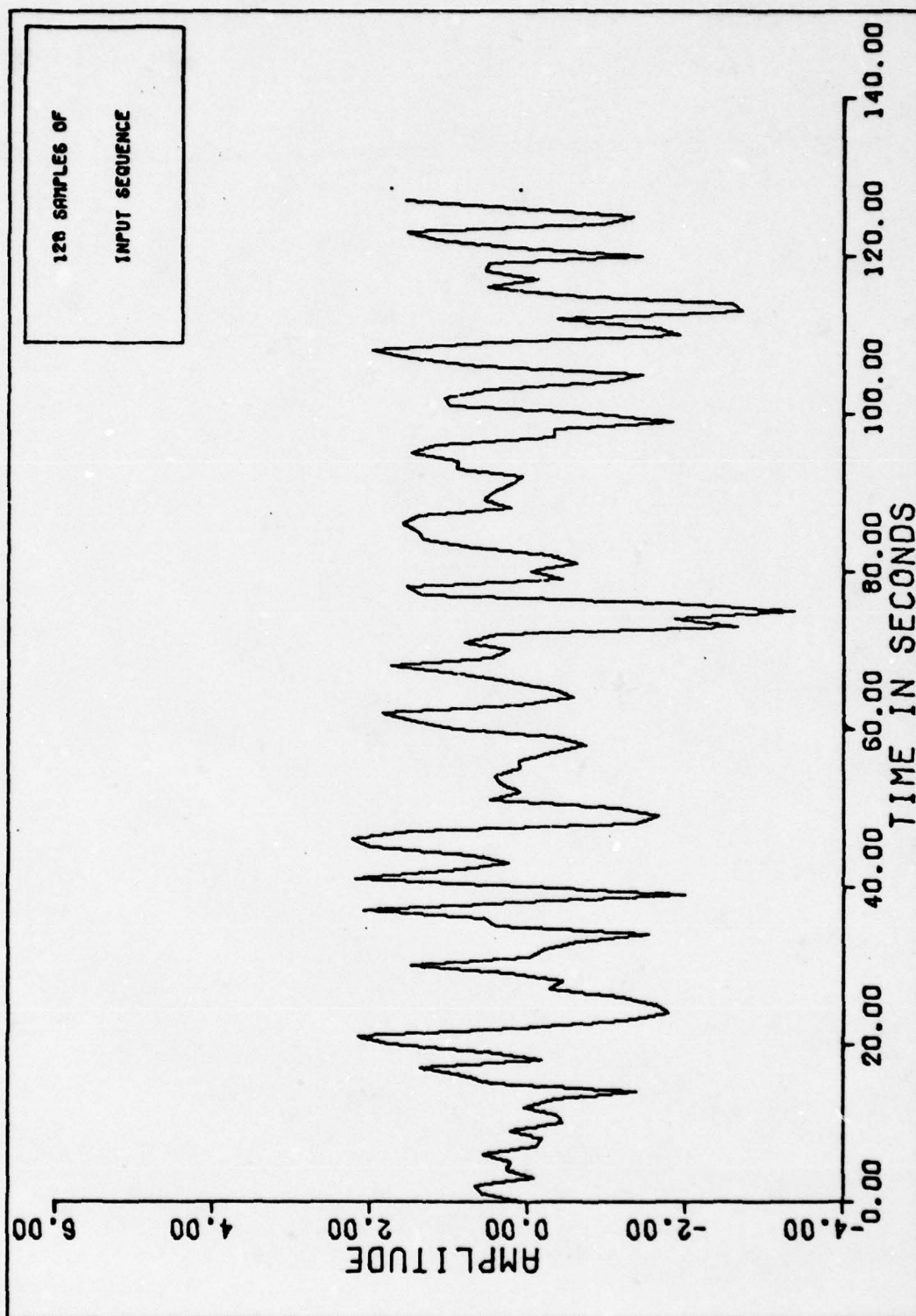


Figure 3. 128 Samples of a Second Order AR Sequence

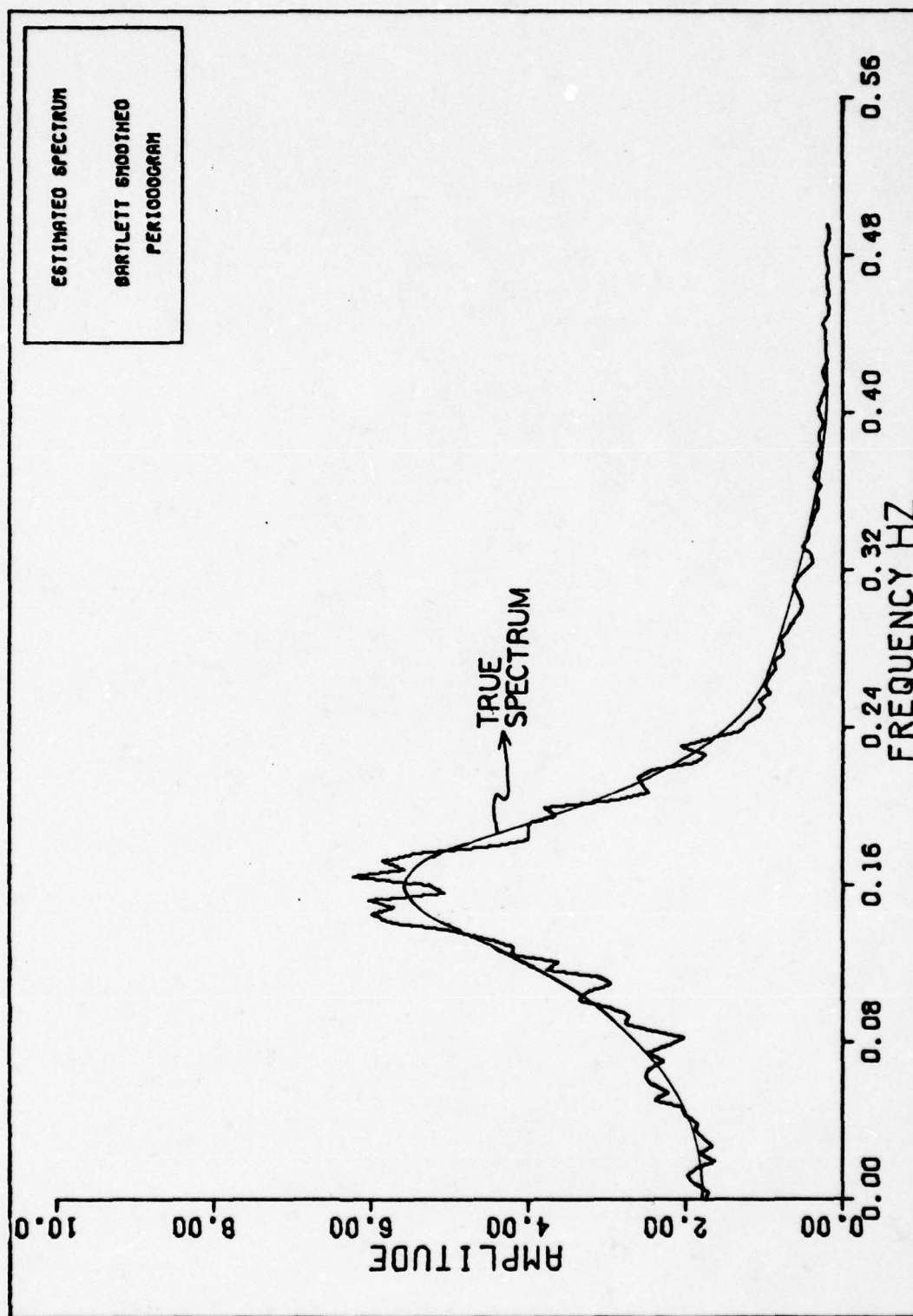


Figure 4. Bartlett Smoothed Periodogram Spectral Estimate of Second Order AR Model

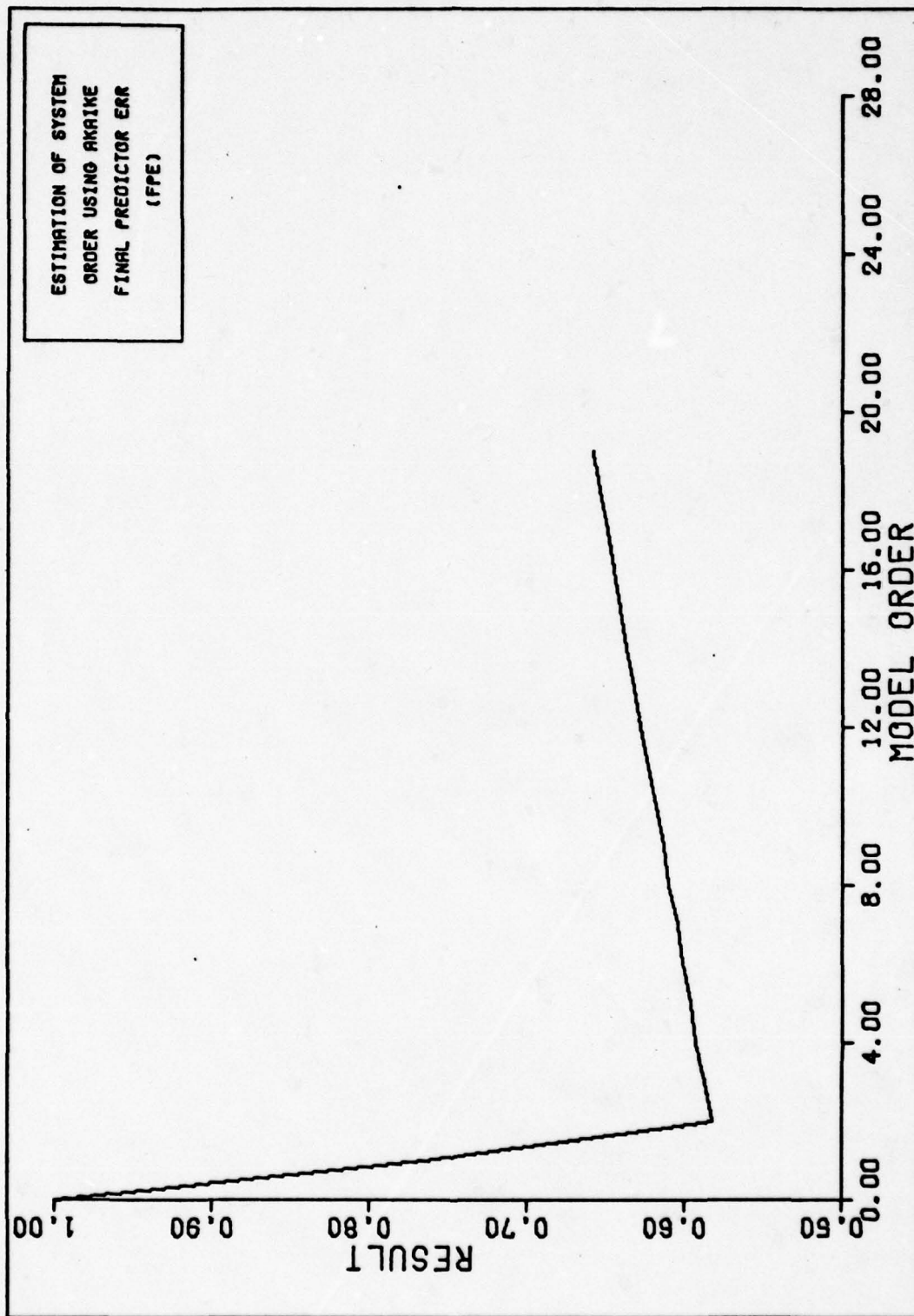


Figure 5. Amplitude of FPE as a Function of Model Order for Second Order AR Model

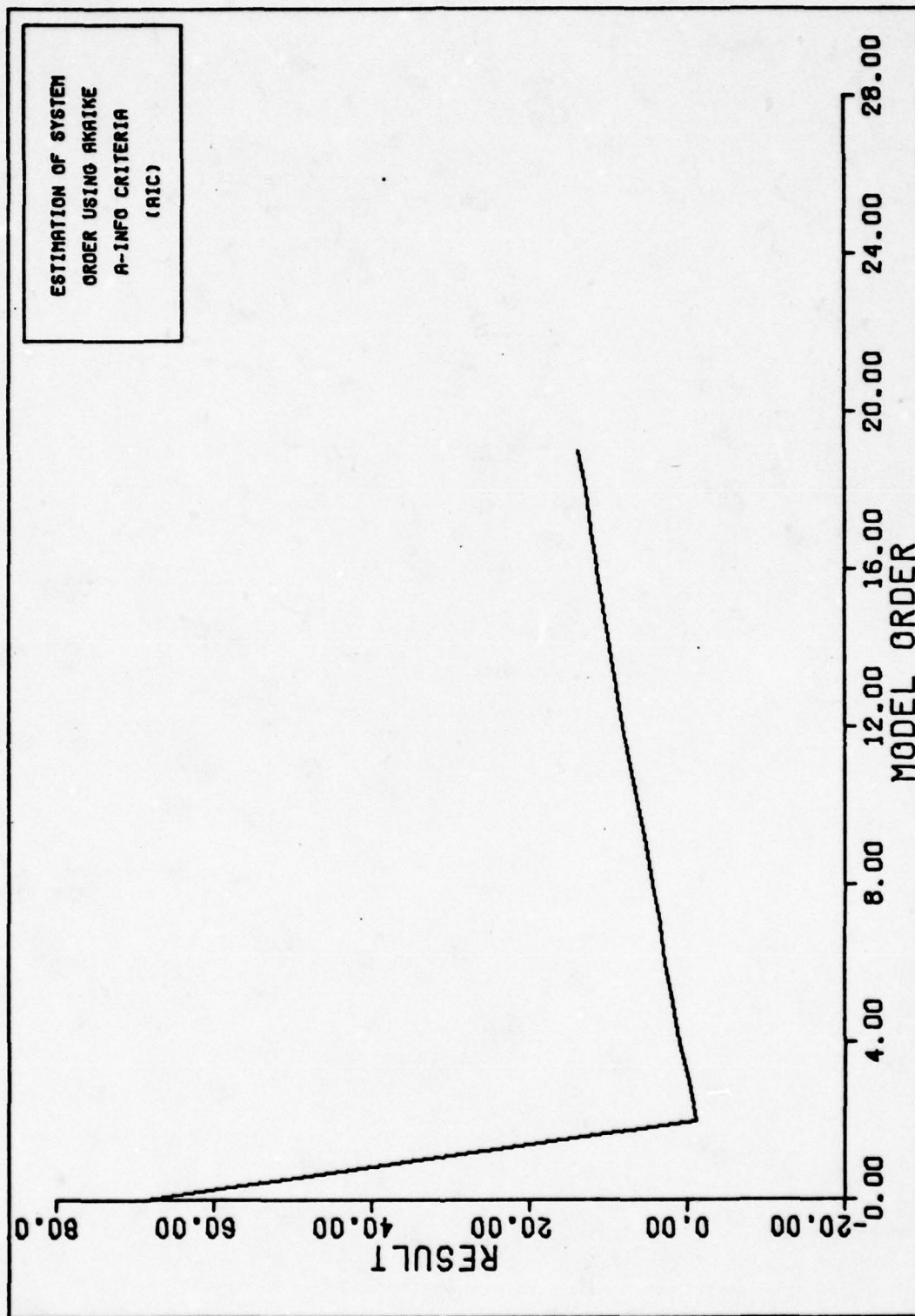


Figure 6. Amplitude of AIC as a Function of Model Order for Second Order AR Model

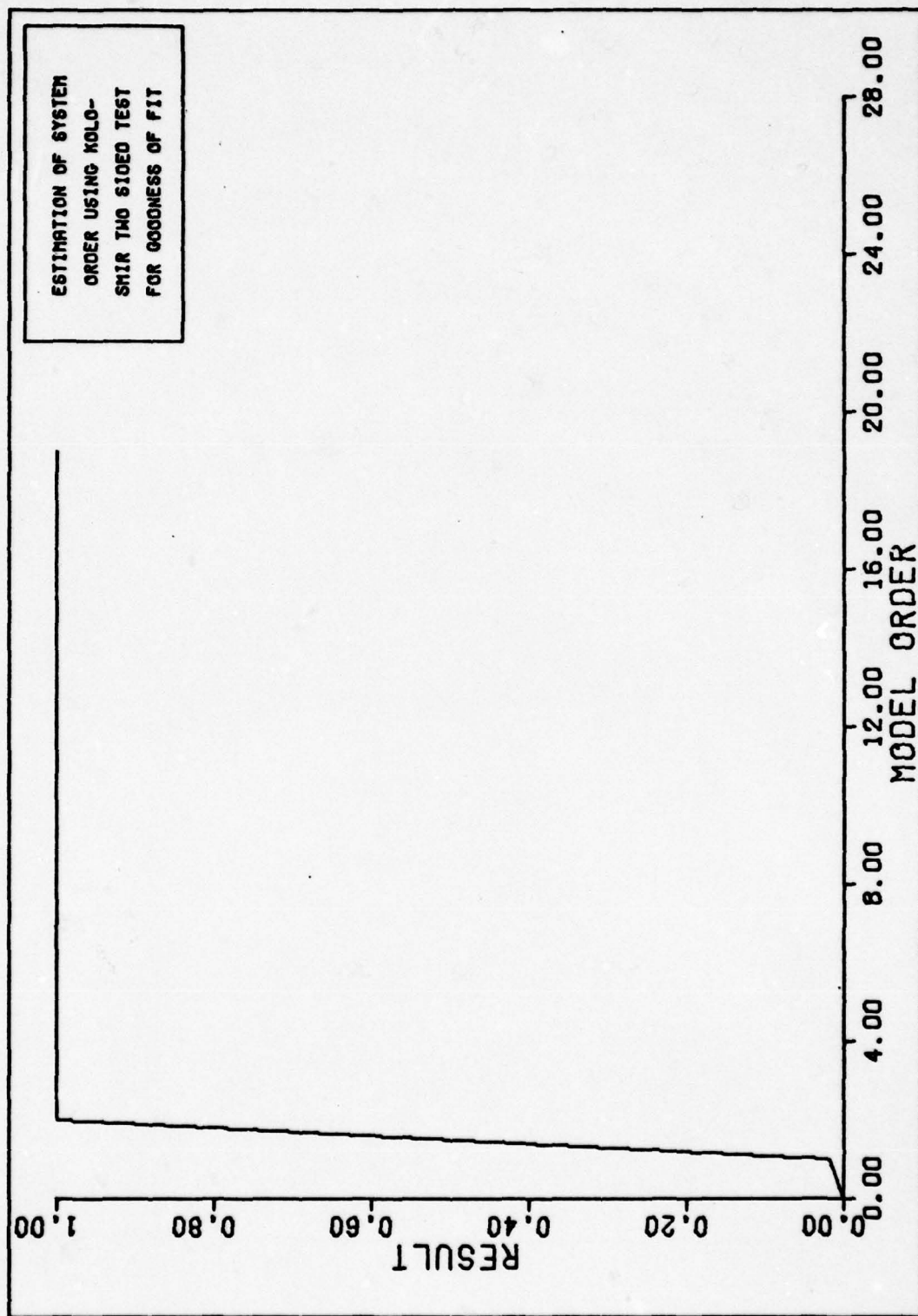


Figure 7. Probability of Kolmogorov-Smirnov Two Sided Test as a Function of Model Order for Second Order AR Model

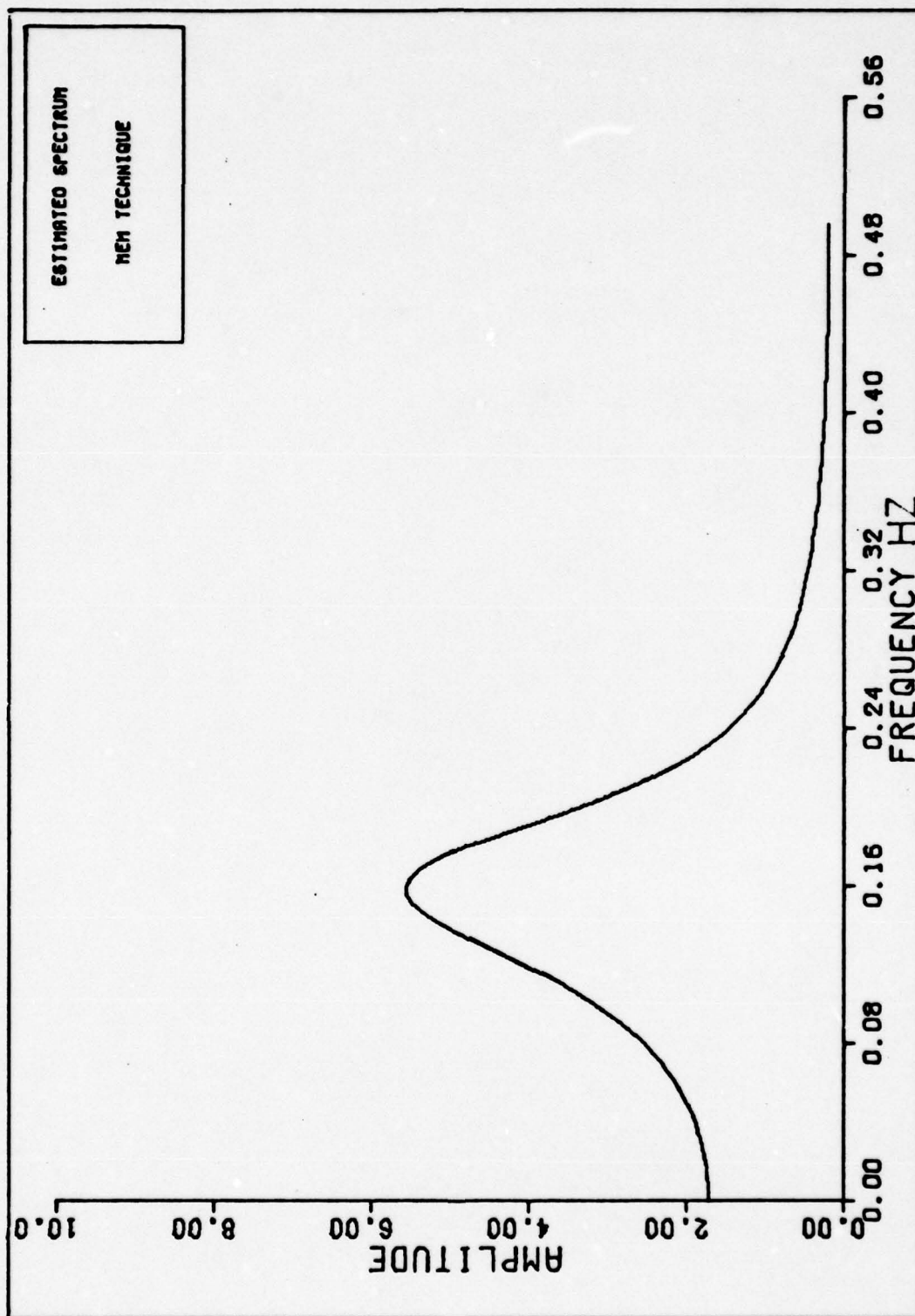


Figure 8. Estimated Mean of Estimated Spectrum Using the MEM Technique, Second Order AR Model

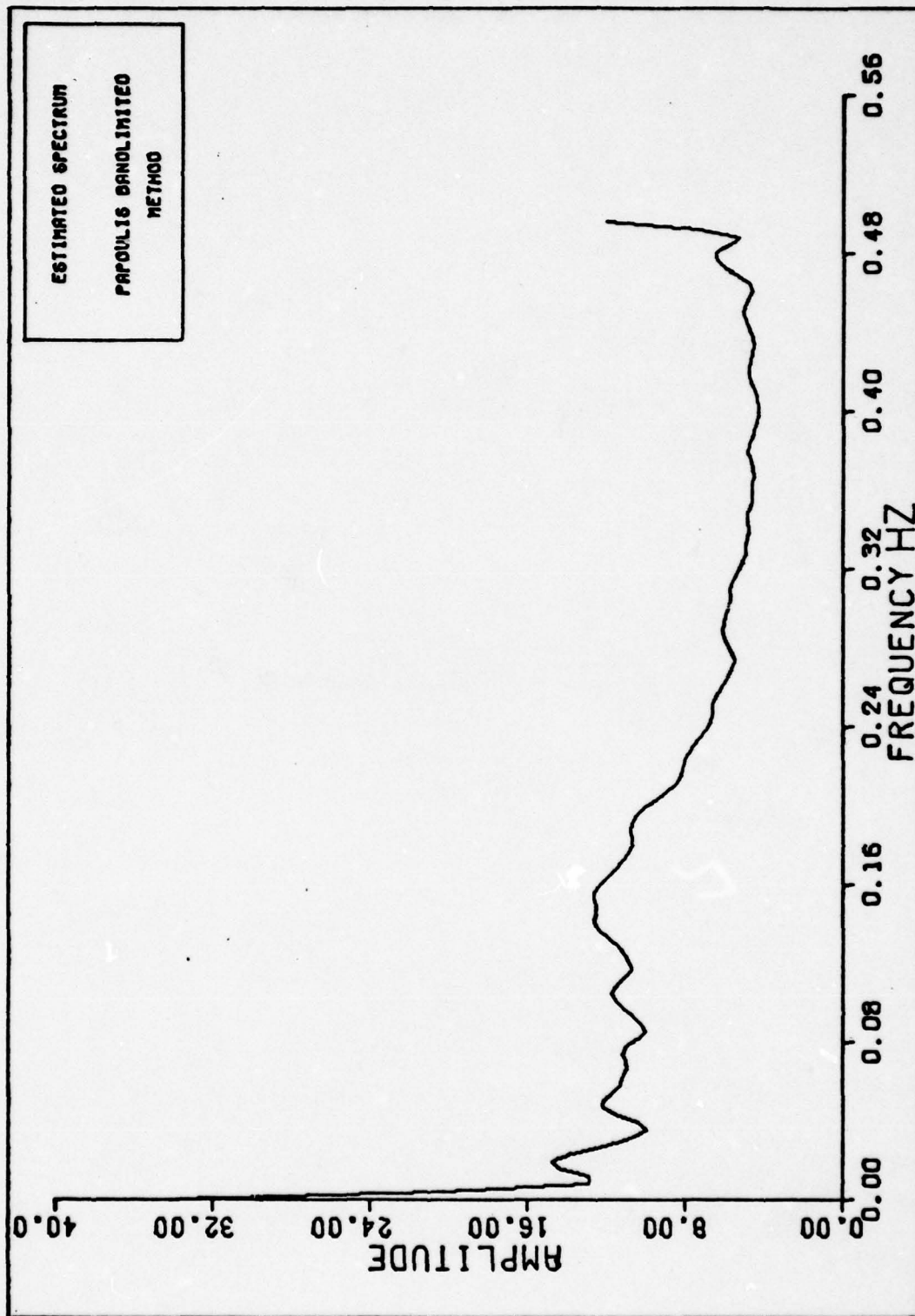


Figure 9. Estimated Mean of Estimated Spectrum Using the Papoulis Technique, Second Order AR Model

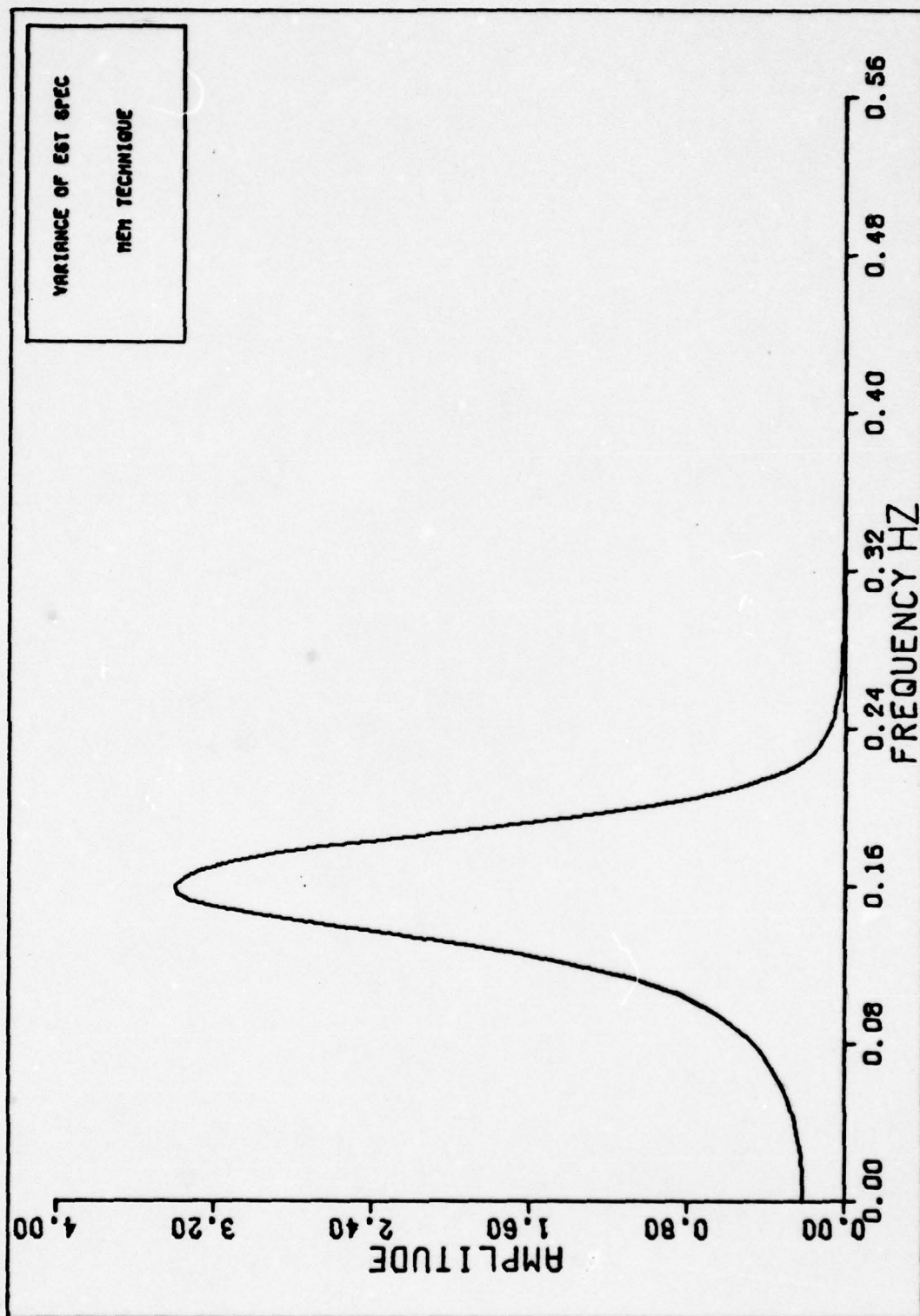


Figure 10. Estimated Variance of Estimated Spectrum Using the MEM Technique, Second Order AR Model

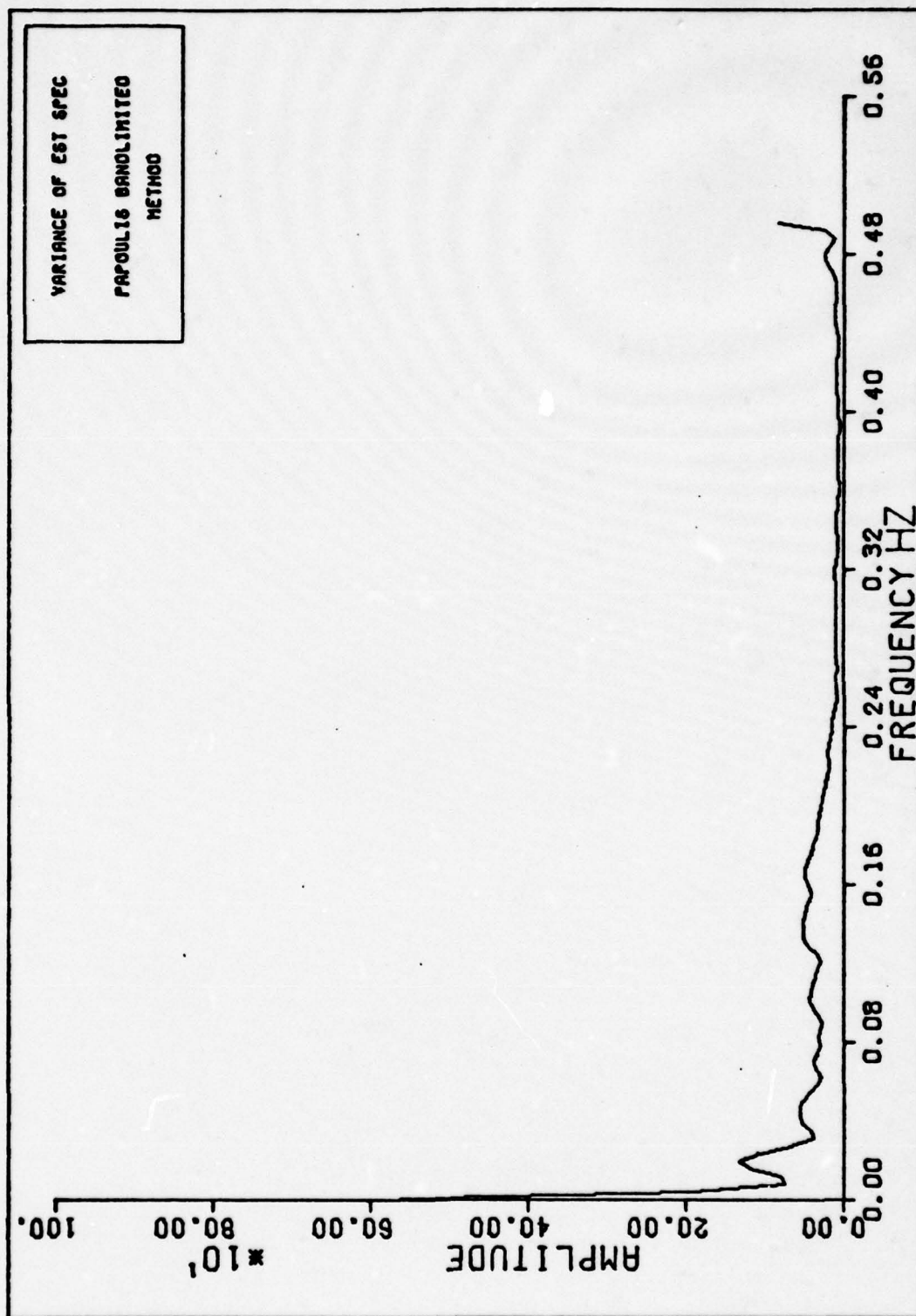


Figure 11. Estimated Variance of Estimated Spectrum Using the Papoulis Technique, Second Order AR Model

(approximately the true spectrum). With only 64 realizations, the mean from the MEM technique appears to be reasonably accurate with a variance depending on the amplitude of the true spectrum. For this particular problem, the estimation errors are relatively small.

The Papoulis technique fails to provide satisfactory results, with a variance much greater than that of the MEM technique. This problem is attributed to the limitation of the number of allowed iterations in the Papoulis estimation routine. It is assumed that the Papoulis technique will do a more creditable estimation of the spectrum if the routine is allowed to iterate beyond 100. This conclusion is suggested by Eq(63) and Papoulis' proof of convergence. However, since the input in this problem is not deterministic, the error will not go to zero as the number of iterations is increased, but will converge to some constant value related to the variance of the noise process $\eta(n)$.

Results from execution of the routine in Figure 2 are even more illustrative of the accuracy of the MEM technique. Figures 12 through 15 show the results of these techniques applied to two input sequences of 128 and 32 samples. The MEM technique is clearly superior for this particular second order AR sequence. Results of this application indicate that the MEM technique estimates the spectral density with a high degree of reliability. This can be observed when the MEM analysis results, Figures 12 and 14, are compared to the true spectrum (by Bartlett technique) Figure 4.

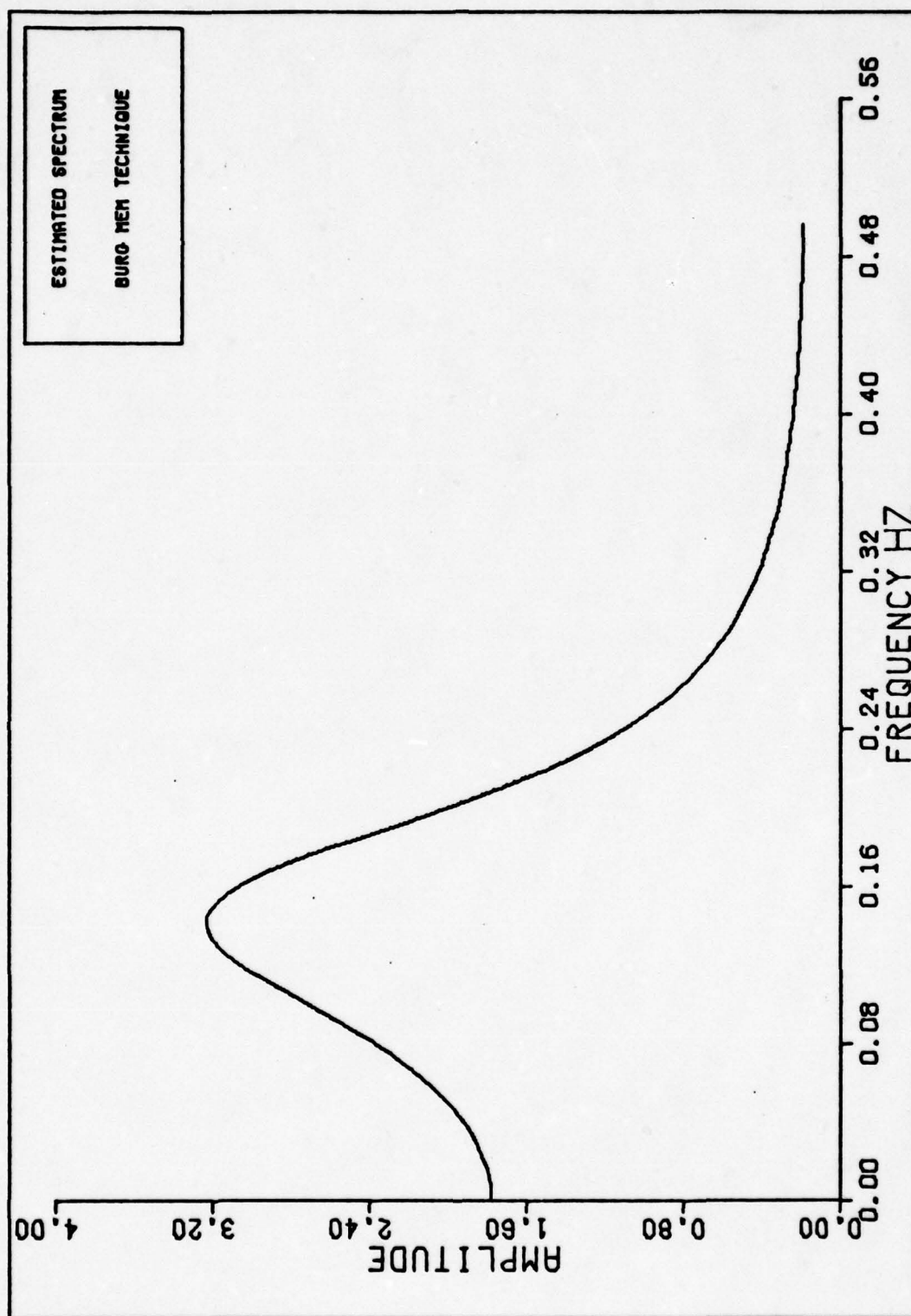


Figure 12. Estimated Spectrum From 128 Samples of Second Order
AR Process Using MEM with Order Equal to Two

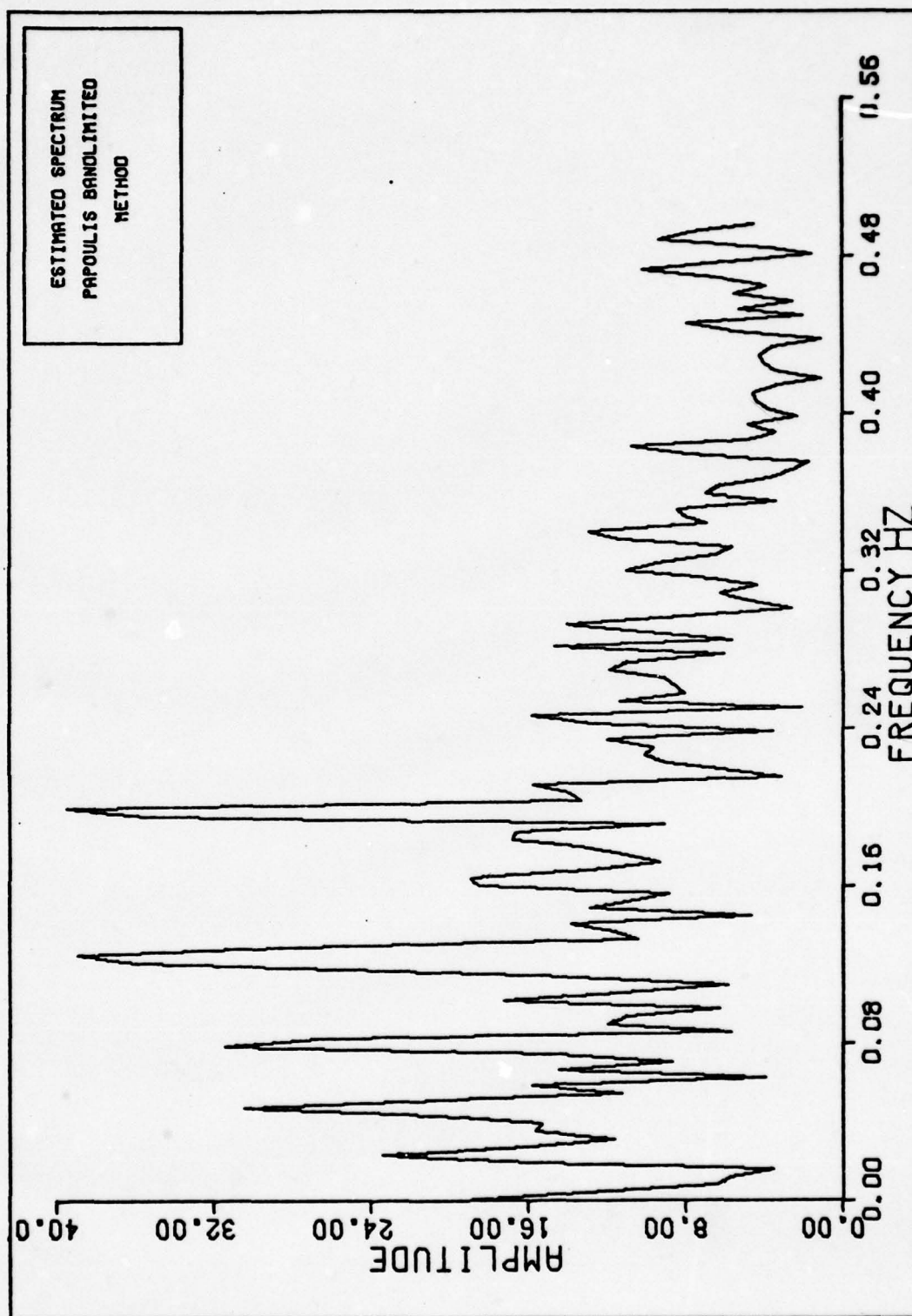


Figure 13. Estimated Spectrum from 128 Samples of Second Order AR Process Using Papoulis Technique

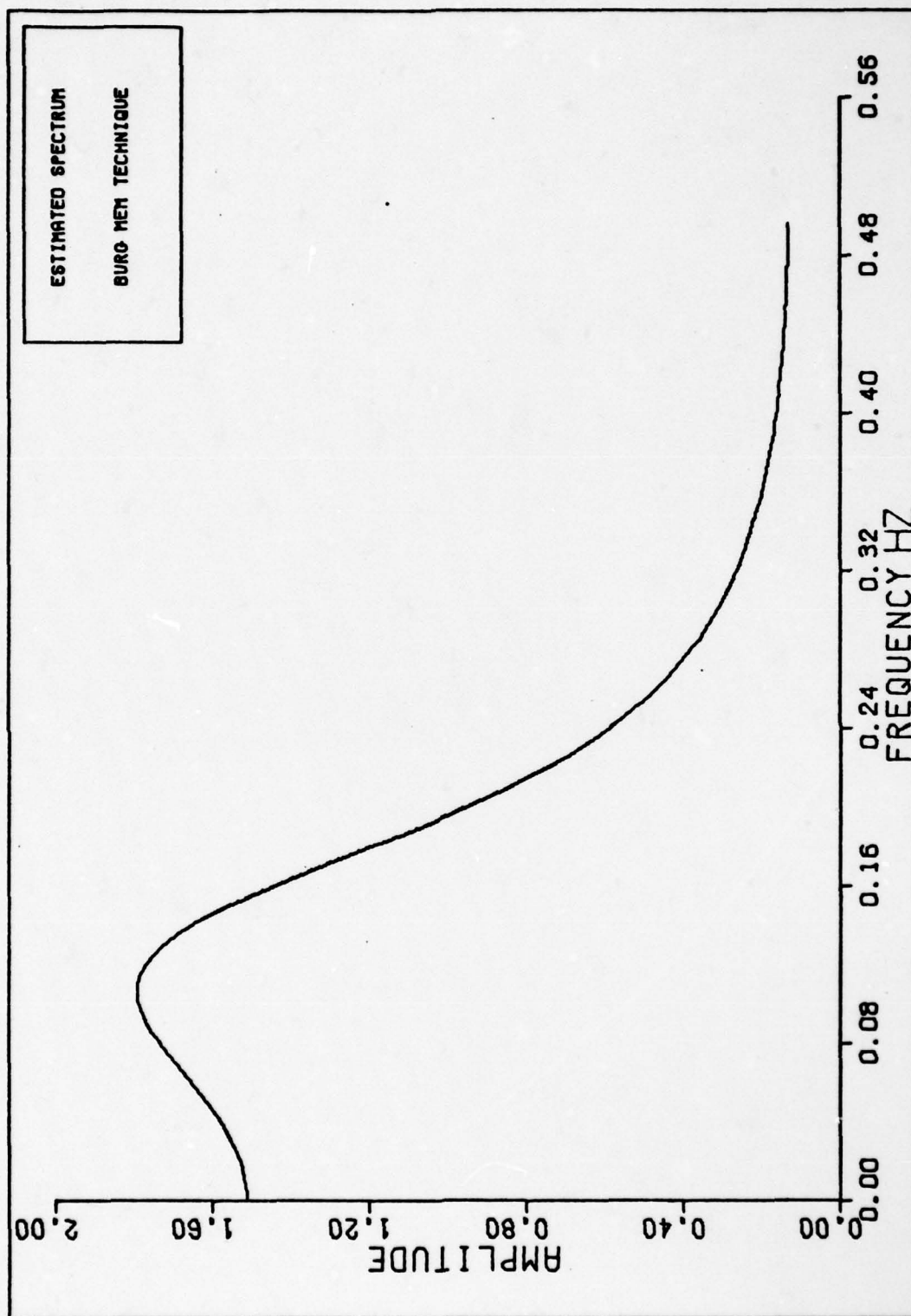


Figure 14. Estimated Spectrum from 32 Samples of Second Order
AR Process Using MEM with Order Equal to Two

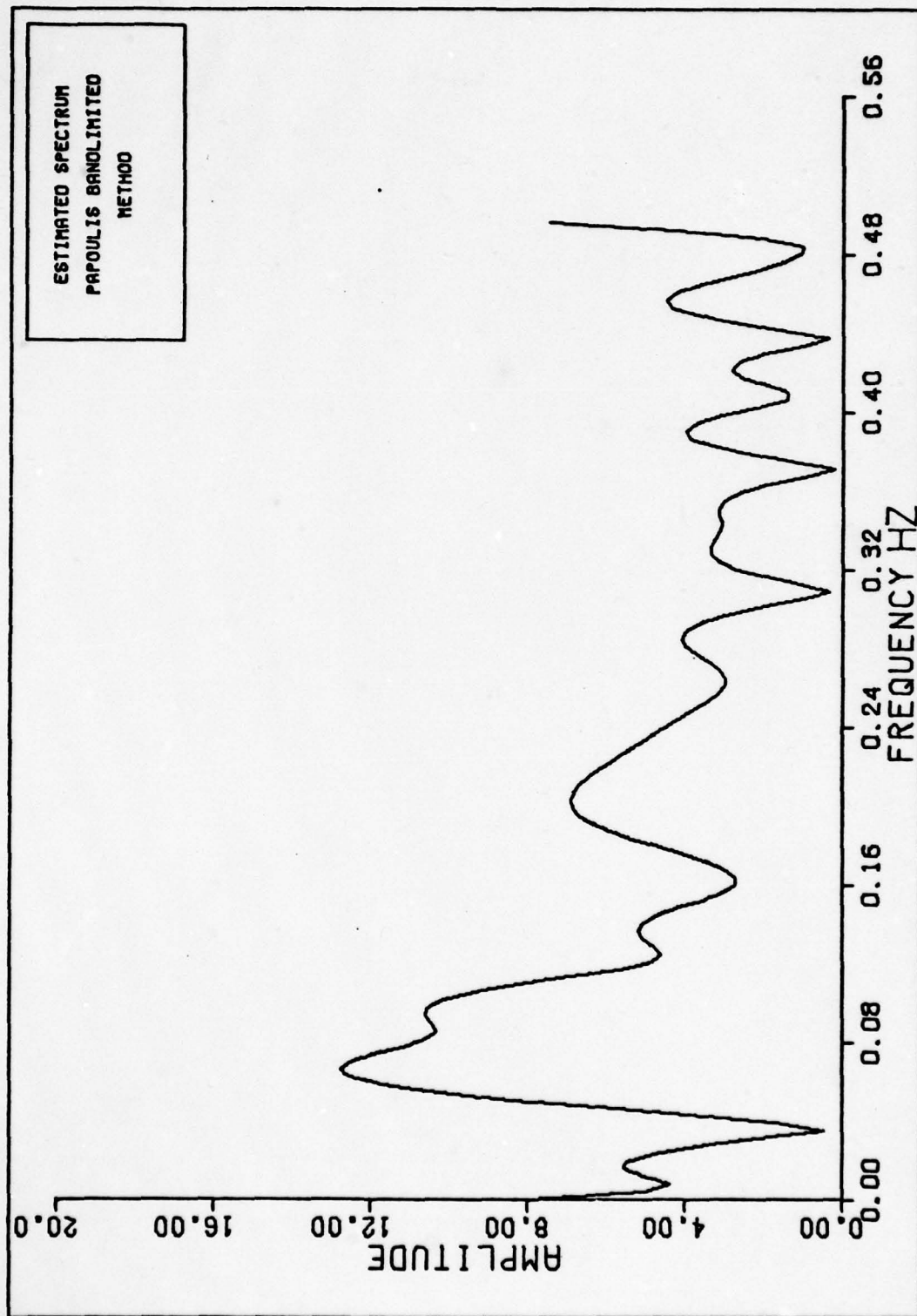


Figure 15. Estimated Spectrum from 32 Samples of Second Order AR Process Using Papoulis Technique

Example Two: ARMA Process

Example two is a departure from the previous example, in that the MEM technique must approximate the system spectral density [Auto-regressive-Moving Average (ARMA)] by an AR Model. This example provides a more rigorous test of the MEM technique. Something other than an AR model is modeled by the MEM technique. Illustrations of the primary results are provided in this section with supplemental data, i.e. AR model order, MEM and Papoulis mean, and MEM and Papoulis variance estimates, provided in Appendix C.

The ARMA sequence is generated by

$$\begin{aligned} x(n) = & 0.5x(n-1) - 0.25x(n-2) + 0.125x(n-3) + \\ & \eta(n) - 1.1\eta(n-1) + 0.24\eta(n-2) \end{aligned} \quad (65)$$

where $\eta(n)$ is defined as in example one. This particular model is the result of a system with three poles and two zeros. It is expected that the spectral data will exhibit the results of cancellation of poles by zeros at some frequency. A plot of 128 samples of the ARMA process is shown in Figure 16. The signal appears to be purely random. Application of the Bartlett smoothed periodogram indicates the expected spectral estimation results (Figure 17).

Application of the MEM model order estimation techniques indicate an AR model order of five (Appendix C). The MEM technique shows a very close relationship between the Bartlett

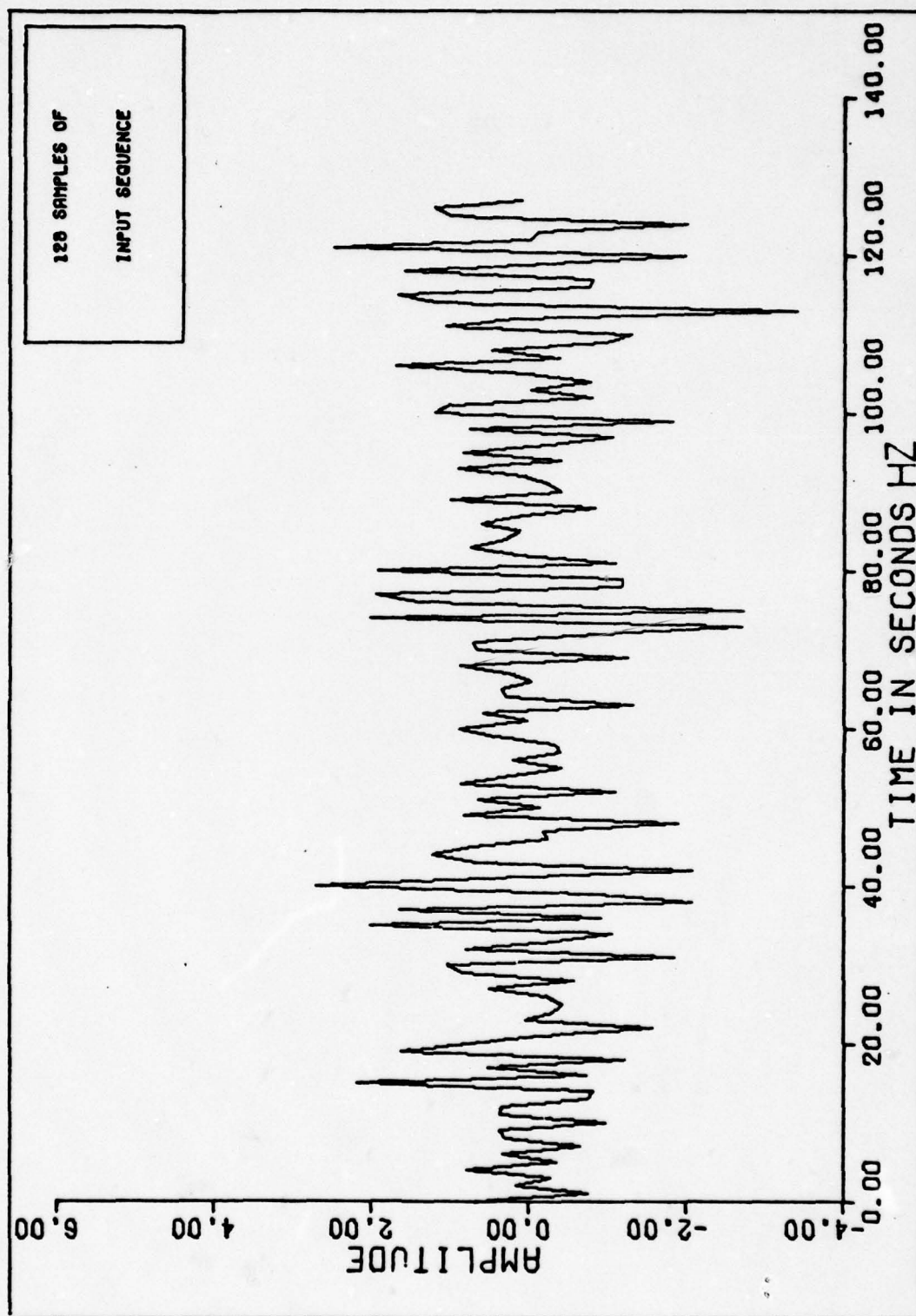


Figure 16. 128 Samples of an ARMA Sequence where the input is Gaussian Noise

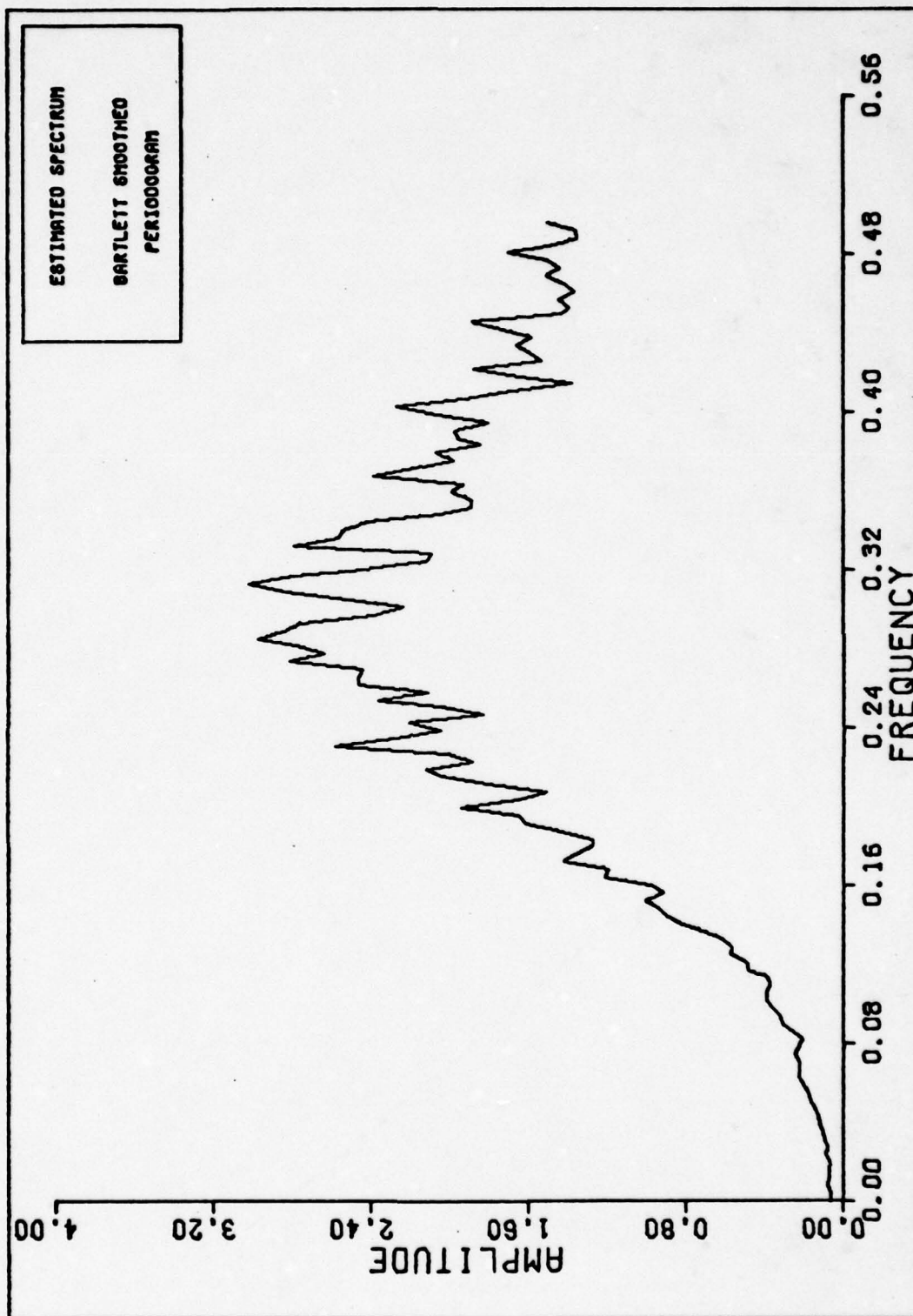


Figure 17. Bartlett Smoothed Periodogram Spectral Estimate of ARMA Input

estimation and the MEM estimated mean. Additionally, the MEM estimated variance is small when compared to the Papoulis technique counterpart. The problems previously encountered in the Papoulis technique continue to be evident in this example.

Figures 18 through 21 show results of application of a fifth order AR MEM model and the Papoulis technique on 128 and 32 samples of the ARMA process. The MEM technique clearly estimates the spectral density with more accuracy than the Papoulis technique. The limitation of 100 iterations restricts accurate estimation by the Papoulis routine.

Example Three: Sum of Sinusoids

Many spectral estimation application problems are a sequence resulting from some form of a sinusoidal process. One case may be a sequence consisting of radar returns. This example exercises the spectral estimation equations to analyze a sinusoidal time sequence, a process that is the result of a sum of two cosines in the presence of a Gaussian noise.

This example is set up to provide an indication of how well the estimation techniques are able to resolve two cosines with different amplitudes and frequencies that are close to each other. The input sequence is generated by

$$x(n) = 3\cos(0.11n) + 2.5\cos(0.14n) + \eta(n) \quad (65)$$

where $\eta(n)$ is Gaussian distributed, zero mean and variance equal to one.

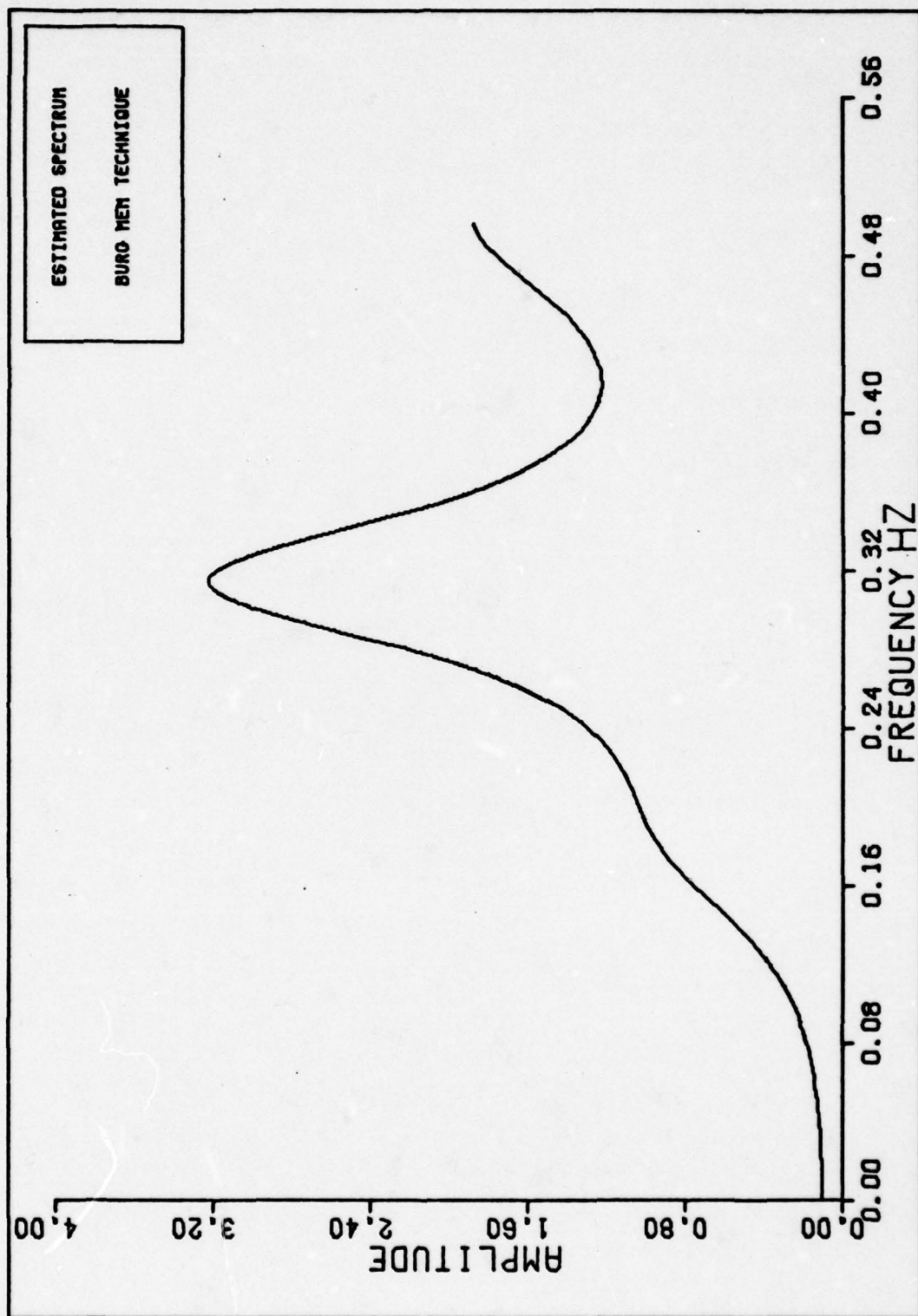


Figure 18. Estimated Spectrum from 128 Samples of ARMA Process
Using MEM with AR Model Order Equal to Five

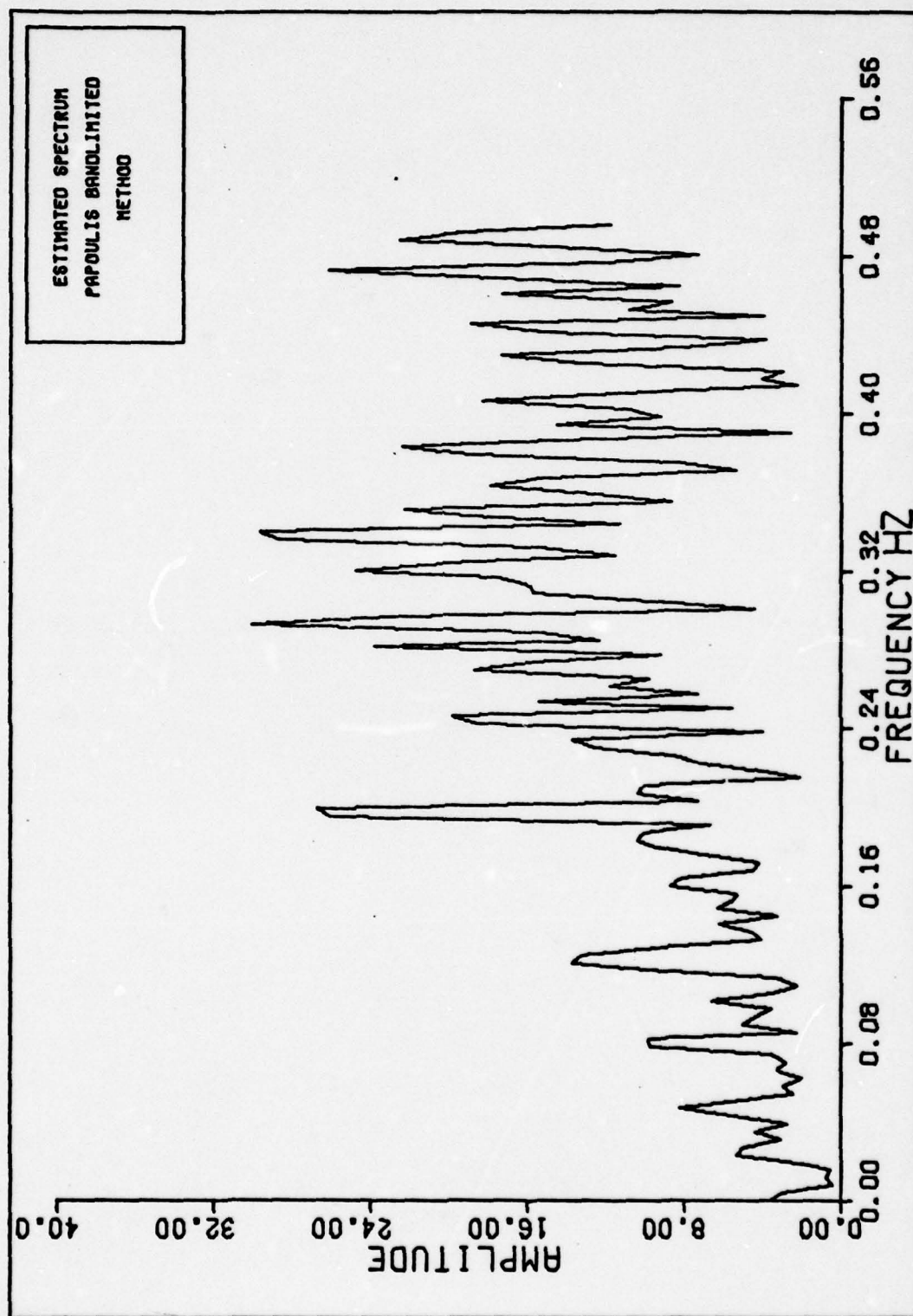


Figure 19. Estimated Spectrum from 128 Samples of ARMA Process
Using Papoulis Techniques

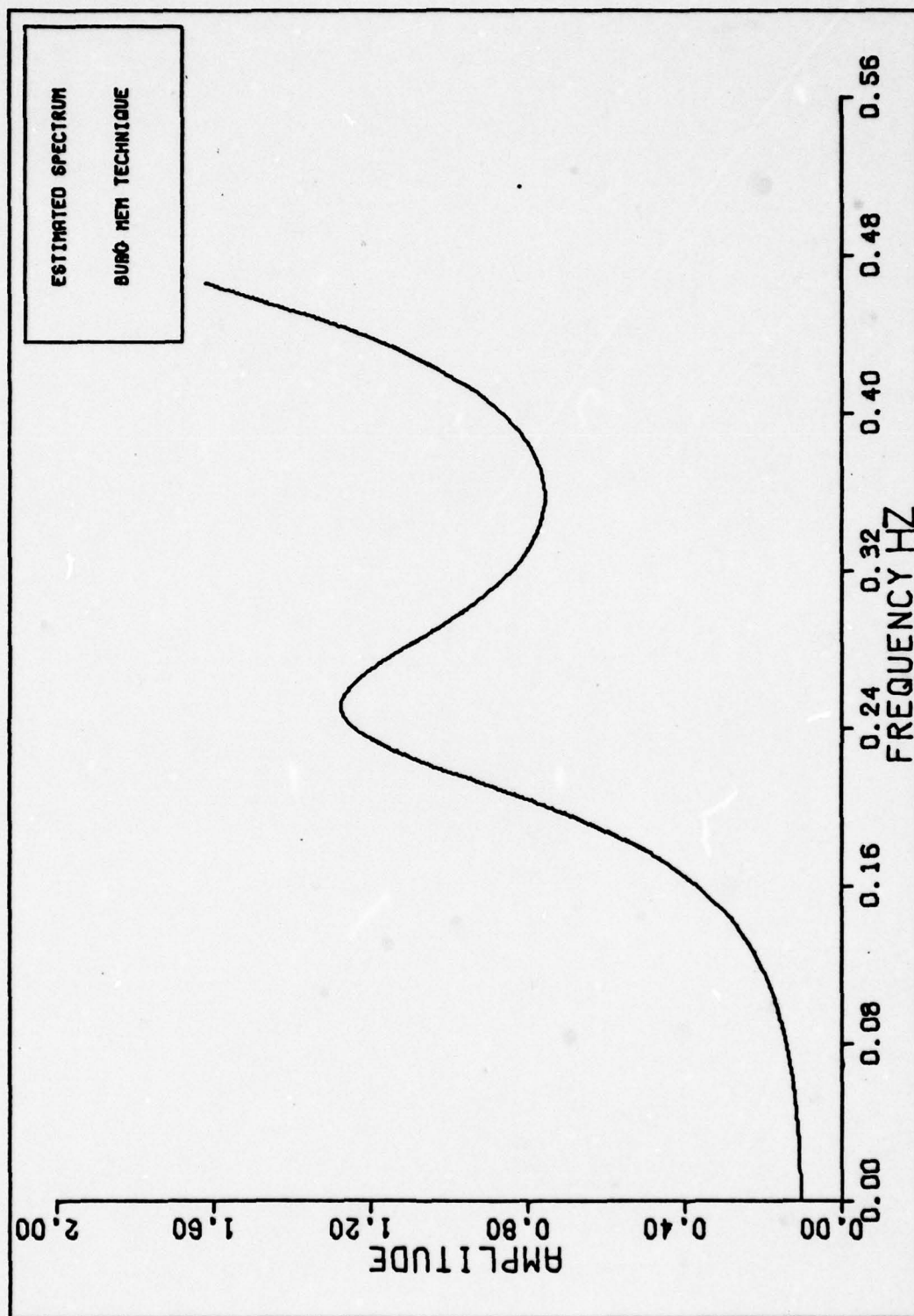


Figure 20. Estimated Spectrum from 32 Samples of ARMA Process
Using MEM with AR Model Order Equal to Five

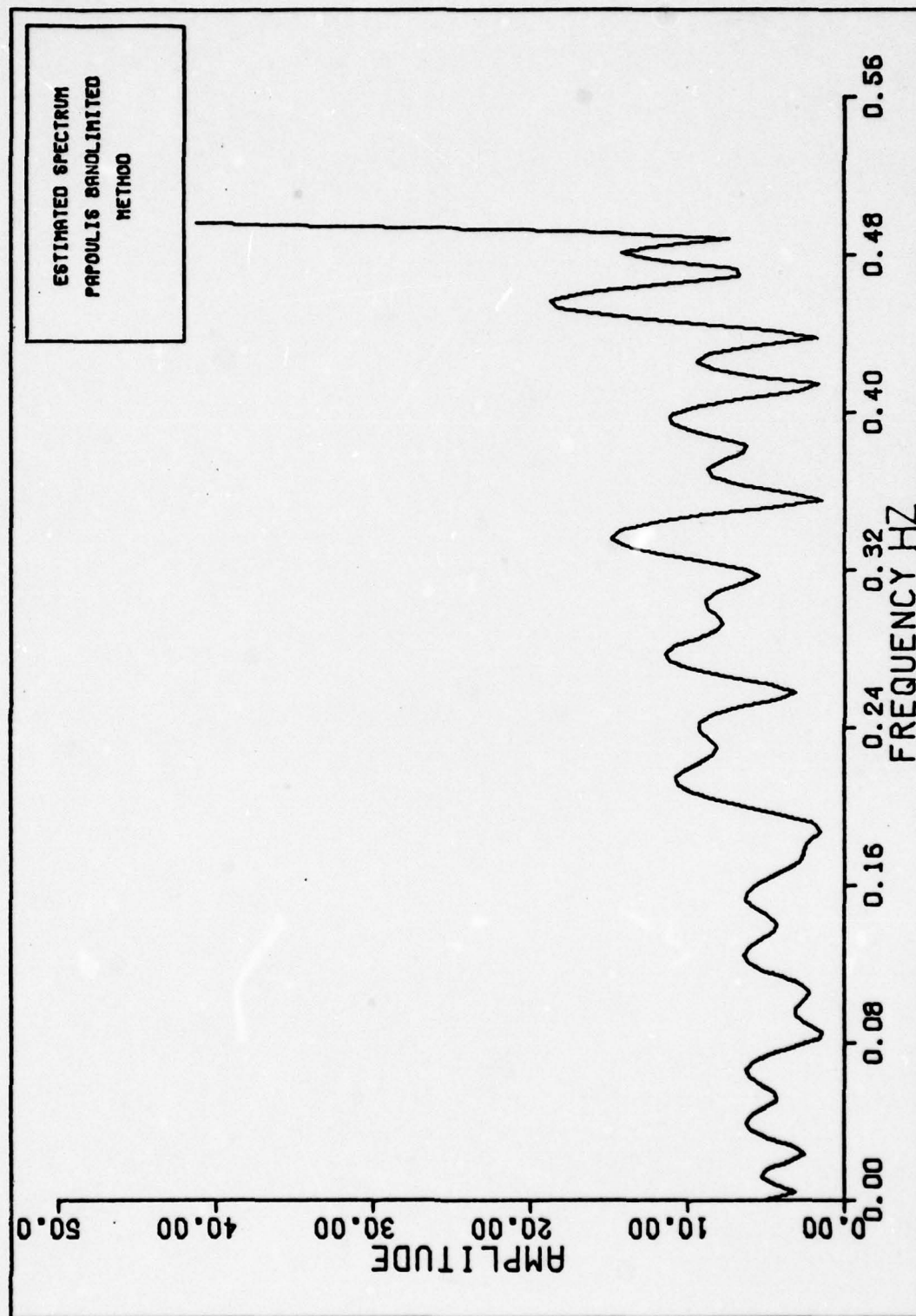


Figure 21. Estimated Spectrum from 32 Samples of ARMA Process
Using Papoulis Techniques

A plot of 128 samples of the input sequence is provided in Figure 22. The expected spectral density should have two narrow spikes at 0.11 and 0.14 Hertz riding on a low level of noise. The spike at 0.11 Hertz should have a higher amplitude than the 0.14 Hertz spike. These expected results are verified by the estimated spectral plot from the Bartlett smoothed periodogram, shown in Figure 23. It appears that the periodogram closely matches the spectral density.

Estimation of the AR model order indicates that the best (minimum FPE and AIC) order is 23 (Appendix C). Also, reasonable values for the estimated mean and variance indicate that the MEM technique appropriately models the input sequence (Appendix C).

The Papoulis analysis indicates that this technique provides increased accuracy over applications in the previous examples. Estimated mean and variance data suggest that the Papoulis spectral estimation technique produces reliable estimates (Appendix C).

Results of spectral estimation of two independent sequences, 128 and 32 samples, are shown in Figures 24 through 27. Both MEM, with AR model order 23, and Papoulis techniques accurately estimate the input spectral content. The 32 sample sequence, when applied to the FPE and AIC equations, suggest an AR model order of 17. For the 32 sample case, noticeable degradation in amplitude resolution of the MEM technique is observed. This degradation is attributed to the large

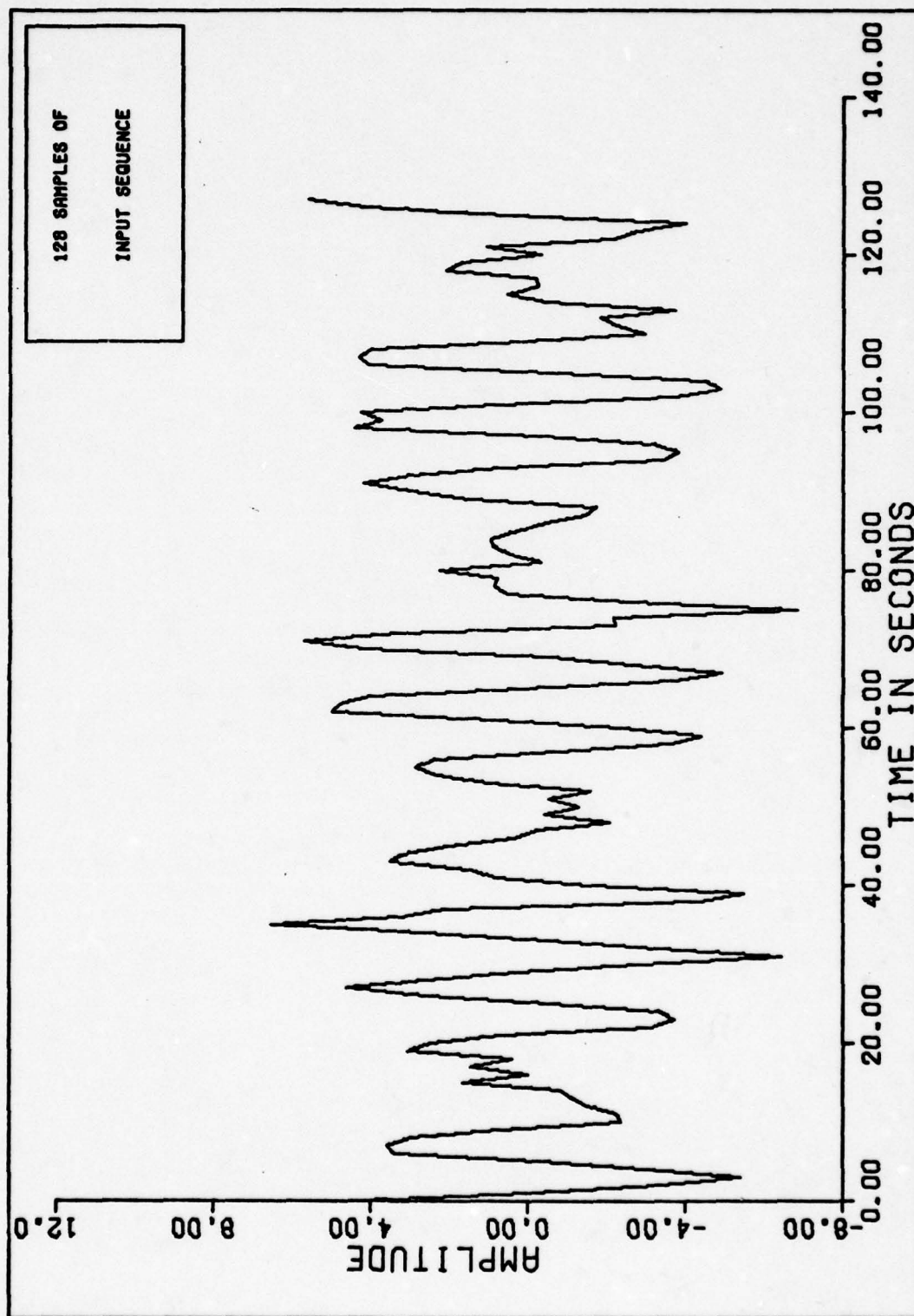


Figure 22. 128 Samples of Sum of Sinusoids Sequence Plus Gaussian Noise

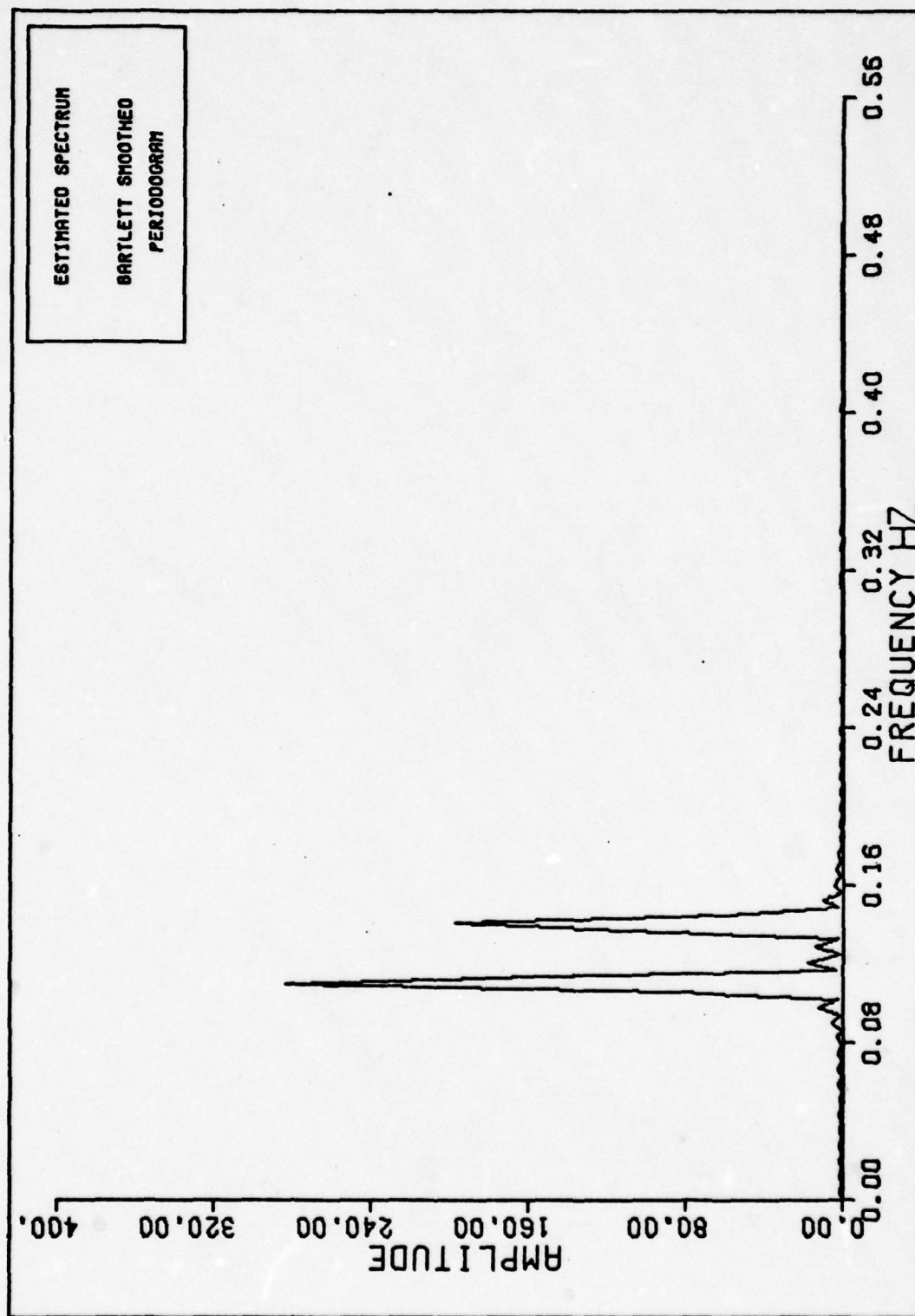


Figure 23. Bartlett Smoothed Periodogram Spectral Estimation of
Sum of Sinusoids

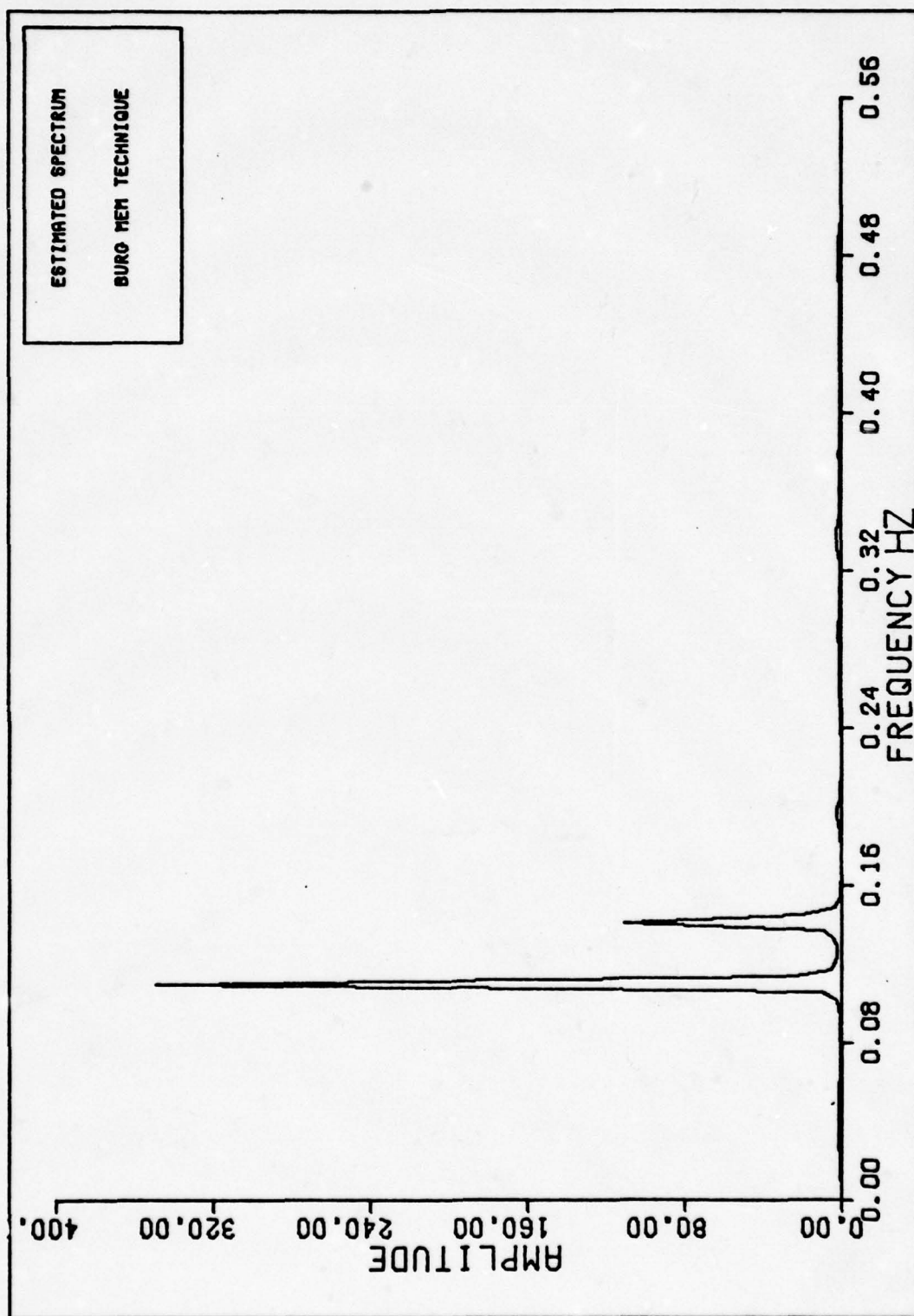


Figure 24. Estimated Spectrum from 128 Samples of Sum of Sinusoids Process
Using MEM with AR Model Order Equal to 23

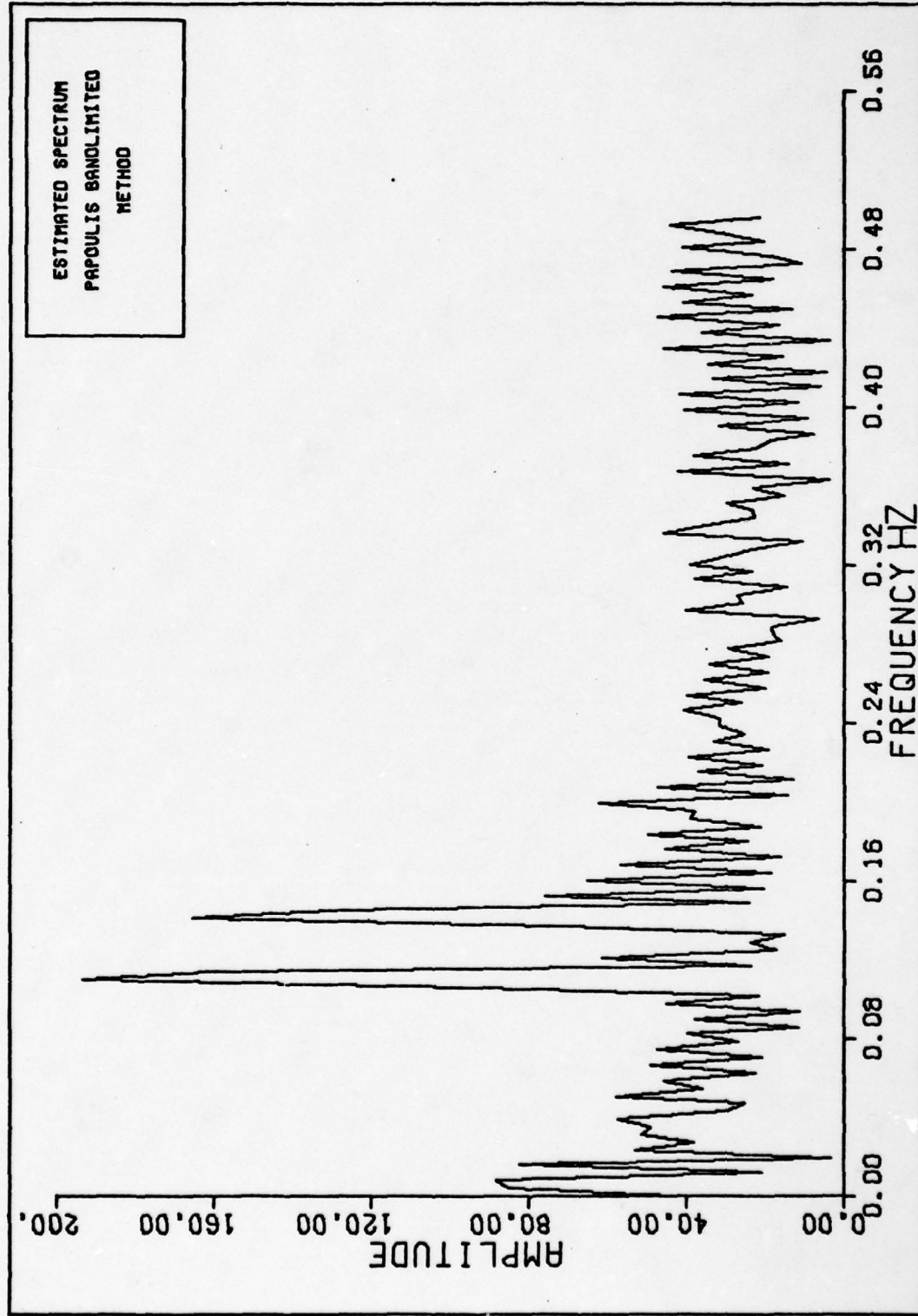


Figure 25. Estimated Spectrum from 128 Samples of Sum of Sinusoids
Process Using Papoulis Techniques

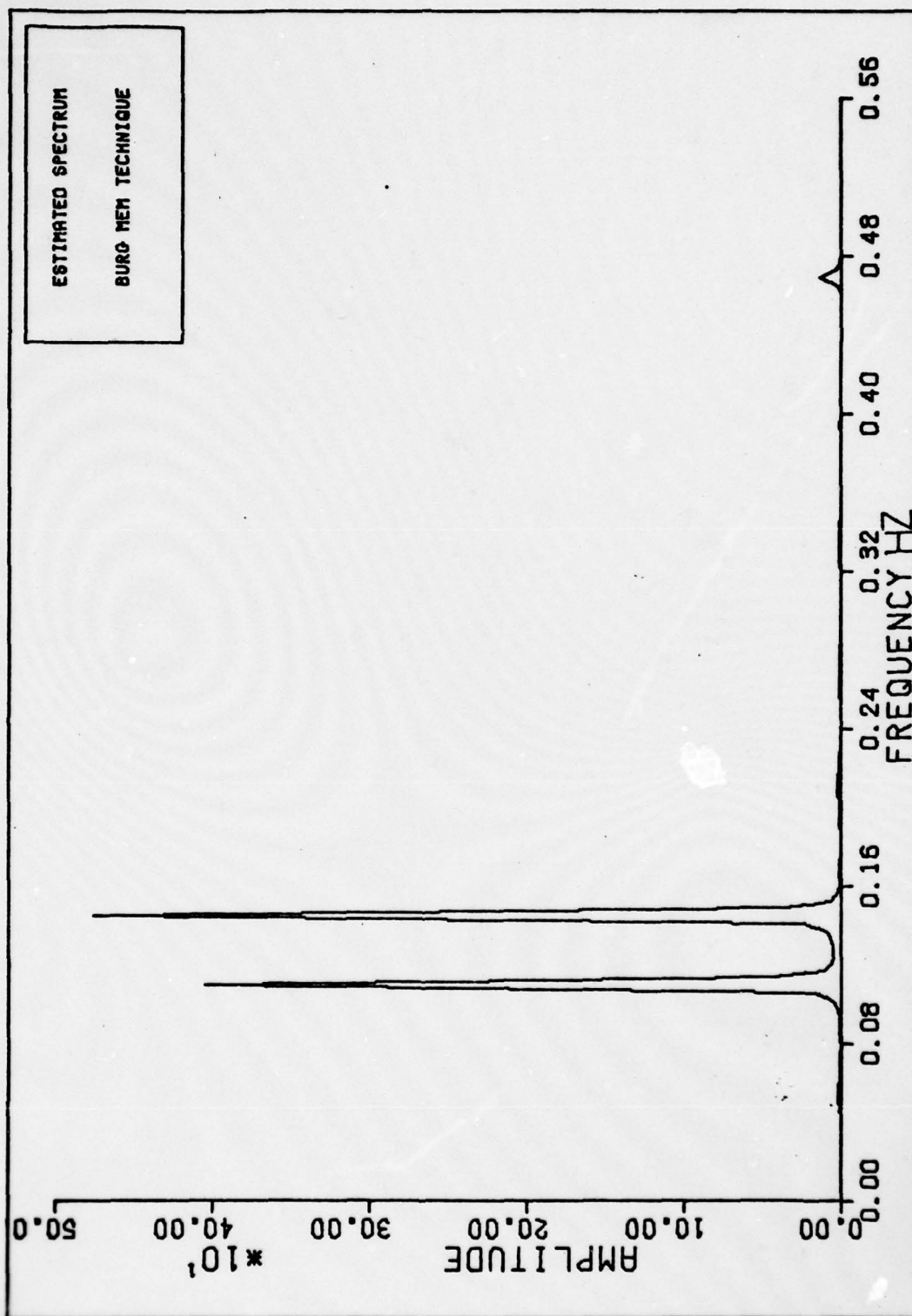


Figure 26. Estimated Spectrum from 32 Samples of Sum of Sinusoids Process
Using MEM with AR Model Order Equal to 17

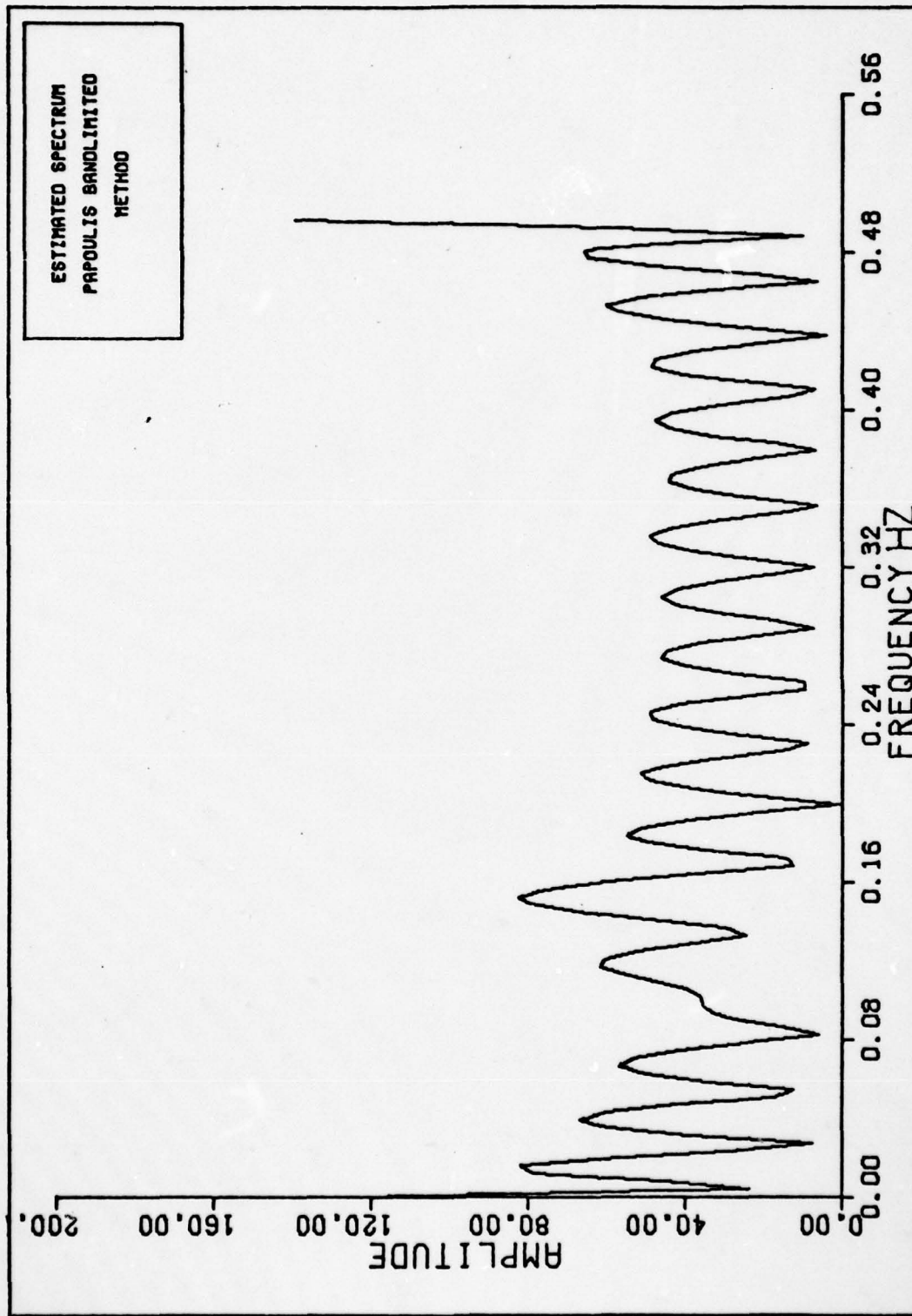


Figure 27. Estimated Spectrum from 32 Samples of Sum of Sinusoids
Process Using Papoulis Technique

estimated variance of the MEM technique (Appendix C). Recall, from Table I, the variance of the estimate is inversely proportional to the number of samples. Therefore, with a larger variance estimate and fewer samples the estimated spectrum will contain larger errors.

Conclusions

The signals analyzed in this section are by no means considered to be an exhaustive list of all possible signals of interest. However, enough data is available, from analysis of the provided examples, to draw realistic conclusions about the spectral estimation techniques under investigation. The three examples indicate the relative qualities of the MEM and Papoulis spectral estimation techniques. In particular, the MEM techniques show considerable applicability for all types of input processes including simple AR, ARMA, and sinusoidal data. This conclusion is tempered by the restrictions placed on the number of iterations for the Papoulis estimation technique. Clearly, the Papoulis technique provides creditable results when the input is sinusoidal and it is expected that the technique can be employed on other types of data if the restrictions are removed.

The analysis of short record input processes is expanded to specific problem signals from data provided by the Rome Air Development Center. The following section provides analysis results showing the relative merits of MEM and Papoulis spectral estimation techniques.

IV. Analysis of Radar Problems

The purpose of this research is to develop spectral density estimation algorithms for specific problems of interest to the government. The major limiting feature of the problem is the restriction to short sequences (128 samples or less). The specific problems evaluated in this section are adaptations of data provided at a recent RADC spectral estimation workshop (Ref 35). These problems represent data typically available from a radar problem. One problem is a sum of sinusoids with a wide range of amplitudes. The other problem is a sum of sinusoids with additive noise. Two different noise sources are added to the second problem. In the first case, only Gaussian noise is added. The problem is evaluated again with additive Gaussian noise plus impulsive interference distributed randomly throughout the data.

Spectral estimation techniques are required in the radar problems to determine the relative amplitudes and frequencies of the time sampled sinusoidal data. The data is assumed to be defined over the range of 0.0 to 200.0 Hertz. One strong sinusoidal waveform is added to other weaker sinusoids. The total dynamic range is approximately 40 db (the weakest signal is no more than 40 db down from the strongest signal).

Problem One

A simple sum of sinusoids with different amplitudes is

evaluated in this problem. The input data is evaluated using the interactive routine outlined in Figure 2. Independent sequences of 128 and 32 samples are evaluated. The sampling interval (Δt) is 0.0025 seconds with a maximum frequency of interest of 200 Hertz.

Problem one is generated by implementing the following equation

$$\begin{aligned} x(n) = & 0.03 \cos(2\pi 78n\Delta t) \\ & +0.90 \cos(2\pi 134n\Delta t) \\ & +1.20 \cos(2\pi 128n\Delta t) \\ & +0.90 \cos(2\pi 143n\Delta t) \\ & +0.04 \cos(2\pi 153n\Delta t) \\ & +0.16 \cos(2\pi 165n\Delta t) , n=1,2,\dots \quad (66) \end{aligned}$$

The dynamic range of amplitudes for this problem is -1.43db-(-33.47db)=32.04db.

Figure 28 shows a 128 point sample of the input sequence $x(n)$. Numerical results from 128 and 32 point samples of the input sequence are provided in Figures 29 through 32. The higher amplitude components are clearly evident from both MEM and Papoulis spectral analysis. Close examination of the actual spectral density estimation data from the MEM algorithm, provide by a computer listing, indicate that the MEM technique is capable of detecting the associated input frequencies with few errors. In particular, the 128 point sample clearly detects all input frequencies. However, MEM is deficient in

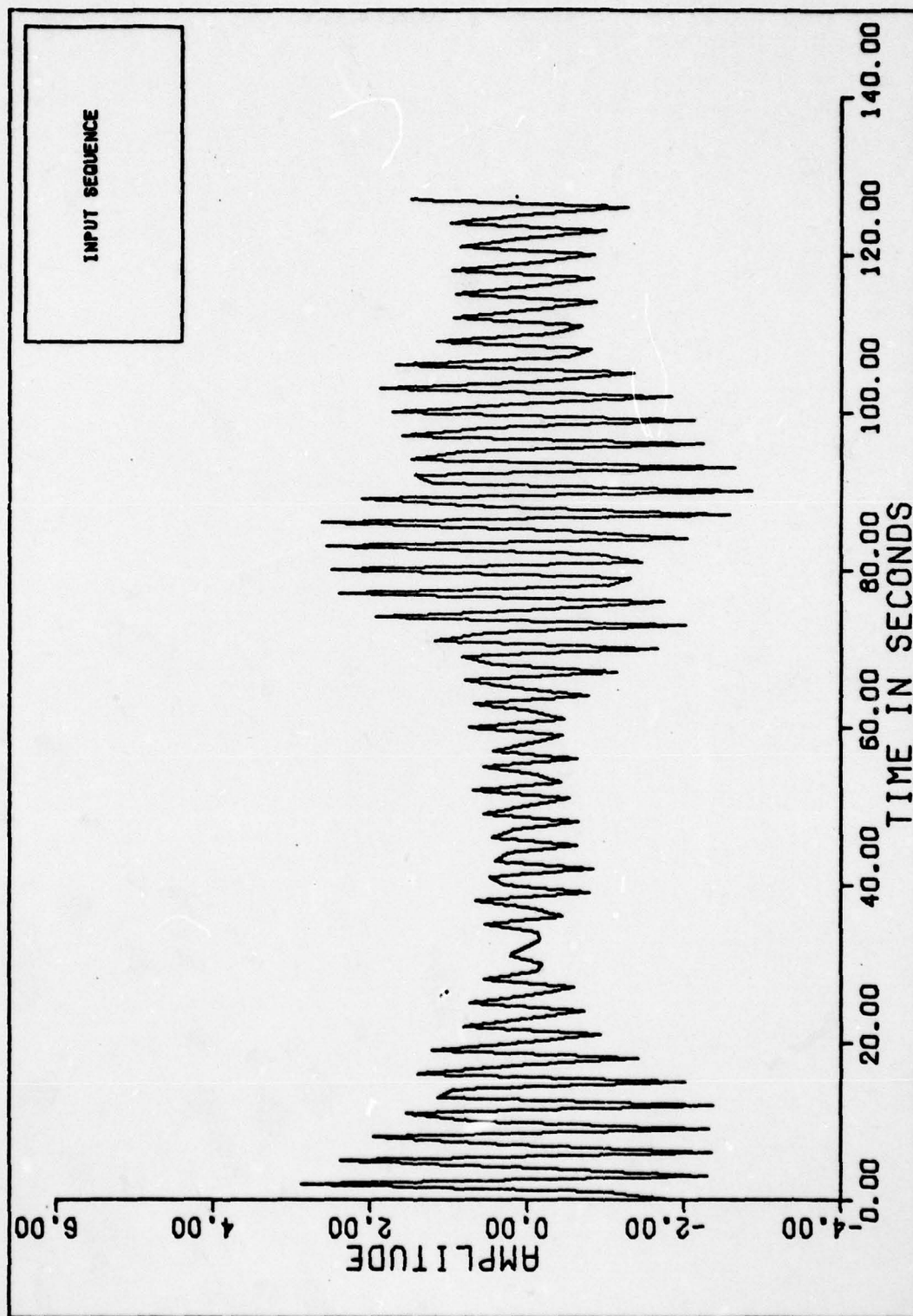


Figure 28. 128 Samples of Sum of Six Sinusoids

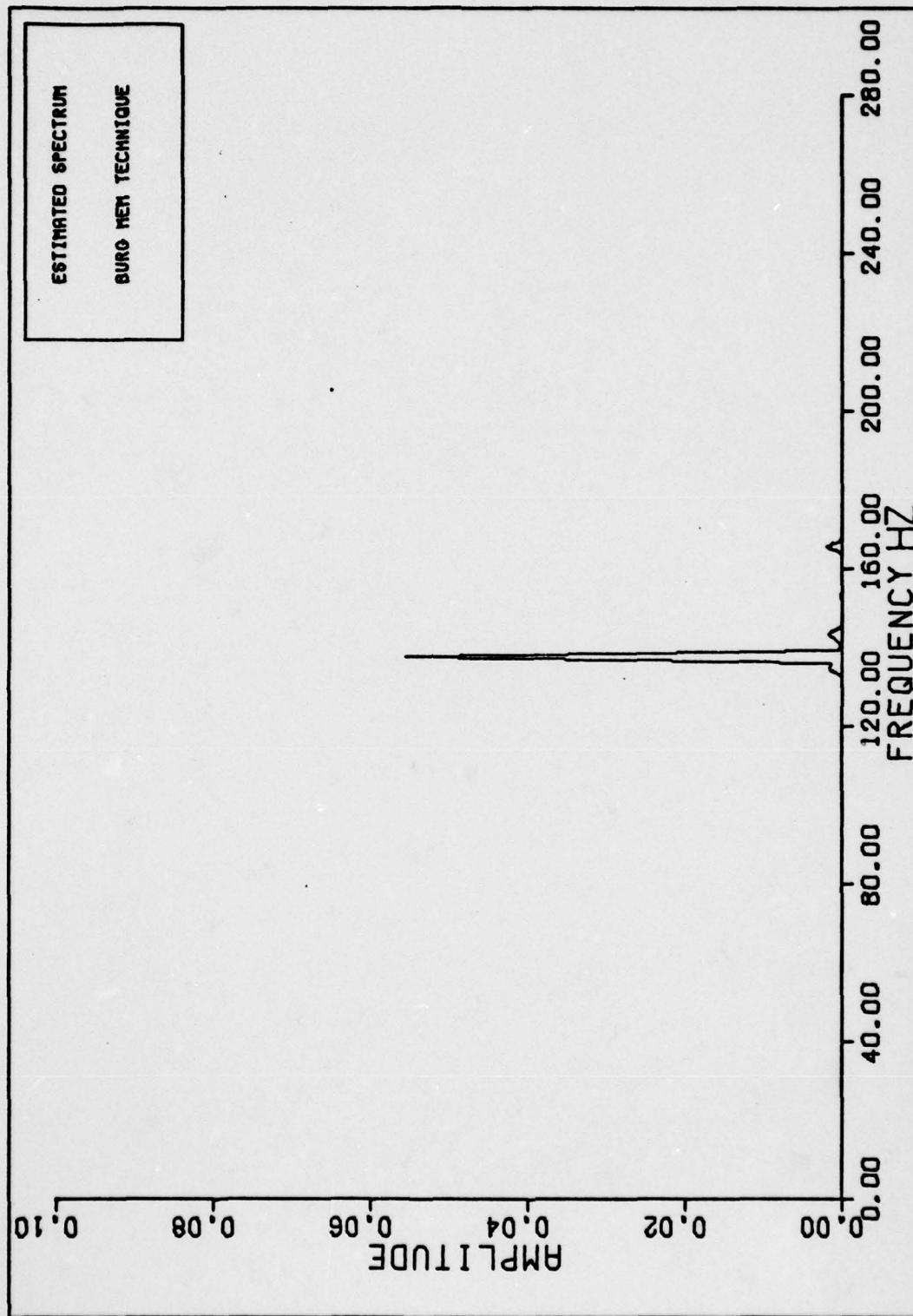


Figure 29. Spectral Estimation from 128 Samples of Six Sinusoids Using MEM Techniques

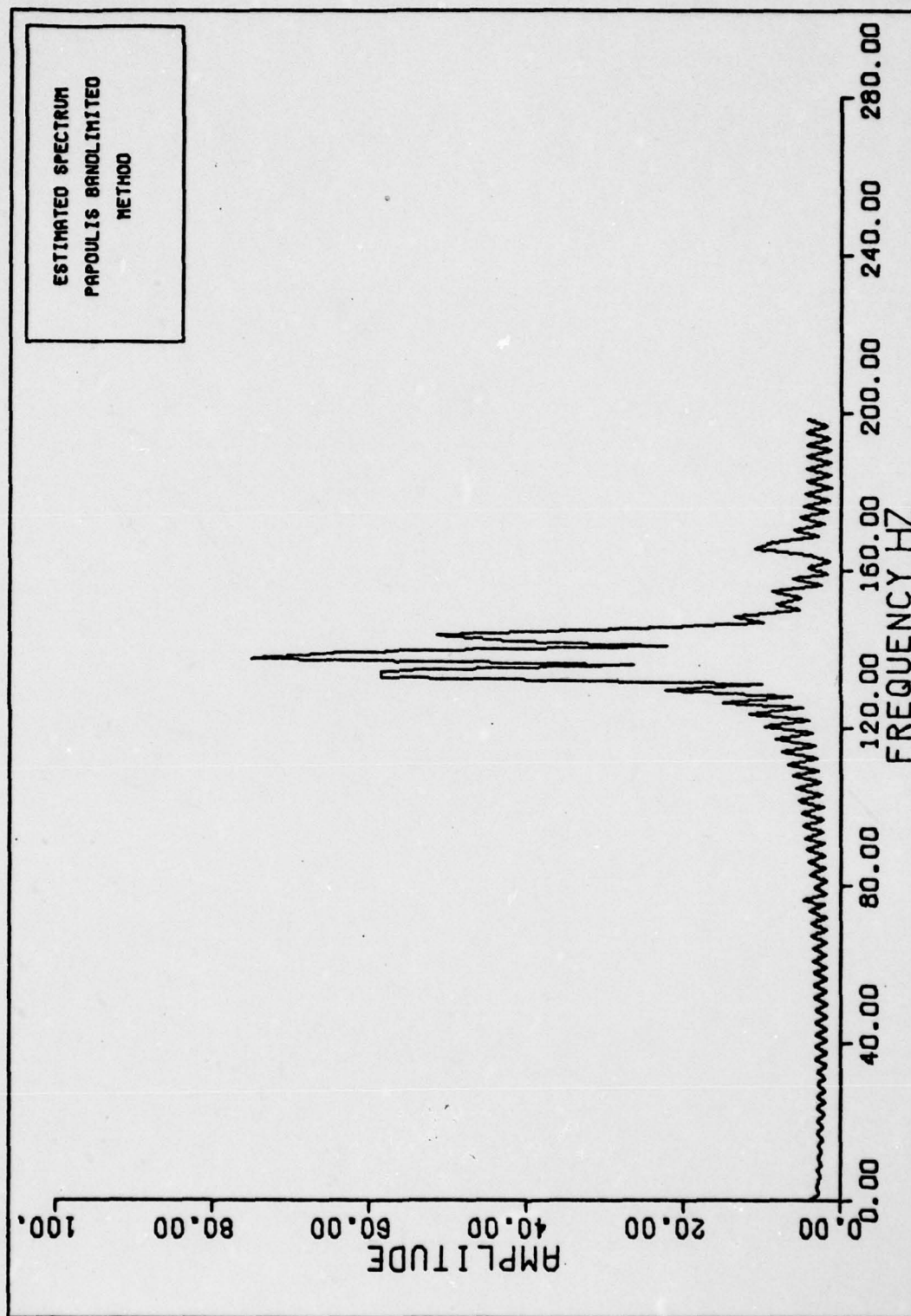


Figure 30. Spectral Estimation from 128 Samples of Six Sinusoids Using Papoulis Techniques

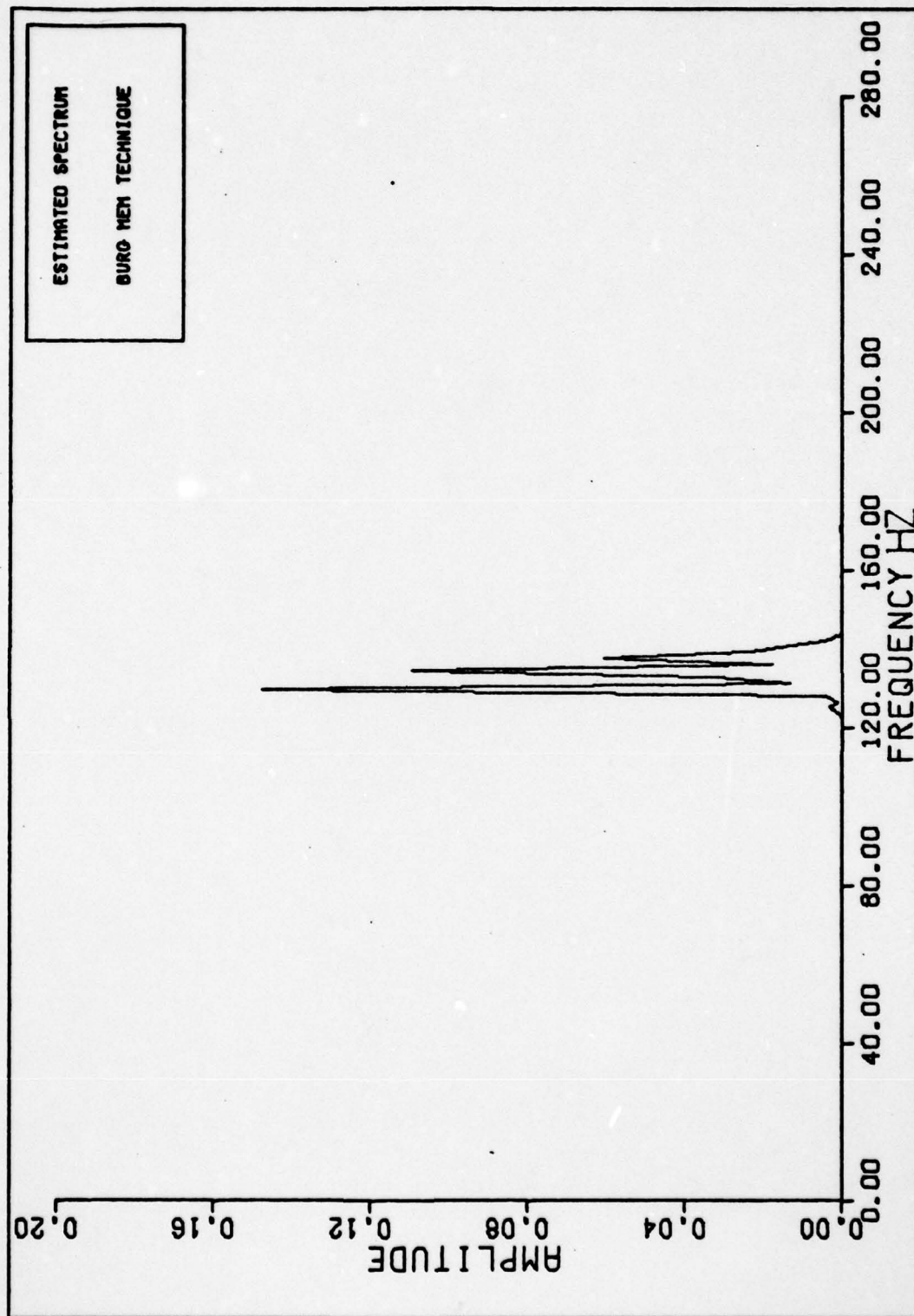


Figure 31. Spectral Estimation from 32 Samples of Six Sinusoids Using MEM Techniques

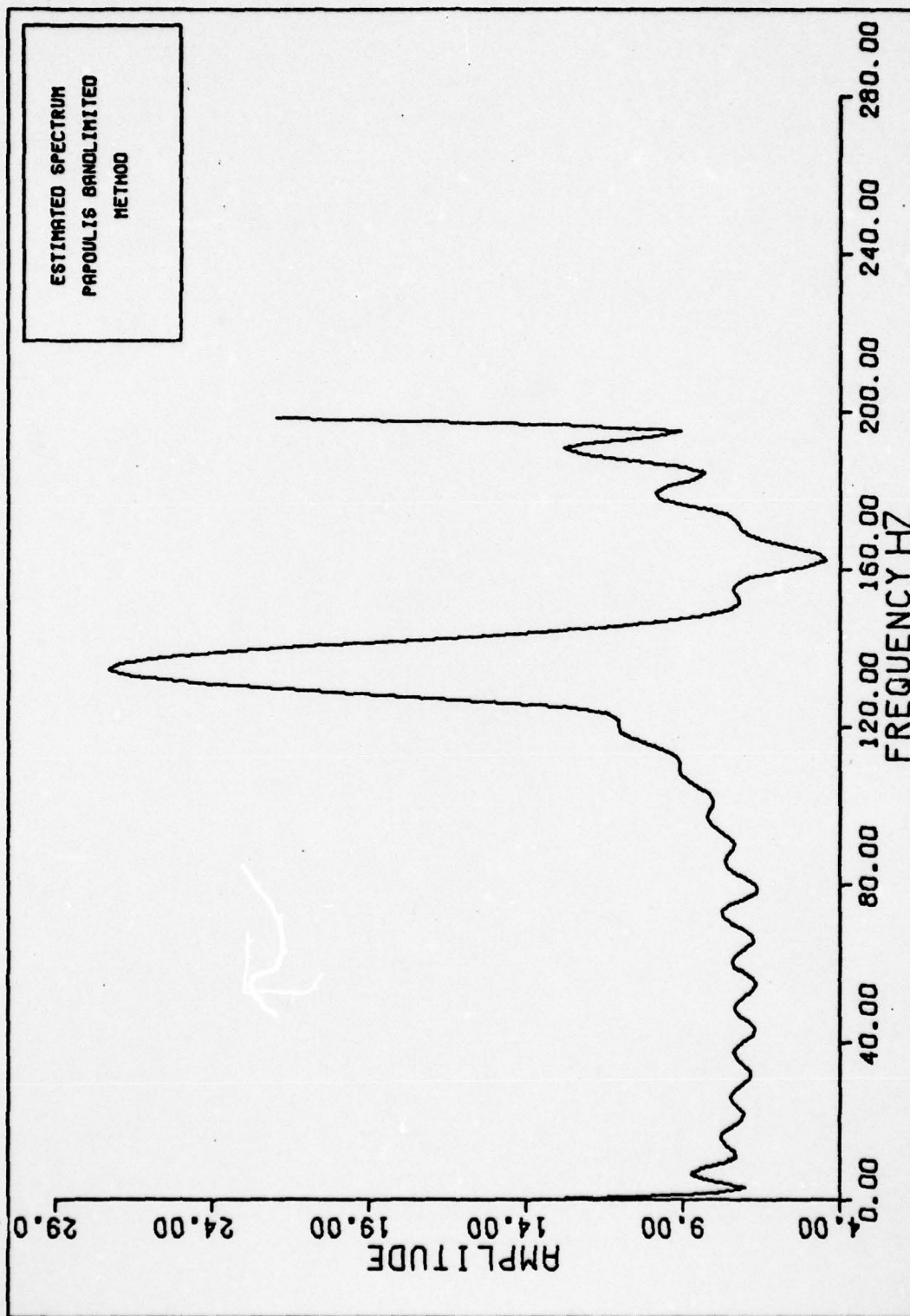


Figure 32. Spectral Estimation from 32 Samples of Six Sinusoids Using Papoulis Techniques

low amplitude estimation, when only 32 samples of the input sequence are available. The latter problem is assumed to be a result of limited model order, i.e. only 32 samples of input, limits model order to less than 32. A higher model order may be required.

Papoulis extrapolation techniques estimate the spectral frequencies of the top four amplitude signals but fail to detect the remaining signals. The Papoulis technique becomes less reliable with fewer input samples, a problem encountered in the last section and related to limitations imposed on the number of iterations.

An additional note of interest is the failure of MEM estimation to estimate the relative amplitudes of the various frequencies. This problem is clearly evident in this and previous examples. Ulrych and Bishop (Ref 39:191-192) attribute this anomaly to the relatively high variance of the MEM spectral estimation techniques when compared to other techniques (also see Table I). The variance is directly proportional to the amplitude of the estimate. Ulrych and Bishop suggest that this problem is allowable if a trade off between variance and resolution is considered. Clearly, the results suggested in Section II are illustrated in this sum of six sinusoids problem. If the Papoulis technique successfully estimates the input frequencies, the relative amplitudes of the generating data is preserved. Analysis results from Section III and this

section indicate resolution limitations of the Papoulis technique when compared to the MEM technique.

Problem Two

The second radar problem considers the case of two closely spaced cosines with additive noise. The second part of this problem includes an additional random noise source that is impulsive. Initially, the sequence of interest is generated by

$$\begin{aligned} x(n) = & 231 \cos(2\pi 51n\Delta t) \\ & + 1314 \cos(2\pi 62n\Delta t) + \eta(n) \end{aligned} \quad (67)$$

where $\eta(n)$ is a Gaussian process with zero mean and variance equal to 36. The large variance indicates a large noise source. Figure 33 shows a 128 point sample of the input sequence. Spectral estimation results from 128 and 32 point input sequences are provided in Figures 34 through 37. Satisfactory results are indicated for both the MEM and Papoulis techniques applied to the 128 point sample. The Papoulis technique fails to differentiate between the two input signals when only 32 points are analyzed. This problem is another indication of the resolution differences between MEM and Papoulis spectral estimation techniques.

An additional noise process is added to Eq(67). Samples from a uniform random number generator are taken at each point n . The uniform generator produces numbers between $[0,1]$.

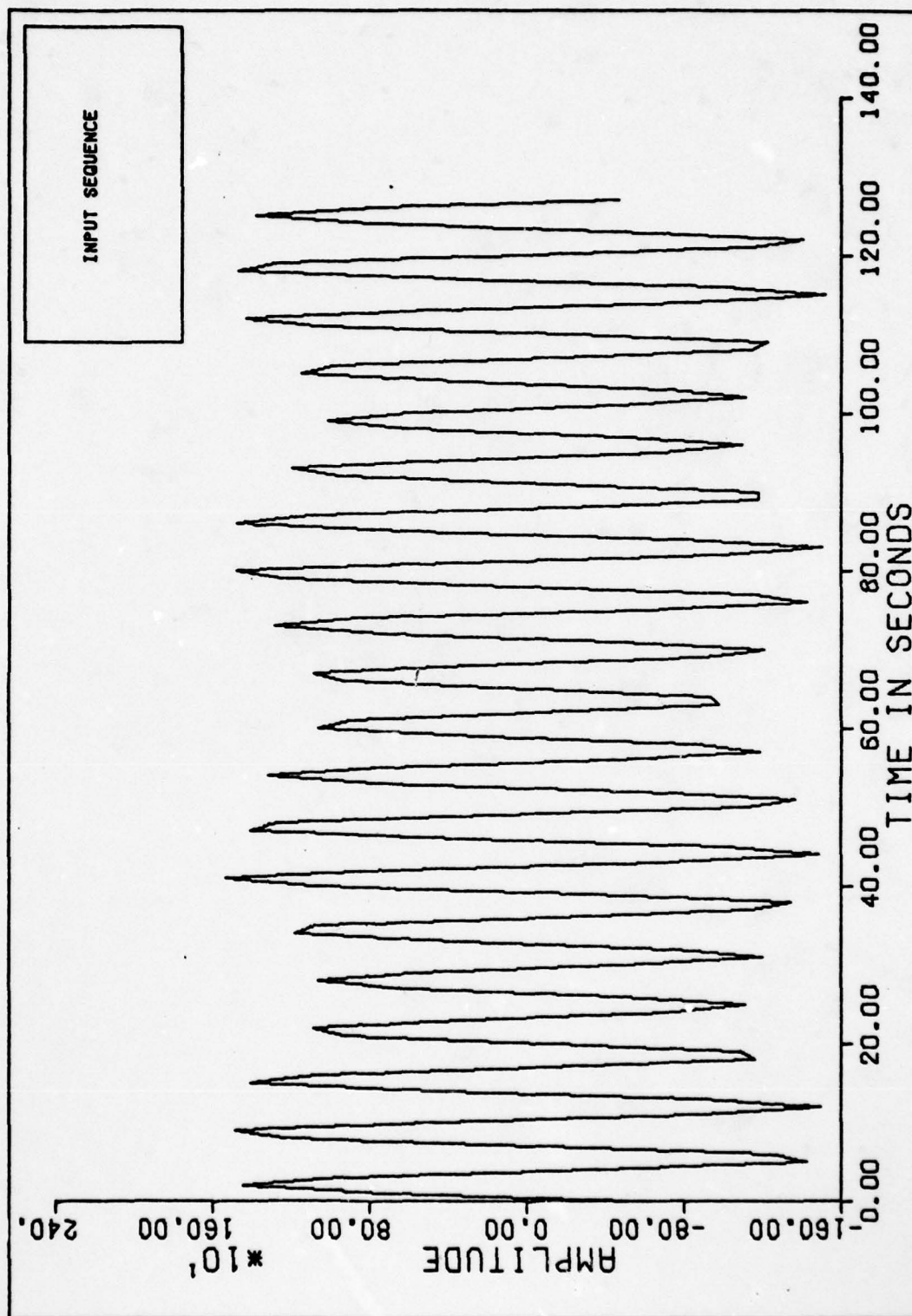


Figure 33. 128 Samples of Sum of Two Sinusoids Plus Noise

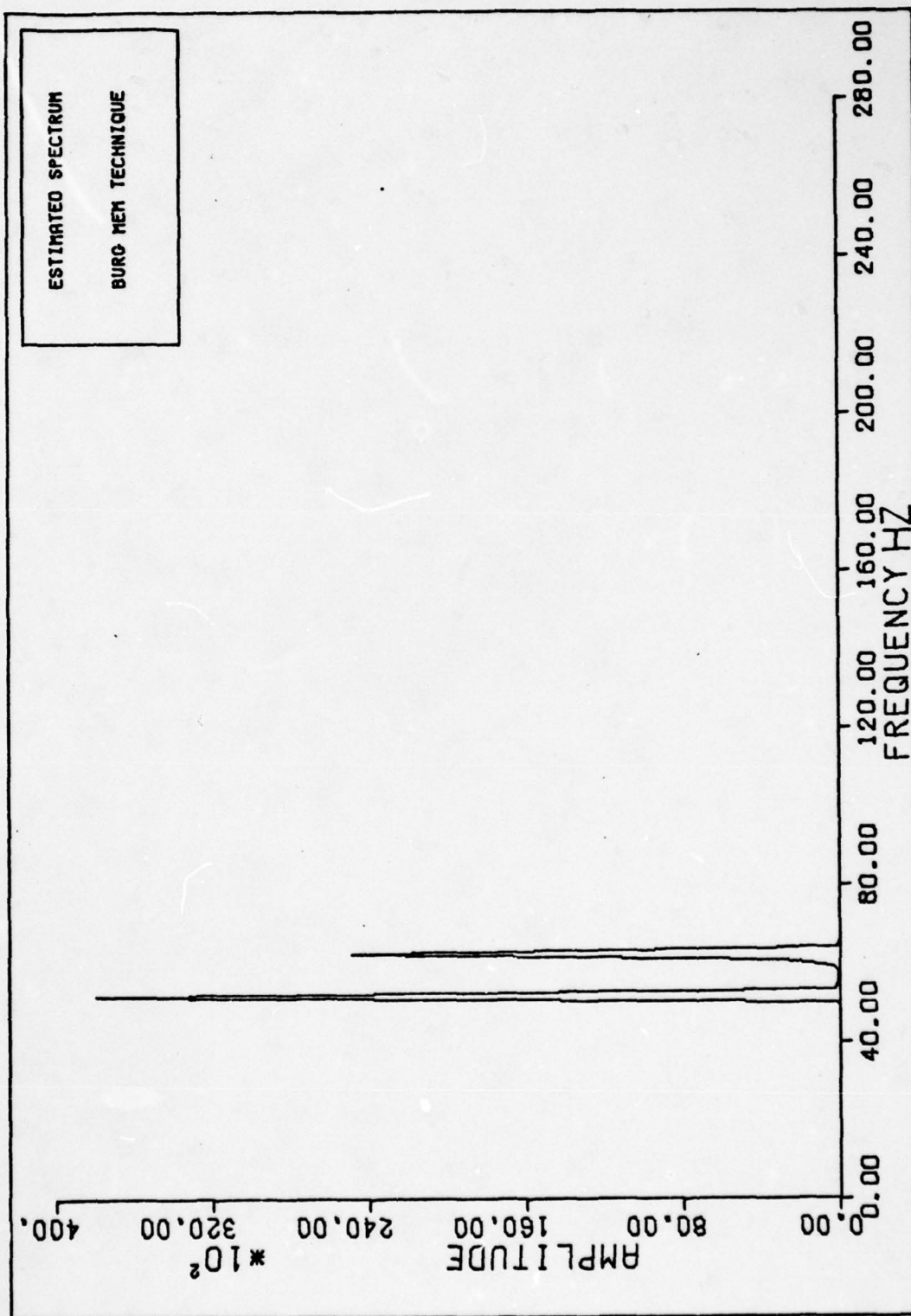


Figure 34. Spectral Estimation from 128 Samples of Two Sinusoids
Plus Noise Using MEM Techniques

AD-A080 156

AIR FORCE INST OF TECH WRIGHT-PATTERSON AFB OH SCHOO--ETC F/G 12/1
SPECTRAL ANALYSIS OF SHORT RECORD TIME SERIES DATA.(U)

UNCLASSIFIED

DEC 79 P B TERRY
AFIT/GE/EE/79-38

NL

2 OF 2

AD-

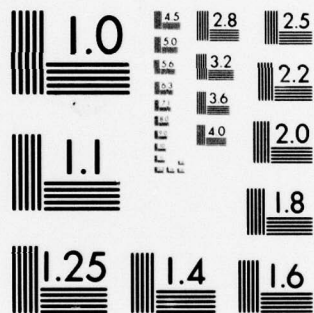
A080156



END
DATE
FILMED

2-80

DDC



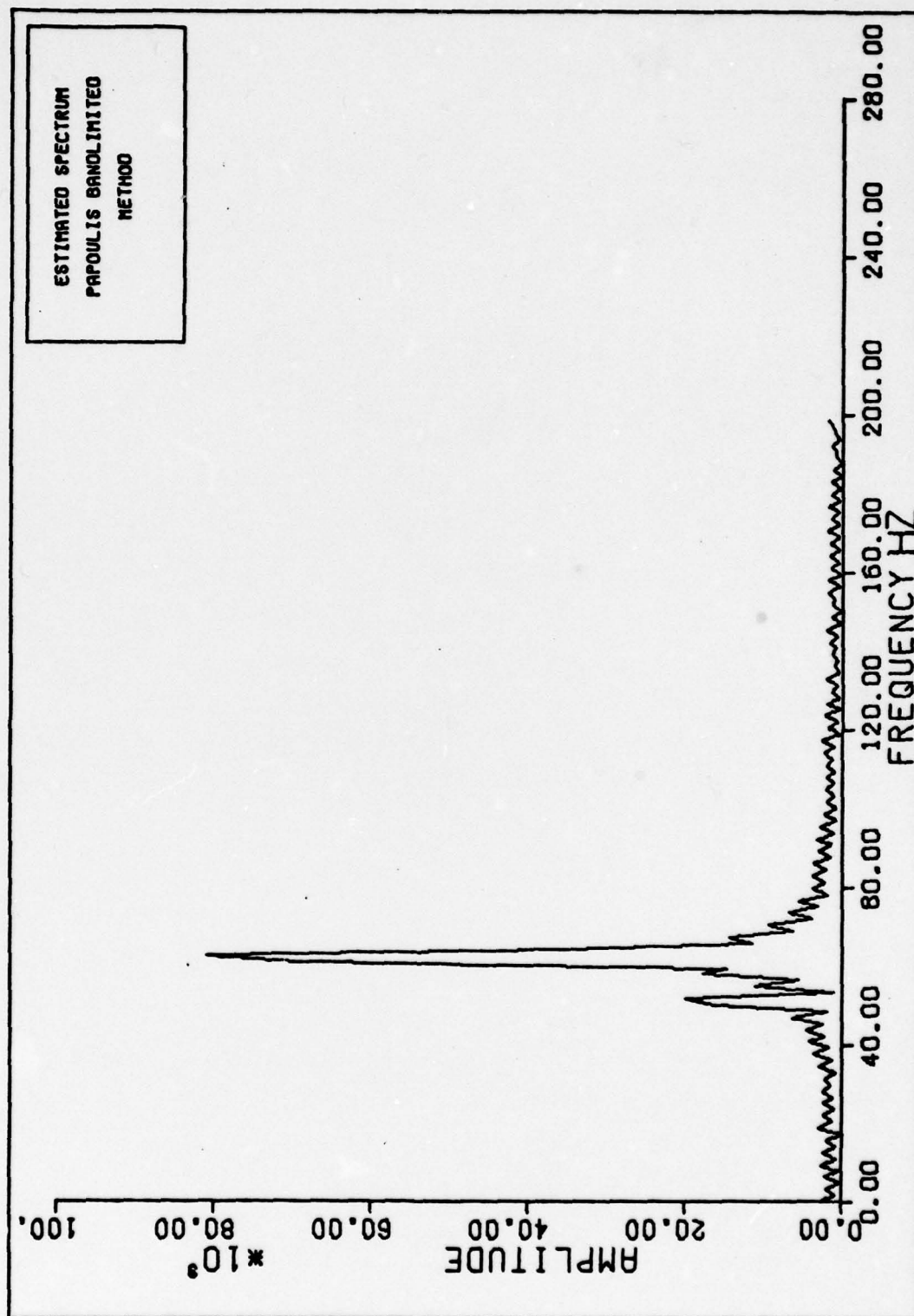


Figure 35. Spectral Estimation from 128 Samples of Two Sinusoids
Plus Noise Using Papoulis Techniques

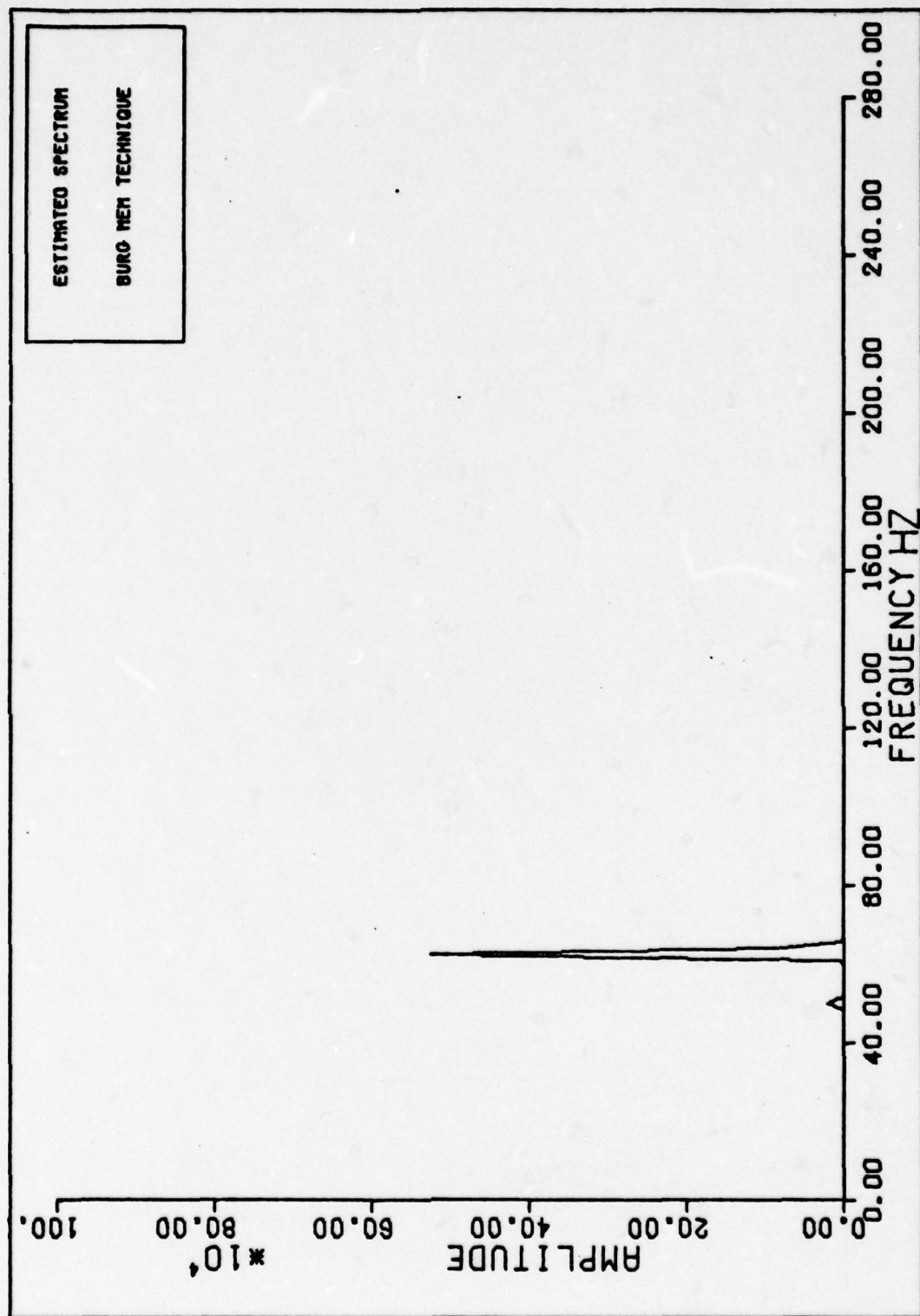


Figure 36. Spectral Estimation from 32 Samples of Two Sinusoids
Plus Noise Using MEM Techniques

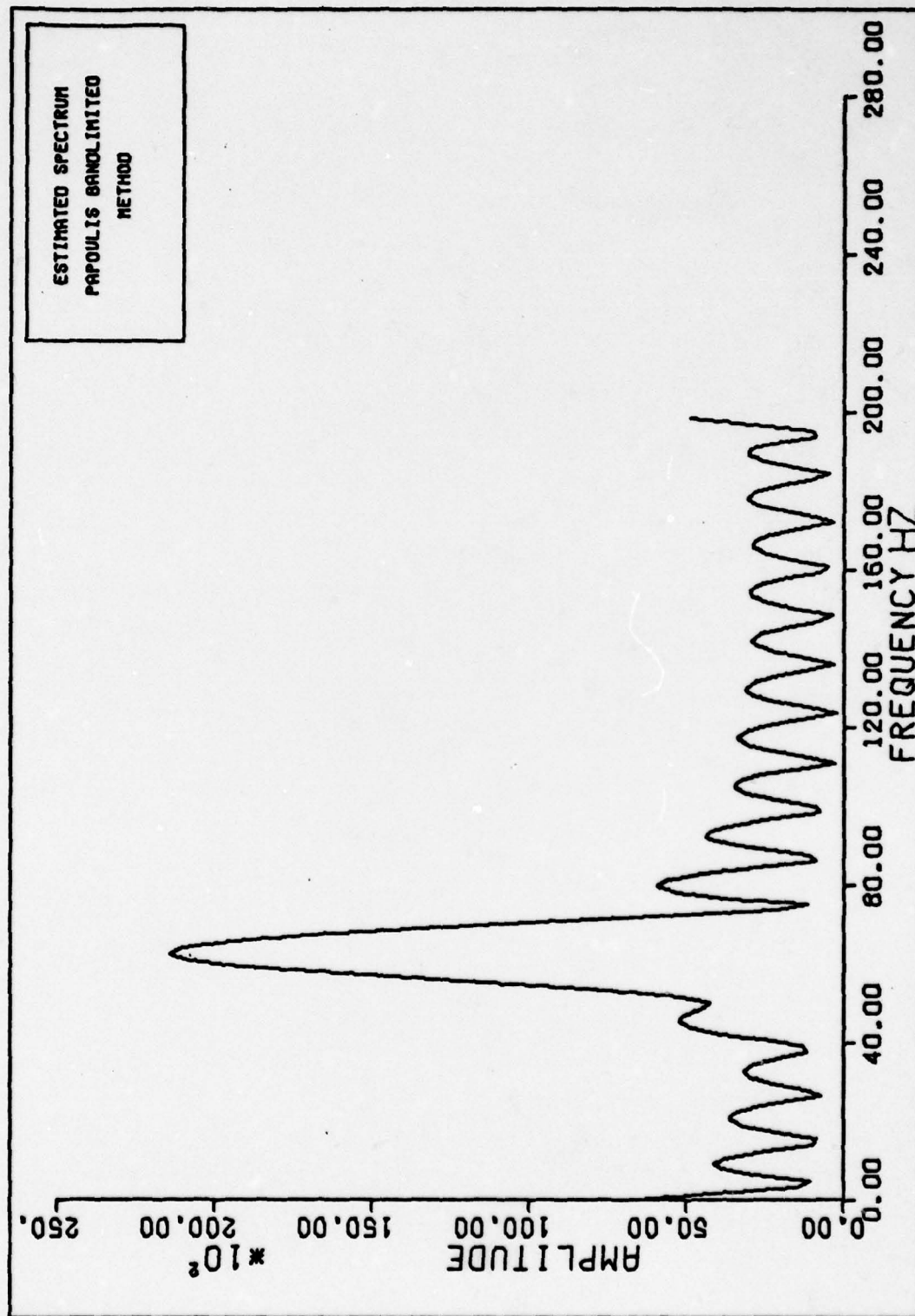


Figure 37. Spectral Estimation from 32 Samples of Two Sinusoids
Plus Noise Using Papoulis Techniques

Whenever a number is greater than an arbitrary value of 0.85, an additional value of 9999 is added to the output $x(n)$. This impulsive signal is added to simulate external perturbations such as lightning and erroneous data coding. It turns out, that an average of ten pulses occur in every 128 samples. A 128 point sample of this sequence is shown in Figure 38. The data are evaluated using MEM and Papoulis spectral estimation techniques. Figures 39 and 40 provide graphic examples of the resulting analysis. Both techniques are unable to resolve both frequencies. However, MEM does indicate a large amplitude node near the two frequencies of interest, i.e. 51 and 62 Hertz. Note the very large impulse near zero. This added impulsive noise reduces the signal to noise ratio of both techniques. Therefore, the resolution of MEM and Papoulis techniques is greatly reduced.

Conclusions

The problems considered in this section represent "real world" radar applications. Papoulis Bandlimited Extrapolation and MEM are capable of resolving many of the signals present in the input sequences. In particular, a sequence of 128 samples can be resolved when the maximum deviation between frequency amplitudes is less than 40 db. Additionally, when resolution is of greater importance than amplitude, the MEM technique exhibits marked superiority over the Papoulis algorithm.

Noise perturbations do degrade the relative accuracy of

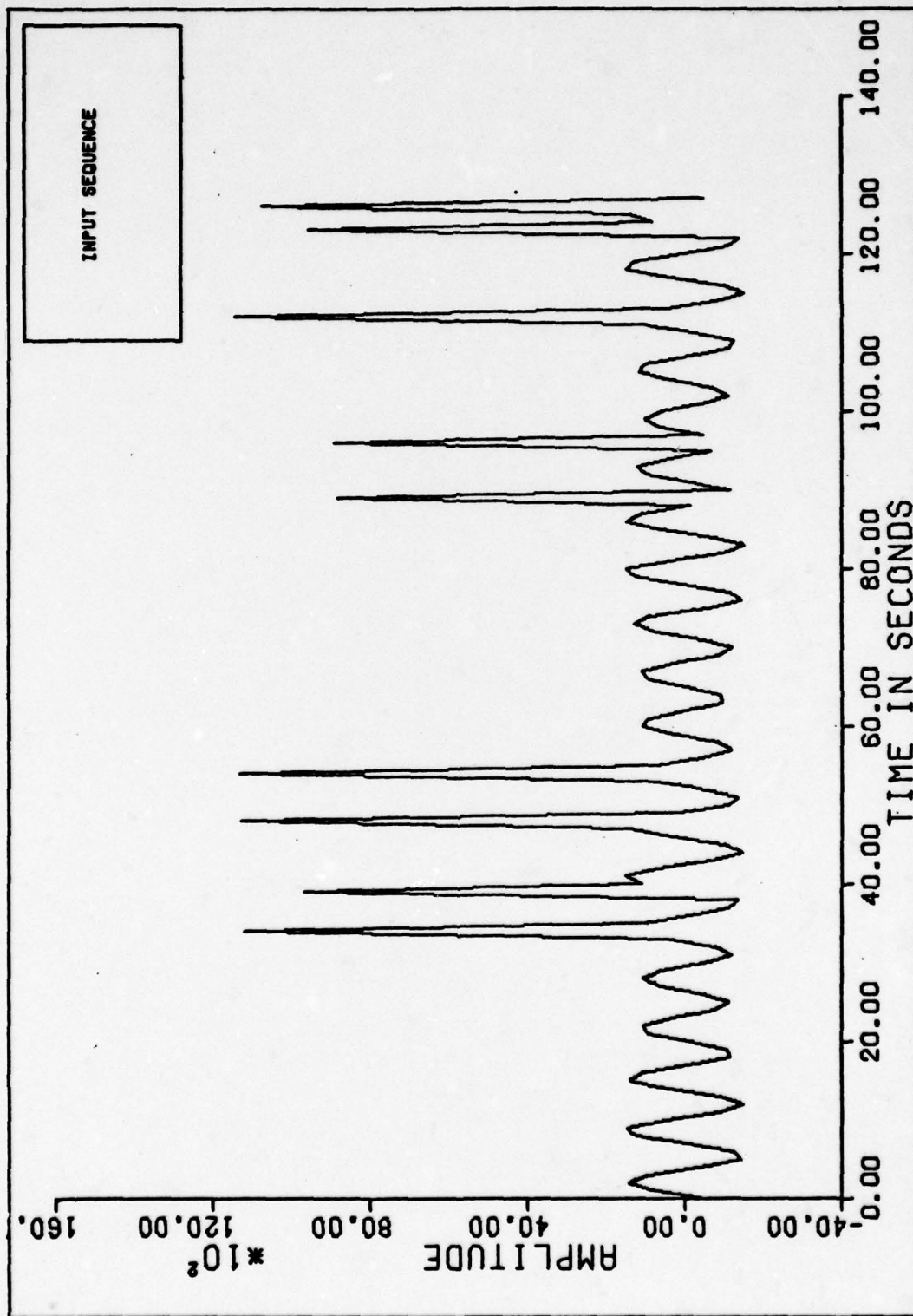


Figure 38. 128 Samples of Sum of Two Sinusoids Plus Noise
Plus Impulsive Noise

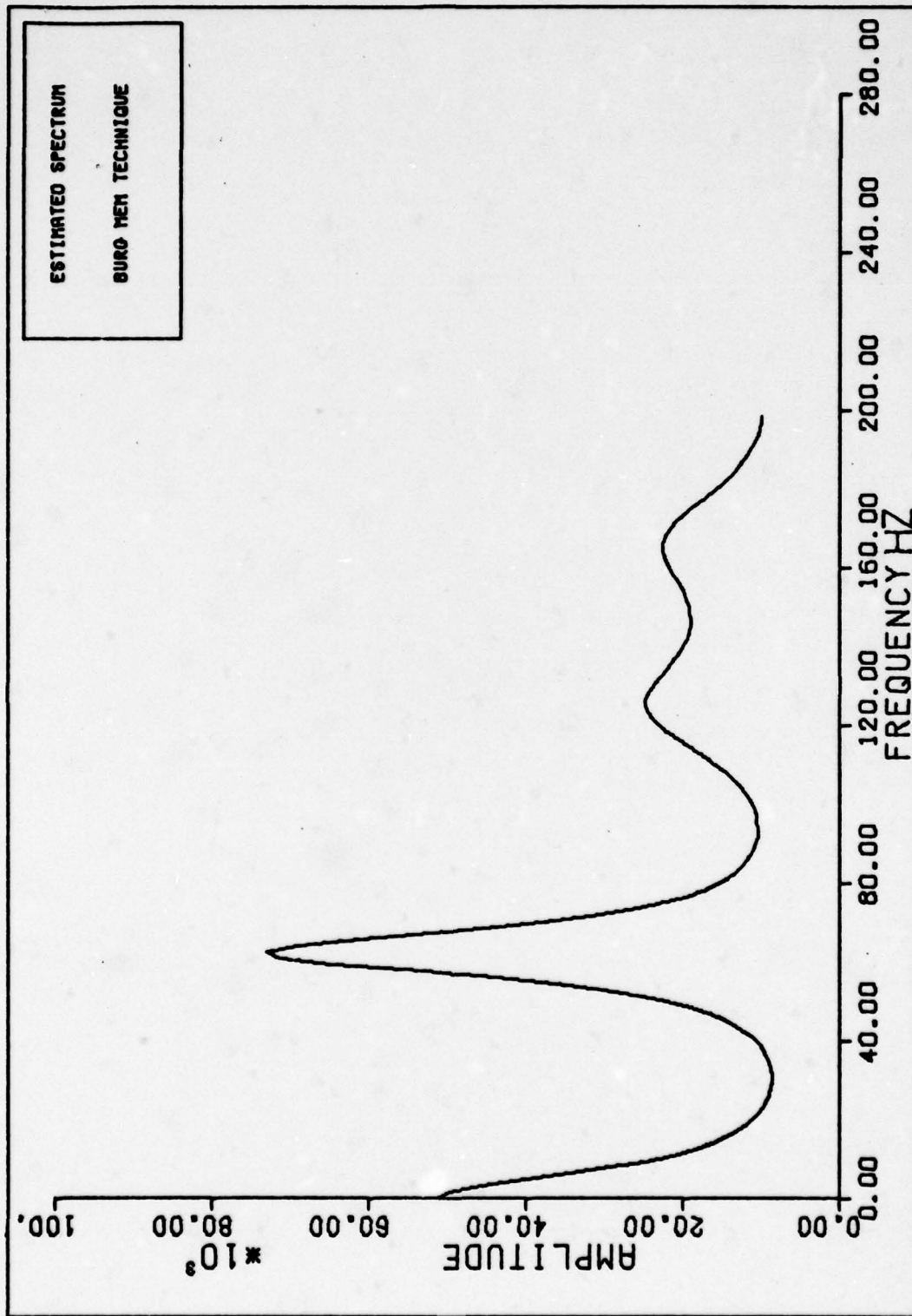


Figure 39. Spectral Estimation from 128 Samples of Two Sinusoids
Plus Noise Plus Impulsive Noise Using MEM Techniques

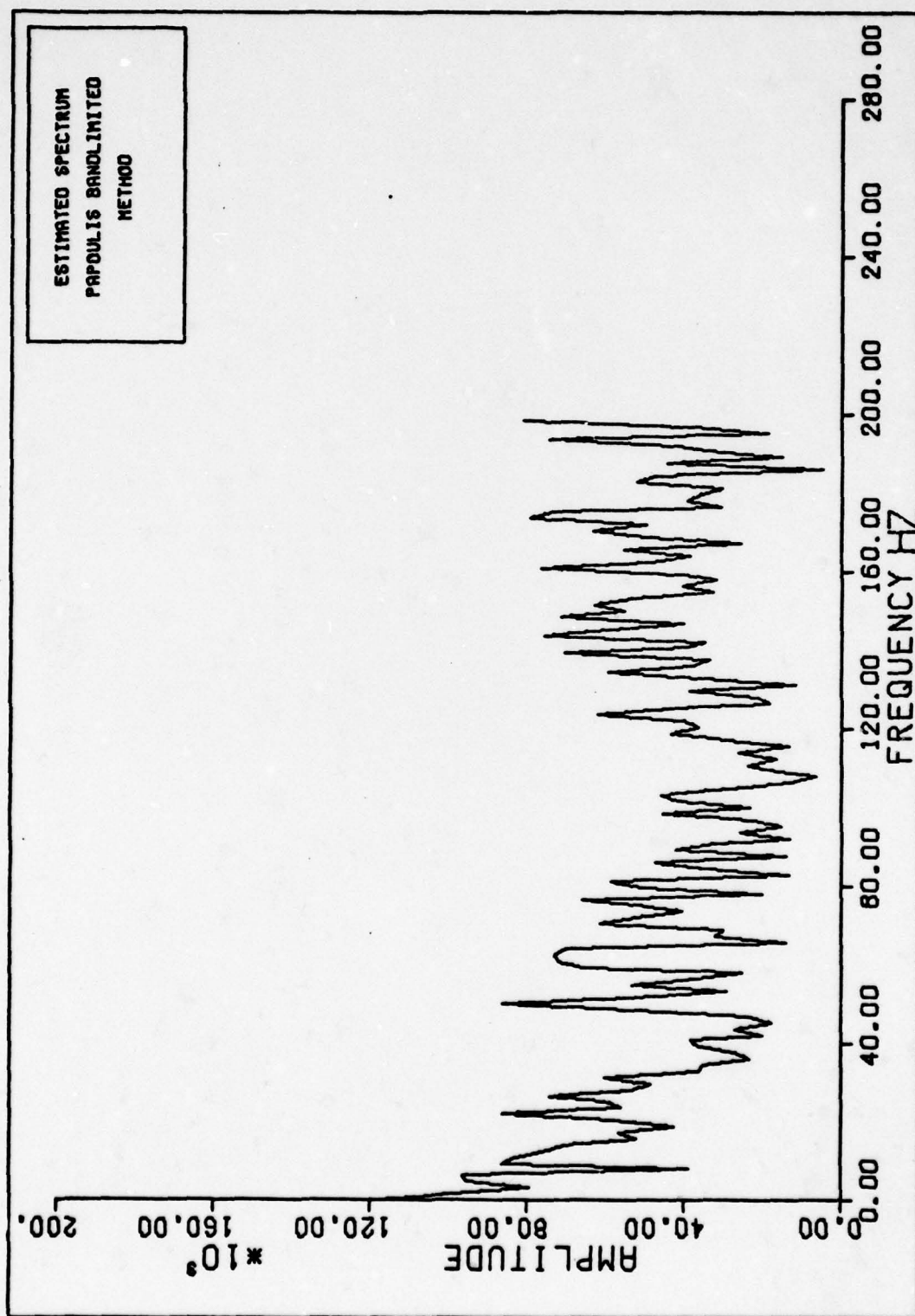


Figure 40. Spectral Estimation from 128 Samples of Two Sinusoids Plus Noise Plus Impulsive Noise Using Papoulis Techniques

each estimation technique. In particular, considerable resolution discrepancies are observed when both impulsive and normal noise are introduced as compared to simple normally distributed noise.

V. Conclusions and Recommendations

Power spectral estimation of short record time series data represents a unique problem. Traditional estimation techniques such as FFT and periodograms do not provide sufficient resolution for adequate analysis. Two techniques are suggested that produce spectral density estimates that are clearly advantageous and computationally desirable. The problems considered in this research are limited to stationary processes. The Maximum Entropy Method applied by Burg and bandlimited extrapolation by Papoulis clearly are desirable algorithms. Each technique exhibit some limitations and certain trade offs between resolution and amplitude.

The spectral estimation techniques are applied to several "real world" problems producing acceptable results in most cases. The Papoulis techniques do not provide the resolution of the MEM technique, but this reduced resolution is attributed to the prelimiting of computer processing time.

This research does not suggest that all possible analysis techniques are considered. Several techniques are currently being evaluated by several individuals. Of particular importance is the work by Makhoul et al (Ref 26) in the area of lattice networks.

Additional areas of evaluation and research are extensions

to methods covered in this thesis. Extension of the techniques to complex signals should be a relatively simple operation. Also, since signals from imaging systems can be evaluated using the techniques of this thesis, two dimensional spectral estimation techniques are a reasonable evolution. Finally, Cadzow (Ref 14) suggests a technique to evaluate an input sequence using MEM when a percentage of the data is incorrectly coded.

Bibliography

1. Akaike, H., "Fitting Autoregressive Models for Prediction," Ann. Inst. Stat. Math., 21:243-247 (1969).
2. -----, "Power Spectrum Estimation Through Autoregressive Model Fitting," Ann. Inst. Stat. Math., 21:407-419(1969).
3. -----, "Autoregressive Model Fitting for Control," Ann. Inst. Stat. Math., 23:163-180.
4. -----, "A New Look at the Statistical Model Identification," IEEE Trans. Autom. Cont., AC19:716-723(December 1974).
5. Anderson, S., "Calculation of Filter Coefficients for Maximum Entropy Spectral Analysis," Geophysics, 39(1):69-72 (February 1974).
6. Anderson, T.W., "Determination of the Order of Dependence of Normally Distributed Time Series," Time Series Analysis, edited by Rosenblatt, New York: Wiley, 1963.
7. Barnard, T.E., "Maximum Entropy Spectrum and the Burg Technique," Technical Report Number 1: Advanced Signal Processing, Texas Instruments, 25 June 1975.
8. Bartlett, M.S., Introduction to Stochastic Processes with Special Reference to Methods and Applications, New York: Cambridge University Press, 1953.
9. Blackman, R.B. and J.W. Turkey, Measurement of Power Spectra, New York: Dover Publications, 1958.
10. Box, G.E. and G.M. Jenkins, Time Series, Forecasting and Control, San Francisco: Holden-Day Inc., 1970.
11. Burg, J.D., Maximum Entropy Spectral Analysis, Paper presented at the 37th Annual International SEG Meeting, Oklahoma City, October 1967.
12. -----, "A New Analysis Technique for Time Series Data," Proceedings of NATO Advanced Study Institute on Signal Processing, Enschede, Neth. Vol.1, August 1968.
13. -----, "Relationship Between Maximum Entropy and Maximum Likelihood Spectra," Geophysics, 37(2):375-376(April 1972).

14. Cadzow, J.A., "Improved Spectral Estimation From Incomplete Sampled-Data Observations," Proceedings of the RADC Spectrum Estimation Workshop. 109-124. RADC, New York, May 1978.
15. Conover, W.J., Non-Parametric Statistics, New York:Wiley, 1971.
16. Durbin, J., "The Fitting of Time Series Models," Rev.Int. Stat.Inst., 28:233-243 (1960).
17. Fine, T.L. and W.G. Hwang, "Consistant Estimation of System Order," IEEE Trans. Auto.Cont., AC-24(3):387-402(June 1979)
18. Fuller, W.A., Introduction to Statistical Time Series, New York: Wiley, 1976.
19. Gerchberg, R.W., "Super-Resolution Through Error Energy Reduction," Optica Acta., 21(9):709-720(1974).
20. Gerhardt, L.A., "Approaches to Spectral Analysis-New and Used," Proceedings of the RADC Spectrum Estimation Workshop. 1-18. RADC, New York, May 1978.
21. Jones, R.H., "Identification and Autoregressive Spectrum Estimation," IEEE Trans. Auto Cont., AC-19(6):894-898 (December 1974).
22. -----, "Autoregressive Order Selection," Geophysics, 41: 771-773(August 1976).
23. Kromer, R., Asymptotic Properties of the AR Spectrum Estimator, PhD Thesis, Stanford University, California, 1970.
24. Lacoss, R.T., "Data Adaptive Spectral Analysis Methods," Geophysics, 36(4):661-675(August 1971).
25. Makhoul, J., "Linear Prediction: A Tutorial Review," Proceedings of the IEEE, 63(4):561-580 (April 1975).
26. Makhoul, J. et al, "Lattice Methods in Spectral Estimation," Proceedings of the RADC Spectrum Estimation Workshop.
27. Maybeck, P.S. Lecture Material EE7.12, Linear Estimation and Control. School of Engineering, Air Force Institute of Technology, Wright-Patterson AFB, 1979.
28. Nuttall, A.H., "Multivariate Linear Predictive Spectral Analysis Employing Weighted Forward and Backward Averaging (A Generalization of Burg's Algorithm)." 13 October 1976. (AD-A031755).

29. Oppenheim, A.V. and R.W. Schafer, Digital Signal Processing, New York: Prentice-Hall, 1975.
30. Papoulis, A., Probability, Random Variables, and Stochastic Processes, New York: McGraw-Hill, 1965.
31. -----, "A New Algorithm in Spectral Analysis and Band-Limited Extrapolation," IEEE Trans. Circ. and Sys., CAS-22(9): 735-742 (September 1975).
32. -----, Signal Analysis, New York: McGraw Hill, 1977.
33. Papoulis, A. and C. Chamzas, "Adaptive Extrapolation and Hidden Periodicities," Proceedings of the RADC Spectrum Estimation Workshop. 85-96. RADC, New York, May 1978.
34. Parzan, E., Statistical Spectral Analysis (single channel case) in 1968, Stanford University Statistics Department Technical Report No.11. California, June 10, 1968.
35. RADC Spectrum Estimation Workshop(Problem and Solutions), RADC, New York, May 1978.
36. Shannon, C.E., "A Mathematical Theory of Communications," Bell Sys. Tech. J., 27: 379-423(1948).
37. Siegel, S., Non-Parametric Statistics, New York: McGraw-Hill, 1956.
38. Smylie, et al, "Irregularities in the Rotation of the Earth as Time Series," Chapter 3 from Methods in Computational Physics, (13), New York: Academic Press, 1973.
39. Ulrych, T.J. and T.Bishop, "Maximum Entropy Spectral Analysis and Autoregressive Decomposition," Reviews of Geophysics and Space Physics, 13:183-200 (1975).
40. Van Den Bos, A. Alternative Interpretation of Maximum Entropy Spectral Analysis," IEEE Trans. Info. Theory, 493-494, July 1971.
41. Van Trees, H.L., Detection, Estimation, and Modulation Theory, New York: Wiley, 1968.
42. Vaughn, G., Lecture material EE6.91, Digital Signal Processing, School of Engineering, Air Force Institute of Technology, Wright-Patterson AFB, 1979.
43. Walker, G., "On Periodicity in Series of Related Terms," Proc. Royal Soc., 131(A):518(1931).

44. Welch, P.D., "Use of FFT for Estimation of Power Spectra," IEEE Trans. Aud. Elect., AU-15:70-73(June 1970).
45. Whittle, P., Hypothesis Testing in Time-Series Analysis, Uppsula, Swed: Almqvist and Wiksell, 1951.
46. Yule, G.U., "On a Method of Investigating Periodicities in Distributed Series, with Special Reference to Wolfer's Sunspot Numbers," Phil. Trans. Roy. Soc., 226(A):267-298 (1927).
47. Ziemer, R.E. and W.H. Tranter, Systems, Modulation, and Noise, Boston: Houghton Mifflin, 1976.

Appendix A

Prolate Spheroidal Expansion

Prolate Spheroidal expansion methods can be used to determine $P(\omega)$ from a sample of an input sequence $x_1(t)$. $x_1(t)$ can be expanded into a series of values dependent upon a set of orthogonal eigenfunctions $\phi_k(t)$

$$\alpha_k = \frac{1}{\lambda_k} \int_{-T}^T x_1(t) \phi_k(t) dt \quad (68)$$

where λ_k are the eigenvalues and T is the sampling interval defined for the Papoulis extrapolation in Section II.

$x_1(t)$ is expanded as

$$x_1(t) = \sum_{k=0}^{\infty} \alpha_k \phi_k(t) \quad (69)$$

since $\phi_k(t)$ are orthogonal eigenfunctions, the Fourier Transforms are a scaled value of ϕ_k

$$\phi_k(t) \longleftrightarrow \frac{B}{\sqrt{\lambda_k}} \phi_k(b\omega) P_{\alpha}(\omega) \quad (70)$$

$$B = \sqrt{2\pi T/\sigma}, b=T/\sigma$$

and since $\phi_k(t)$ is defined over T ,

$$\phi_k(t) \leftrightarrow B\sqrt{\lambda_k} \phi_k(b\omega) \quad (71)$$

The fourier Transform of the input sequence is

$$P(\omega) = B \sum_{k=0}^{\infty} \frac{\alpha_k}{\sqrt{\lambda_k}} \phi_k(b\omega) \quad (72)$$

where $|\omega| \leq \sigma$.

Papoulis (Ref31:737) shows that the technique suggested in Section II converges. The input function can be expressed as

$$x(t) = \sum_{k=0}^{\infty} \alpha_k \phi_k(t) \quad (73)$$

and from Eqs(56) and (69),

$$x_n = x(t) - \sum_{k=0}^{\infty} \alpha_k (1-\lambda_k)^n \phi_k(t) \quad (74)$$

Finally, $x_n \rightarrow x(t)$ as $n \rightarrow \infty$. This is shown by Eq(63).

Therefore, $E_n \rightarrow 0$ as $n \rightarrow \infty$, but

$$E = \sum_{k=0}^{\infty} \alpha_k^2 \quad (75)$$

is the energy in $x(t)$ and is finite. Since the eigenvalues λ_k are less than one, $1-\lambda_k < 1$ and $1-\lambda_k \leq 1-\lambda_N$ when $k \leq N$. Therefore, the energy in the n th iteration of the Papoulis technique is

$$E_n = \sum_{k=0}^N \alpha_k^2 + \sum_{k>N} \alpha_k^2 (1-\lambda_k)^{2n}$$

$$< (1-\lambda_N)^{2n} \sum_{k=0}^N \alpha_k^2 + \sum_{k>N} \alpha_k^2 < \epsilon \quad (76)$$

where ϵ is some arbitrary value. Therefore $(1-\lambda_N)^{2n} \rightarrow 0$ as $n \rightarrow \infty$ and $P_n(\omega)$ converges to $P(\omega)$ as the number of iterations increases.

Appendix B

Subroutines Used for Spectral Estimation

Several algorithms are used in the analysis sections of this paper. This appendix provides a brief explanation of each routine along with a FORTRAN IV listing. All subroutines are compiled into object code and stored in an ASD computer system program library called MEMBIN. A listing of the subroutine names and functions is provided in Table II. The applicable equations for each routine are repeated in this section from section II.

Subroutine AAIC

Calculates the Akaike A-Information Criterion using Eq(54)

$$(AIC)_p = N \ln (P_{p+1}) + 2(1+p) \quad (54)$$

where N is the number of samples; \ln is the natural logarithm, p is the particular model order and P_{p+1} is the innovations (estimation error) power.

```
C*****
C
C      SUBROUTINE AAIC(N,M,P,AIC)
C
C      AAIC CALCULATES THE AKAIKE A-INFORMATION CRITERION
C      VALUE FROM THE INNOVATION ERROR VARIANCE (POWER)
C      VECTOR P() (1,2).
C
C      CALLED BY: CALL AAIC(N,M,P,AIC)
C
C      N IS THE TOTAL NUMBER OF INPUT SAMPLES
C      M IS THE MODEL ORDER PLUS ONE
C      P() ARE THE ERROR POWER VALUES FOR ORDERS UP TO M
C      AIC() ARE THE CALCULATED INFORMATION CRITERION VALUES
```


TABLE II

Subroutine Identification

| Routine Name | Function Performed | External Calls Required |
|--------------|---|-----------------------------|
| AAIC | Calculates the Akaike A-Information Criteria (ATC) | None |
| AFPE | Calculates the Akaike Final Predictor Error (FPE) | None |
| BTLET | Computes a Bartlett Smoothed Periodogram | FFT |
| FFT | Decimation in Frequency Discrete Fourier Transform | None |
| HGRAPH | Generates plotting Data for CALCOMP x,y data | AXIS, SYMBOL PLOT, SCALE |
| KOLSMR | Calculates the Probability that the MEM Coefficients Produce a True estimate. | PDF, NKS1 (IMSL Routine) |
| MEMCO1 | Calculates the Innovations Power, Estimation Coefficients, and Autocorrelation values for the MEM Technique | None |
| PAPO | Calculates the Spectrum using the Papoulis Bandlimited Extrapolation Routine | FFT |
| PDF | Calculates the Values for a Theoretical Uniform Distribution. | None |
| PSPEC | Calculates the Power Spectral Density using the MEM Estimation Coefficients | None |

```

C
C 1. AKAIKE, H., "A NEW LOOK AT THE STATISTICAL MODEL IDENTIFI-
C   ATION", IEEE TRANS. AUTOM. CONT., VOL. AC-19, 796-7, DEC 71.
C 2. JONES, R. H., "IDENTIFICATION AND AUTOREGRESSIVE SPECTRUM
C   ESTIMATION", IEEE TRANS. AUTOM. CONT., VOL. AC-19, 716-23,
C   DEC 71.
C
C *****
C
C   DIMENSION P(1),AIC(1)
C GENERATE THE STARTING SCALE FACTOR
C   AIC(1)=N*ALOG(P(1))
C   IF(M.EQ.1)RETURN
C GET THE AIC VALUES
C   DO 10 I=2,M
C     AIC(I)=N*ALOG(P(I))+2*(I-1)
10  CONTINUE
C   RETURN
C   END

```

Subroutine AFPE

Calculates the Akaike Final Predictor Error using Eq(52)

$$(FPE)_p = \begin{cases} \frac{N+P+1}{N-P-1} P_{p+1} , & 0 \leq P \leq N/2 \\ \frac{N+P+1}{N-P-1} \left(\frac{P_{p+1}}{(1.5-P/N)} \right) , & N/2 \leq P \leq N \end{cases} \quad (52)$$

where N is the number of samples, p is the particular model order, and P_{p+1} is the innovations power. This equation is an adjustment to Akaike's FPE formula, suggested by Jones.

```

C *****
C
C   SUBROUTINE AFPE(N,M,P,FFE)
C
C AFPE CALCULATES THE AKAIKE FINAL PREDICTOR ERROR
C CALLED BY: CALL AFPE(N,M,P,FFE)
C
C N IS THE TOTAL NUMBER OF SAMPLES

```

```

C M IS THE MODEL ORDER PLUS ONE
C P(I) ARE THE ERROR INNOVATIONS (POWER)
C FPE(I) ARE THE CALCULATED FPE VALUES
C
C 1. AKAIKE, H., "FITTING AUTOREGRESSIVE MODELS FOR PREDICTION",
C   ANN. INST. STAT. MATH., VOL. 21, 23-7, 1973.
C 2. JONES, R.H., "AUTOREGRESSIVE ORDER SELECTION", GEOPHYS.,
C   VOL. 41, 171-3, AUG 76.
C
C *****
C
C   DIMENSION P(1), FPE(1)
C   GENERATE THE SCALE FACTOR
C   FPE(1) = (FLOAT(N+1)/FLOAT(N-1)) * P(1)
C   IF (M.EQ.1) RETURN
C   NORMALIZE RESULTS
C   FTEMP = FPE(1)
C   FPE(1) = 1.
C   GET THE FPE VALUES
C   NN = N/2 + 1
C   DO 10 I = 2, M
C   FPE(I) = (FLOAT(N+I-1)/FLOAT(N-I-1)) * P(1)
C   IM1 = I - 1
C   IF (IM1.LT.NN) GO TO 20
C   FPE(I) = FPE(I) / (1.0 - (I-1)/N)
20  FPE(I) = FPE(I) / FTEMP
10  CONTINUE
C   RETURN
C   END

```

Subroutine BTLET

BTLET determines the estimated spectrum by applying the Bartlett smoothed Periodogram equations.

$$\hat{P}_p(\omega) = \frac{1}{N} \left| X_N(\omega) \right|^2 \quad (11)$$

$$\hat{P}_B(\omega) = \frac{1}{K} \sum_{i=1}^K \hat{P}_{pi}(\omega) \quad (12)$$

where $X_N(\omega)$ is the N-point DFT. There are k, N-point periodograms, $\hat{P}_{pi}(\omega)$.

THIS PAGE IS BEST QUALITY FRAGSICAM
FROM COPY FURNISHED TO DDG

```

C*****
C
C      SUBROUTINE BTLET(N,M,MCON,DT,FLO,FHI,X,Y)
C
C      BTLET COMPUTES THE ESTIMATED POWER SPECTRUM USING THE
C      BARTLETT SMOOTHED PERIODOGRAM METHOD (1).
C
C      CALLED BY:  CALL BTLET(N,M,MCON,DT,FLO,FHI,X,Y)
C
C      N      IS THE NUMBER OF SAMPLES PER WINDOW
C      M      IS THE NUMBER OF PERIODOGRAMS USED
C      MCON   IS USED TO COMPUTE N FOR ROUTINE FFT, N=2**MCON
C      DT     IS THE TIME SAMPLE INTERVAL
C      FLO    IS THE LOW FREQUENCY OF INTEREST
C      FHI    IS THE HIGH FREQUENCY OF INTEREST
C      X()    ARE THE FREQUENCY SAMPLES
C      Y()    ARE THE AMPLITUDES AT THE FREQUENCIES
C
C      REQUIRED ROUTINES FROM LIBRARY: FFT
C      REQUIRES (N+M)M DATA POINTS IN LOCAL FILE TAPE6.
C
C      1. OPPENHEIM, A.V. AND S.W. SCHAFER, "DIGITAL SIGNAL PROCESS-
C         ING", NEW YORK: PRENTICE-HALL, 1966.
C*****
C
C      DIMENSION X(1),Y(1)
C      COMPLEX A,XF(300)
C      NP50=N+10
C      MNP1=MCON+1
C      NN=2*N
C      NP1=N+1
C      OF IS THE CHANGE IN FREQUENCY FOR EACH SAMPLE.
C      OF=(FHI-FLO)/FLOAT(N)
C      FREQ=.
C      DO 10 I=1,N
C      Y(I)=0.
C      X(I)=FREQ
C      FREQ=FREQ+OF
C 10  DO 20 I=1,M
C      DO 30 J=1,NP50
C      READ(6,500)XIN
C      IF(J.LE.50)GO TO 30
C      XF(J-50)=XIN
C 30  CONTINUE
C      DO 15 J=MNP1,NN
C 15  XF(J)=(0.,0.)
C      GET THE OFT
C      CALL FFT(XF,MNP1,1.)

```

```

      DO 40 J=1,N
      A=CONJG(XF(J))
      ABV=XF(J)*A
40    Y(J)=Y(J)+ABV
20    CONTINUE
      DO 50 I=1,N
50    Y(I)=Y(I)/(FLOAT(M)+FLOAT(N))
      REWIND 5
600   FORMAT(F27.10)
      RETURN
      END

```

Subroutine FFT

FFT calculates a 2^M point DFT or IDFT of the input data.

The routine is a standard decimation in frequency application.

```

C*****
C
C      SUBROUTINE FFT(X,M,XI)
C
C  FFT COMPUTES THE DFT FOR A VECTOR INPUT X() THAT HAS
C  LOG(BASE 2)M POINTS. FOR FORWARD FFT, XI = 1., FOR
C  REVERSE (IDFT) XI = -1.
C  THE ROUTINE IS A DECIMATION IN FREQUENCY (1).
C
C  CALLED BY:  CALL FFT(X,M,XI)
C
C  X() ARE THE INPUT VALUES TO BE TRANSFORMED, RESULT
C  IS IN X() ON RETURN
C  M  IS THE MULTIPLYING FACTOR, M=LOG(BASE 2)M
C  XI DETERMINES IF A FFT OR IFFT IS PERFORMED,
C  XI = 1. IS FOR FFT, XI = -1. IS FOR IDFT
C
C  1. OPPENHEIM, A.V. AND R.W. SCHAFER, "DIGITAL SIGNAL PROCESS-
C  ING", NEW YORK: PRENTICE-HALL, 1975.
C
C*****
C
C      COMPLEX X(1),U,W,T
C      N=2**M
C      NV2=N/2
C      NM1=N-1
C  BIT REVERSAL PART
C      J=1
C      PI=3.1415926535898
C      DO 7 I=1,NM1
C      IF(I.GE.J)GO TO 1
C      T=X(J)
C      X(J)=X(I)
C      X(I)=T
5      K=NV2

```

```

6      IF(K.GE.J)GO TO 7
      J=J-K
      K=K/2
      GO TO 5
7      J=J+K
      DO 20 L=1,M
      LE=27-L
      LE1=LE/2
      U=(1.,0.)
      W=CEXP(CMPLX(0.,-XI*P1/LE1))
C BUTTERFLY CALCULATIONS PART
      DO 20 J=1,LE1
      DO 10 I=J,N,LE
      IP=I+LE1
      T=X(IP)*U
      X(IP)=X(I)-T
10     X(I)=X(I)+T
20     U=U*W
      IF(XI.GT.0.)RETURN
      DO 30 I=1,N
30     X(I)=X(I)/N
      RETURN
      END

```

Subroutine HGRAPH

Given some input data, x and y, and the appropriate labeling information, HGRAPH provides an 8½ inch by 11 inch CALCOMP plot of the data (Ref 42)

```

C*****
C
      SUBROUTINE HGRAPH(X,Y,N,ID,NO,NP,NS)
C
C HGRAPH PROVIDES A CALCOMP PLOT OF THE INPUTS Y AND Y
C WITH THE LABELS PROVIDED BY ARRAY ID (1).
C
C CALLED BY: CALL HGRAPH(X,Y,N,ID,NO,NP,NS)
C
C HGRAPH MUST BE PRECEDED BY CALL PLOT(.,-4.,-3) AND
C CALL PLOT(0.,0.03,-3) INITIALLY TO SET UP CALCOMP PLOTTER.
C

```



```

C X() ARE THE X ORDINATES
C Y() ARE THE Y ORDINATES
C N IS THE NUMBER OF POINTS IN X,Y
C ID() ARE THE LABEL DATA VALUES
C NO, NP, SMS ARE PEN CONTROLS
C
C REQUIRED ROUTINES: SCALE, PLOT, SYMBOL, LINE.
C
C 1. VAUGHN, G., LECTURE MATERIAL EEE.91, DIGITAL SIGNAL PROC-
C     ESSING, SCHOOL OF ENGINEERING, AFIT, 1976.
C
C*****
      DIMENSION X(1), Y(1), ID(1)
      IF(NO.EQ.2) CALL PLOT(-1.8, 2.1, -3)
      IF(NO.EQ.2) GO TO 30
      IF(NO.LT.2) GO TO 10
      CALL SCALE(X, 7., N, 1)
      CALL SCALE(Y, 5., N, 1)
10    CALL PLOT(0., 11., 2)
      CALL PLOT(8.5, 11., 2)
      CALL PLOT(8.5, 0., 2)
      CALL PLOT(0., 0., 2)
      CALL PLOT(1.35, 1.35, -3)
      CALL PLOT(0., 8.3, -2)
      IF(ID(1).EQ.999) GO TO 2:
      CALL PLOT(.1, -.1, -3)
      CALL PLOT(0., -2., -2)
      DO 21 I=1, 7, 2
20    CALL SYMBOL((I+1.5)*.1, .3, .7, ID(I), 90., 20)
      CALL PLOT(0., 0., 3)
      CALL PLOT(1., 0., 2)
      CALL PLOT(1., 2., 2)
      CALL PLOT(0., 2., -2)
      CALL PLOT(-.1, .1, -3)
25    CALL PLOT(5.8, 0., -2)
      CALL PLOT(0., -8.3, -2)
      CALL PLOT(-5.8, 0., -2)
      CALL SYMBOL(.5, -.2, .1, ID(13), 0., 50)
      CALL PLOT(5.3, .7, -3)
      CALL AXIS(0., 0., ID(9), -20, 7., 90., X(N+1), X(N+2))
      CALL AXIS(0., 0., ID(11), 20, 5., 180., Y(N+1), Y(N+2))
30    Y(N+2)=-Y(N+2)
      CALL LINE(Y, X, N, 1, NF, NS)
      Y(N+2)=-Y(N+2)
      CALL PLOT(1.8, -2.1, -3)
      RETURN
      END

```

Subroutine KOLSMR

Given a set of M estimation Coefficients, determine if the AR model accurately models the input data sequence. An error vector is generated

$$e(n) = x(n) - \hat{x}(n) \quad 1 \leq n \leq N \quad (48)$$

where

$$\hat{x}(n) = \sum_{j=1}^P \hat{\beta}_{pj} x(n-j) \quad (47)$$

Assuming Eq(17) is correct we proceed. If $\hat{x}(n)$ accurately estimates the input, $e(n)$ will be a white noise process. The routine generates $e(n)$ then calculates the spectrum by the Bartlett smoothed periodogram technique. A bandlimited sample of the frequency data is integrated (Simpsons integration) to produce a quasi distribution function. The distribution function is evaluated by a Kolmogorov-Smirnov two sided test to determine how well it approximates a uniform distribution. The results are a probability measure of goodness of fit.

```
C*****
C
C      SUBROUTINE KOLSMR(MODN,M,BTA,PRB4)
C
C KOLSMR COMPUTES THE PROBABILITY THAT THE SYSTEM OF ORDER
C M IS CORRECT. THE TEST IS ACCOMPLISHED BY THE KOLMOGOROV-
C SMIRNOV SINGLE SAMPLE TEST FOR GOODNESS OF FIT (1).
C
C CALLED BY: CALL KOLSMR(MODN,M,BTA,PRB4)
C
C (N+50)50 POINTS OF DATA MUST BE AVAILABLE IN A LOCAL FILE
C TAPE6.
```

```

C
C MODN IS THE # TO CALCULATE # OF SAMPLES
C M IS THE MODEL ORDER PLUS ONE
C BTA() ARE THE ESTIMATION COEFFICIENTS
C PRBM IS THE PROBABILITY THAT THE SYSTEM (MODEL) IS
C CORRECT
C
C ROUTINES REQUIRED: PDF,NKS1 (AN IMSL ROUTINE)
C
C 1. BOX, G.E. AND A. JENKINS, "TIME SERIES ANALYSIS FORECASTING
C AND CONTROL",HOLDEN-DAY,1970.
C
C *****
C
C PDF IS CALLED BY IMSL ROUTINE NKS1, THE KOLO-SMIR ROUTINE.
C EXTERNAL PDF
C DIMENSION XM(100),ER(300),BTA(1),E(1000),PDIF(6)
C COMPLEX Z,XF(300)
C N=2*M*MODN
C SKIP 10 POINTS BEFORE EACH WINDOW
C NP5=N+50
C ZERO OUT THE ARRAYS
C DO 10 I=1,M
10 XM(I)=0.
C DO 20 J=1,N
C XF(J)=(0.,0.)
20 ER(J)=0.
C CALCULATE THE ESTIMATED OUTPUT
C EST OF X(I)=SUM(BTA(I)*X(1-1))(I=1,M)
C X=J.
C MM1=M-1
C MM2=MM1-1
C NP5JX=NP5+50
C WE WANT 50 WINDOWS OF N SAMPLES (ERFORS) EACH
C DO 30 I=1,NP5JX
C IF(MM1.LT.2)GO TO 45
C DO 40 J=1,MM2
40 XM(MM1-J+1)=XM(MM1-J)
45 XM(1)=X
C SUM=0.
C DO 50 J=1,MM1
50 SUM=SUM+BTA(J+1)*XM(J)
C READ(6,500) X
C FIND THE ERROR FOR THIS SAMPLE
30 E(I)=X-SUM
C NOW DO THE BARTLETT SMOOTHED PERIODOGRAM ON 50 WINDOWS
C N POINTS/WINDOW

```


THIS PAGE IS BEST QUALITY FRAGRANCE
FROM COPY FURNISHED TO DDC

```

AV=0.
DO 80 K=1,50
DO 70 J=1,NP00
IF(J.LE.5) GO TO 70
XF(J-70)=E(J+K*NP00)-NP00
70 CONTINUE
CALL FFT(YF,MOON,1.)
DO 80 J=1,N
A=CONJG(XF(J))
ABV=XF(J)*A
80 ER(J)=ER(J)+ABV
60 CONTINUE
DO 90 I=1,N
ER(I)=ER(I)/(50.*N)
90 AV=AV+ER(I)
C WE NOW HAVE A SMOOTHED SPECTRUM OF THE ERROR, IF WGN,
C WILL BE FLAT. LET THE N VALUES REPRESENT A DENSITY
C FUNCTION FOR SUM R.V.
C SCALE AND INTEGRATE TO GET THE DISTRIBUTION OF THE
C PROCESS.
SUM=0.
ERM1=0.
ERM2=0.
C DO A SIMPSONS INTEGRATION
DO 110 I=1,N
ER(I)=ER(I)/AV
SUM=SUM+(ERM2+4.*ERM1+ER(I))/6.
ERM2=ERM1
ERM1=ER(I)
110 ER(I)=SUM
C NOW TEST FOR UNIFORM OVER THE INTERVAL ( 0.3 TO 1.0 )
CALL NKS1(PDF,ER,N,PDIF,IER)
PRBM=PDIF(6)
REWIND 5
500 FORMAT(F20.10)
RETURN
END

```

Subroutine MEMCO1

With an N point input sequence of data and some assumed model order P , determine the estimation coefficients $\hat{\beta}_{pi}$, innovations power P_{p+1} , and the autocorrelation coefficients ϕ_1 , this routine carries out the recursions outlined by Anderson (Ref 6).

THIS PAGE IS BEST QUALITY PRINTING
FROM COPY FURNISHED TO DDC

```
C*****
C
C      SUBROUTINE MEMCO1(N,M,X,PHI,BTA,P)
C
C      MEMCO1 CALCULATES THE ESTIMATION VALUES FOR AN MTH
C      ORDER AD INPUT. MEMCO1 IS AN ADAPTATION OF AN ALGORITHM
C      BY N. ANDERSON (1).
C
C      CALLED BY: CALL MEMCO1(N,M,X,PHI,BTA,P)
C
C      N IS THE TOTAL # OF SAMPLES
C      M IS THE MODEL ORDER PLUS ONE
C      X() ARE THE INPUT VALUES
C      PHI() ARE THE CALCULATED AUTOCORRELATION COEFFICIENTS
C      BTA() ARE THE CALCULATED ESTIMATION ERROR COEFFICIENTS
C      P() ARE THE INNOVATION VARIANCE (POWER) VALUES
C
C      1. ANDERSON, N., "CALCULATION OF FILTER COEFFICIENTS FOR
C      MAXIMUM ENTROPY SPECTRAL ANALYSIS", GEOPHYS., VOL. 39,
C      NO. 1, 33-42, FEB 74.
C
C*****
C
C      DIMENSION X(1),PHI(1),BTA(1),P(1),B1(500),B2(500),BTA(100)
C      FIND P(1) AND PHI(1)
C      SUM=0.
C      DO 10 I=1,N
10    SUM=SUM+X(I)**2.
C      P(1)=SUM/FLCAT(N)
C      PHI(1)=P(1)
C      BTA(1)=1.
C      IF(M.EQ.1)RETURN
C      NOW COMPLETE THE REGRESSION
C      NM1=N-1
C      DO 20 J=1,NM1
C      B1(I)=X(I)
20    B2(I)=X(I+1)
C      I=2
30    SNOM=0.
C      SDEN=0.
C      NMIP1=N-I+1
C      DO 40 J=1,NMIP1
C      SNOM=SNOM+B1(J)*B2(J)
40    SDEN=SDEN+(B1(J)**2.+B2(J)**2.)
C      BTA(I)=2.*SNOM/SDEN
C      P(I)=P(I-1)*(1.-BTA(I)**2.)
C      SUM=0.
C      DO 50 K=2,I
50    SUM=SUM-PHI(I-K+1)*BTA(K)
C      PHI(I)=SUM
C      IF(M.EQ.2)RETURN
```

```

        IF (I.EQ.2) GO TO 70
        IM1=I-1
        DO 60 K=2,IM1
60      BTA(K)=1BTA(K)-BTA(I)*ABTA(I-K+1)
        IF (I.EQ.N) RETURN
70      I=I+1
        IM1=I-1
        DO 80 K=2,IM1
80      ABTA(K)=BTA(K)
        NMIP1=N-I+1
        DO 90 K=1,NMIP1
        B1(K)=B1(K)-ABTA(I-1)*B2(K)
90      B2(K)=B2(K+1)-ABTA(I-1)*B1(K+1)
        GO TO 30
    END

```

THIS PAGE IS BEST QUALITY PRINTED
FROM COPY FORWARDED TO DOD

Subroutine PAPO

Given a sample of an input time process, this subroutine determines an estimate of the frequency spectrum using the techniques developed by Papoulis Eqs(56) through (60).

C*****

C

SUBROUTINE PAPO(N,IT,DER,FHI,DT,X,PP,FRO,ITT)

C

C PAPO CALCULATES THE SPECTRAL DENSITY USING THE METHODS
C DESCRIBED BY PAPOULIS (1).

C

C CALLED BY: CALL PAPO(N,IT,DER,FHI,DT,X,PP,FRO,ITT)

C

C M IS THE NUMBER THAT IS USED TO CALCULATE THE TOTAL
C NUMBER OF SAMPLES. $N=2*M$

C IT IS THE TIME SAMPLE WINDOW FOR THE ITERATION

C DER IS REQUIRED MINIMUM CHANGE IN MSE FROM ONE ITERATION
C TO THE NEXT

C FHI IS THE HIGHEST FREQUENCY OF INTEREST

C DT IS THE TIME SAMPLE INTERVAL

C X() ARE THE TIME SAMPLE INPUT VARIABLES

C PP() ARE THE CALCULATED POWER SPECTRUM OUTPUT VALUES

C FRO() ARE THE FREQUENCY SAMPLE POINTS

C ITT IS THE TOTAL NUMBER OF ITERATIONS TO MEET THE DER
C VALUE, OR THE DEFAULT VALUE 100

C

C REQUIRED ROUTINES: FFT

C

C 1. PAPOULIS, A., "A NEW ALGORITHM IN SPECTRAL ANALYSIS AND BAND-
C LIMITED EXTRAPOLATION", IEEE TRANS. CIR. SYS., VOL. CAS-22,
C NO. 9, SEP 75.

C

C*****

C

THIS PAGE IS BEST QUALITY FRAGGABLE
FROM COPY FURNISHED TO DDO

```
      DIMENSION FRQ(1),X(1),FF(1)
      COMPLEX FWN(300),A
      N=2**M
      ND2P1=1+N/2
C  GENERATE FREQUENCY POINTS
      DF=(2.*FHI)/FLOAT(N)
      FREQ=.
      DO 5 I=1,N
      FRQ(I)=FREQ
5      FREQ=FREQ+DF
      ERM1=.
C  GENERATE INITIAL SAMPLE WINDOW, FWN(I)=X(I), (1.LE.IT), ELSE
C  FWN(I)=0
      DO 10 I=1,N
      IF (1.GT.IT) GO TO 20
      FWN(I)=X(I)
      GO TO 10
20      FWN(I)=(0.,0.)
10      CONTINUE
C  GET THE FFT
      CALL FFT(FWN,M,1.)
      IIT=1
30      DO 40 J=ND2P1,N
40      FWN(J)=(0.,0.)
      CALL FFT(FWN,M,-1.)
C  TEST FOR MSE LESS THAN DER
      ER=.
      TM1=.
      DO 45 L=1,IT
      A=CONJG(FWN(L))
      A1=A*FWN(L)
      A2=(ABS(X(L)))**2.
      AVAL=A1+A2-2.*SORT(A1)*SORT(A2)
      ER=ER+(TM1+AVAL)/2.
45      TM1=AVAL
      OLTER=ERM1-ABS(ER)
      ER=ABS(ER)
      ERM1=ER
      IF (IIT.LE.1) GO TO 47
C  IF MSE LESS THAN DER, DONE
      IF (OLTER.LE.DER) GO TO 60
C  IF 100 ITERATIONS, DONE
      IF (IIT.GE.100) GO TO 60
C  ELSE, DO ANOTHER ITERATION
47      DO 50 J=1,IT
50      FWN(J)=X(J)
      CALL FFT(FWN,M,1.)
```

```

      ITT=ITT+1
      GO TO 70
C DONE, GET FREQUENCY SPECTRUM
60   CALL FFT(FWN,N,1.)
      DER=ER
      DO /G T=1,N
      PP(I)=FWN(I)*CONJG(FWN(I))
70   PP(L)=SORT(PP(I))
      RETURN
      END

```

THIS PAGE IS BEST QUALITY MICROFILMED
FROM COPY SUBMITTED TO DDC

Subroutine PDF

PDF generate uniform distribution deviates using the following algorithm:

INPUT Y

OUTPUT F

A=0.

B=1.

1. If Y is greater than A, GO to 4 .
2. F=0
3. GO TO 8
4. If Y is less than B, GO to 7 .
5. F=1.
6. GO to 8
7. $F = \frac{Y-A}{B-A}$
8. RETURN to calling routine

```

C *****
C
C      SUBROUTINE PDF(Y,F)
C
C      PDF COMPUTES THE THEORETICAL UNIFORM DISTRIBUTION FUNCTION
C
C      CALLED BY:  CALL PDF(Y,F)
C
C      Y IS INPUT
C      F IS OUTPUT
C
C *****
C
C      A=J.
C      B=1.
C      IF(Y.GT.A)GO TO 5
C      F=0.
C      GO TO 10
5      IF(Y.LT.B)GO TO 10
C      F=1.
C      GO TO 10
10     F=(Y-A)/(B-A)
15     RETURN
C      END

```

Subroutine PSPEC

This subroutine calculates the estimated power spectrum using Eq(18) from the values of $\hat{\beta}_n$ and P_{M+1} determined in the routine MEMCO1.

$$P(\omega) = \frac{P_{M+1}\Delta t}{\left| 1 - \sum_{n=1}^M \hat{\beta}_n e^{-j\omega n \Delta t} \right|^2} \quad (18)$$

where Δt is the input sampling interval and M is the AR model order.


```

C*****
C
C      SUBROUTINE PSPEC(IPTS,IORD,DT,FL,FHI,PM,BTA,PS,F)
C
C  PSPEC COMPUTES THE ESTIMATED POWER SPECTRUM USING THE
C  MEM EQUATION (1).
C
C  CALLED BY:  CALL PSPEC(IPTS,IORD,DT,FL,FHI,PM,BTA,PS,F)
C
C  IPTS IS THE NUMBER OF POINTS COMPUTED
C  IORD IS THE MODEL ORDER PLUS ONE
C  DT IS THE TIME SAMPLE INTERVAL
C  FL IS THE LOW FREQUENCY
C  FHI IS THE HIGHEST FREQUENCY
C  PM IS THE ERROR INNOVATIONS VARIANCE (POWER) FOR
C      FOR ORDER M
C  BTA() ARE THE ESTIMATION COEFFICIENTS
C  PS() ARE THE COMPUTED POWER SPECTRUM POINTS
C  F() ARE THE FREQUENCY POINTS
C
C  1. ANDERSON, N., "CALCULATION OF FILTER COEFFICIENTS FOR
C      MAXIMUM ENTROPY SPECTRAL ANALYSIS", GEOPHYS., VOL. 39,
C      NO. 1, 69-72, FEB 74.
C*****
C
C      DIMENSION BTA(1),PS(1),F(1)
C      COMPLEX A,3
C      DF=(FHI-FL)/IPTS
C      PI=3.1415926535898
C      FREQ=FL
C      DO 10 I=1,IPTS
C      F(I)=FREQ
C      IF(IORD.GT.1)GO TO 5
C      PS(I)=PM*DT
C      GO TO 15
C  5      X=2.*PI.*F(I)*DT
C      CSUM=0.
C      SSUM=0.
C      DO 20 J=2,IORD
C      CSUM=CSUM+BTA(J)*COS((J-1)*X)
C  20      SSUM=SSUM+BTA(J)*SIN((J-1)*X)
C      CSUM=1.-CSUM
C      A=CMPLX(CSUM,SSUM)
C      B=CONJG(A)
C      ABVAL=A*B
C      PS(I)=(PM*DT)/ABVAL
C  15      FREQ=FREQ+DF
C  10      CONTINUE
C      RETURN
C      END

```

THIS PAGE IS BEST QUALITY FRAGMENT
FROM COPY FURNISHED TO LOG

Appendix C

Additional Plots from Analysis of Known Process in Section II

The following figures are additional analysis results from examples two and three of Section II. Figures 41 through 47 show additional results from analysis of the ARMA process. The additional data from the sum of two cosines is provided in Figures 48 through 54.

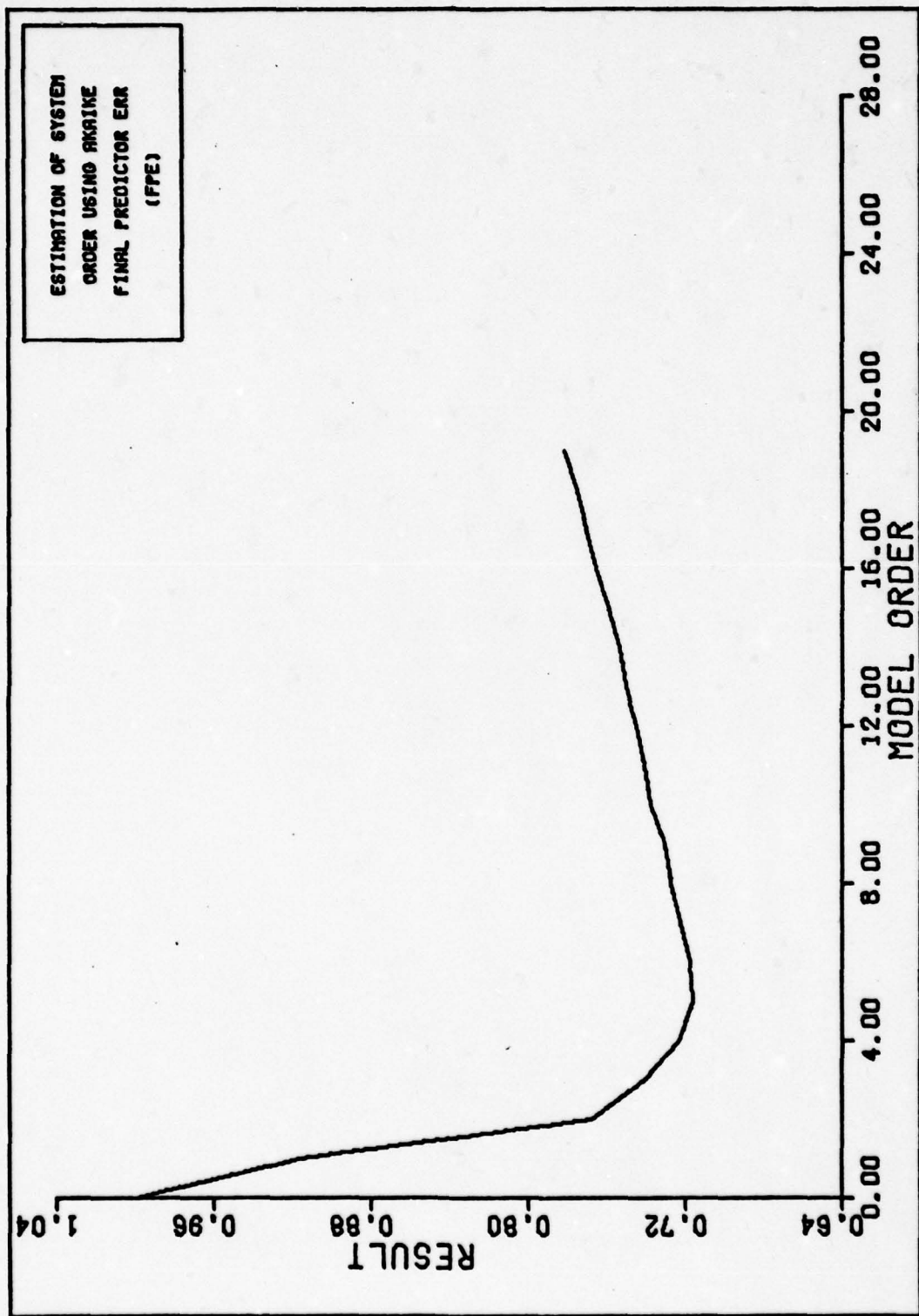


Figure 41. Amplitude of FPE as a Function of Model Order for ARMA Model

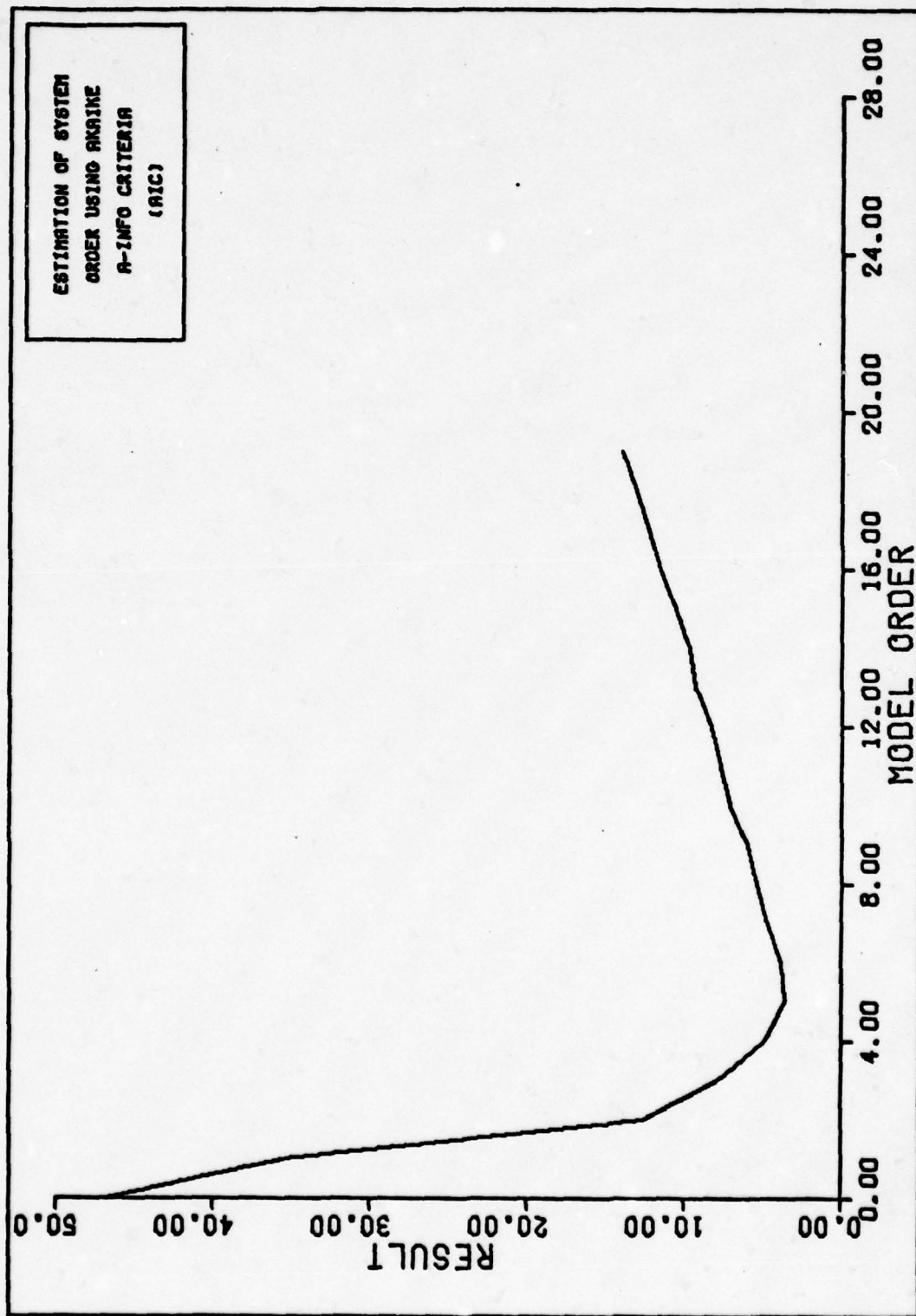


Figure 42. Amplitude of AIC as a Function of Model Order for ARMA Model

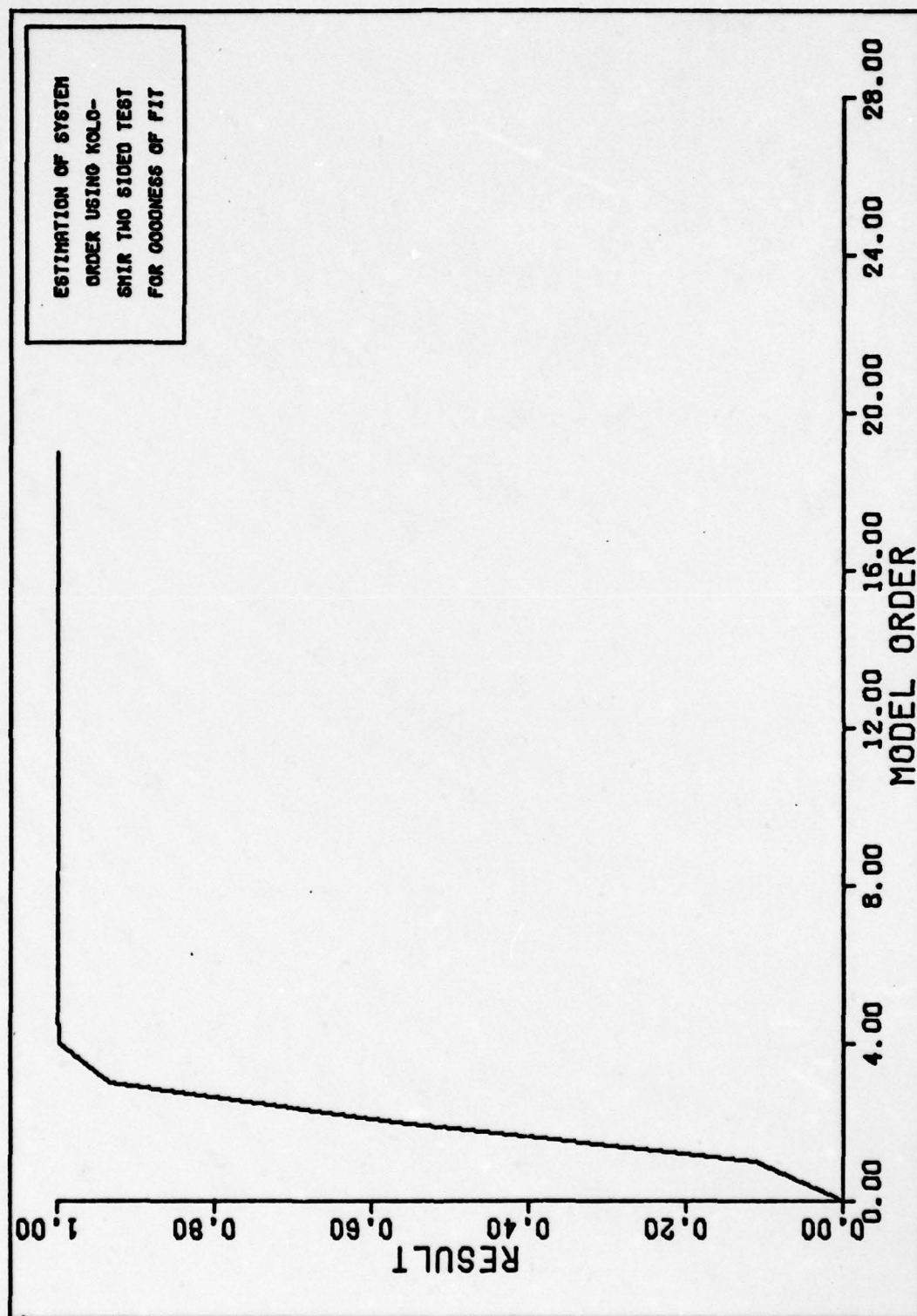


Figure 43. Probability of Kolmogorov-Smirnov Two Sided Test as a
Function of Model Order for ARMA Model

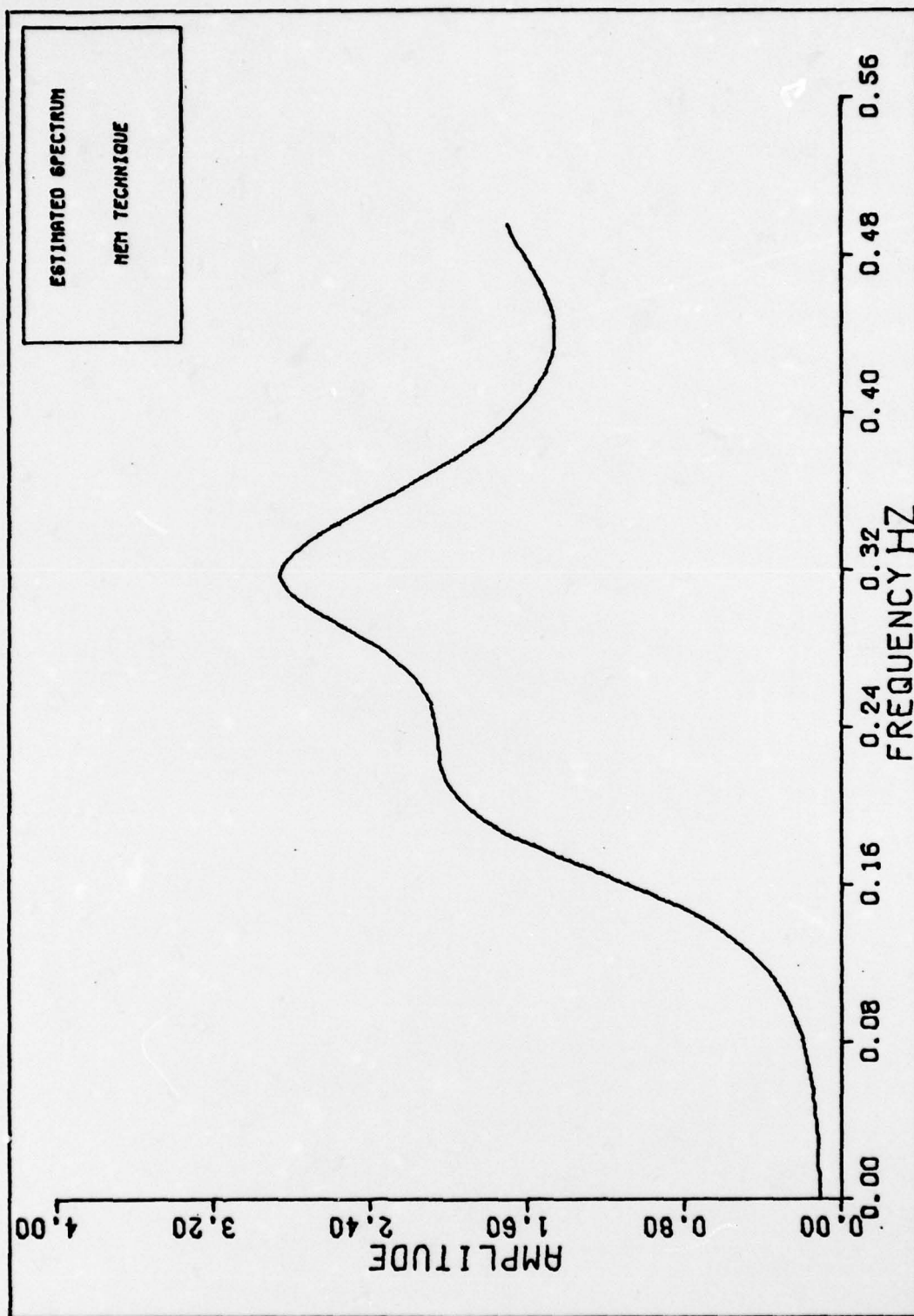


Figure 44. Estimated Mean of Estimated Spectrum Using the MEM Technique, ARMA Model

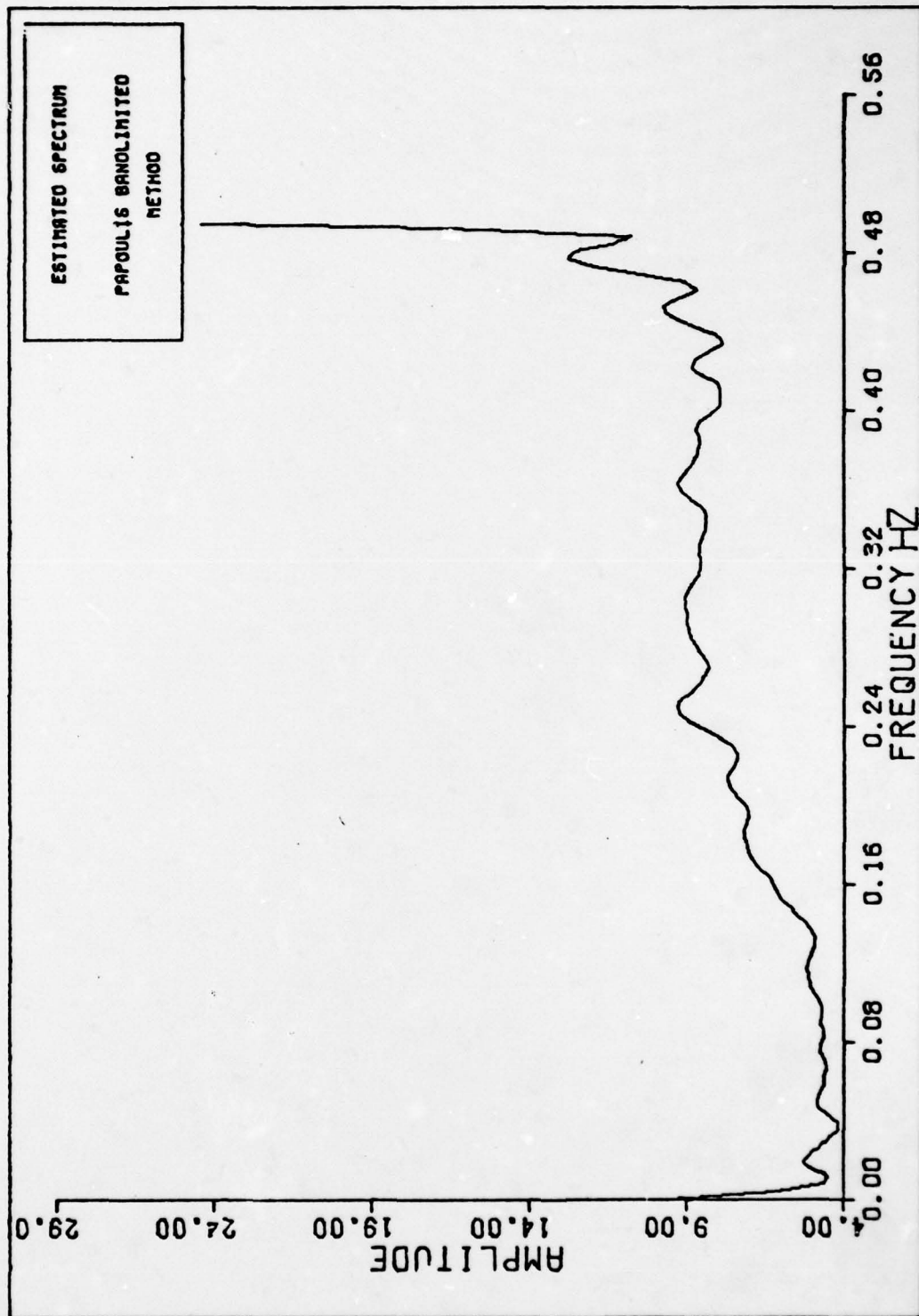


Figure 45. Estimated Mean of Estimated Spectrum Using the Papoulis Technique, ARMA Model

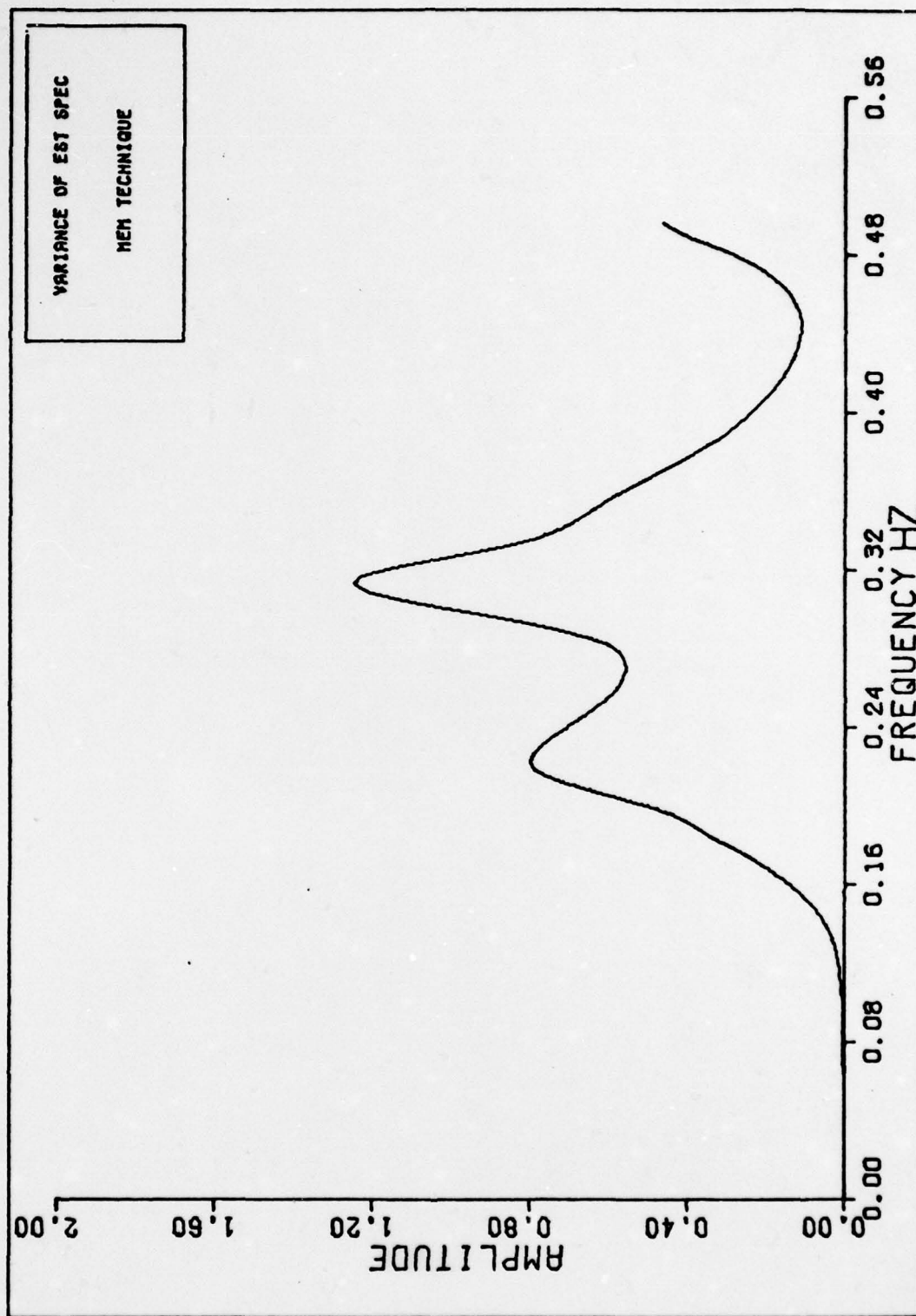


Figure 46. Estimated Variance of Estimated Spectrum Using the MEM Technique, ARMA Model

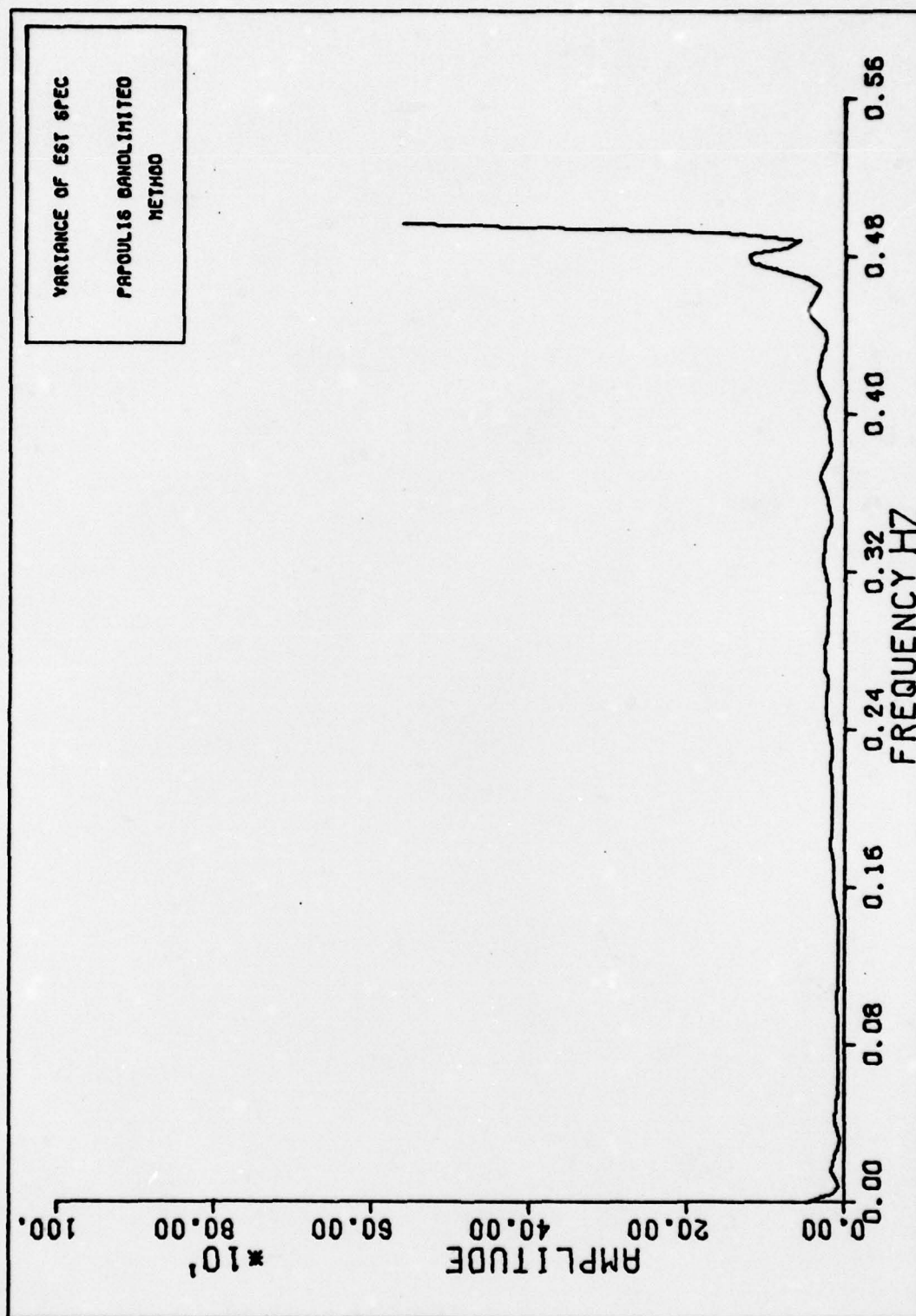


Figure 47. Estimated Variance of Estimated Spectrum Using the Papoulis Technique, ARMA Model

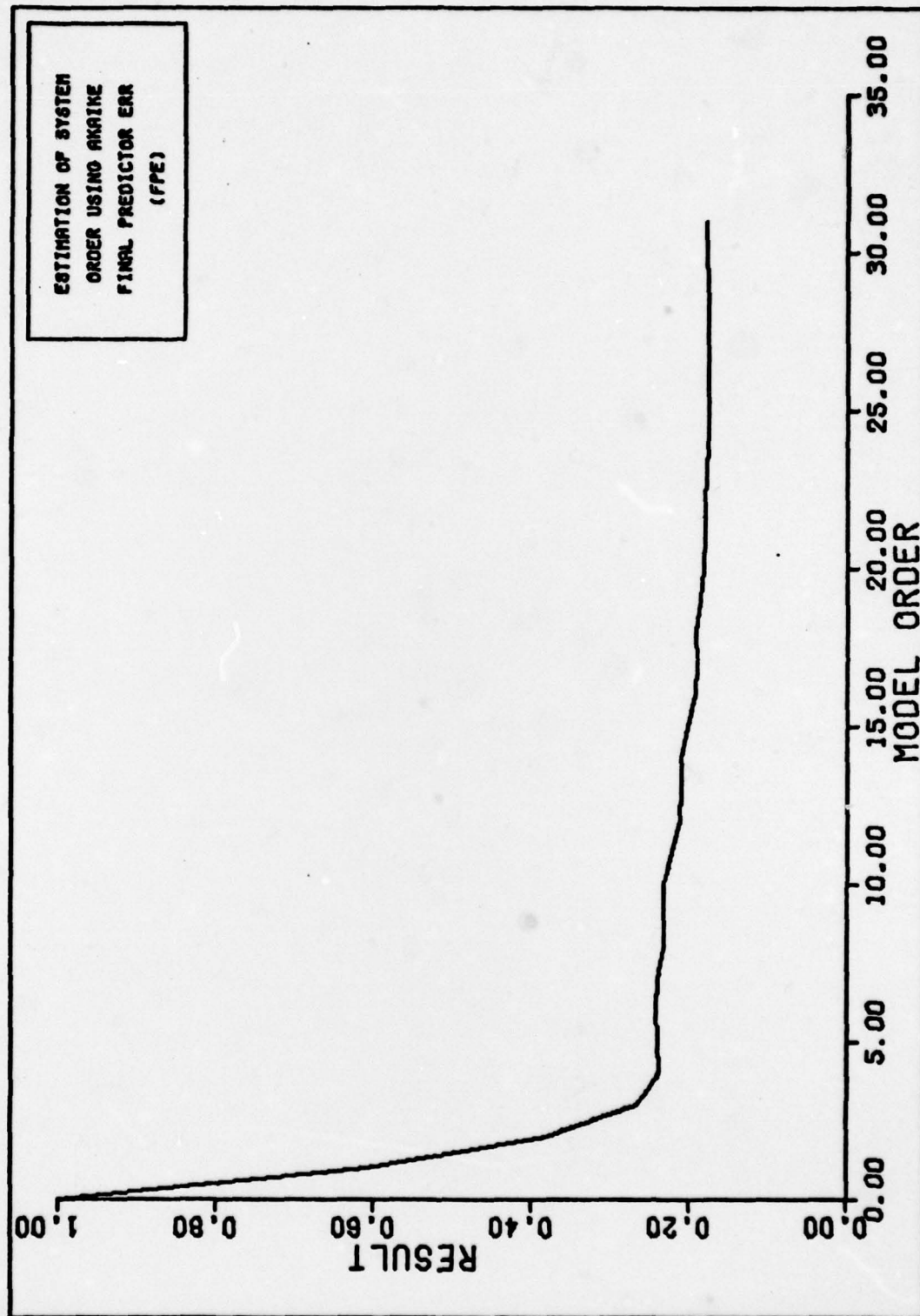


Figure 48. Amplitude of FPE as a Function of Model Order for
Sum of Sinusoids Input

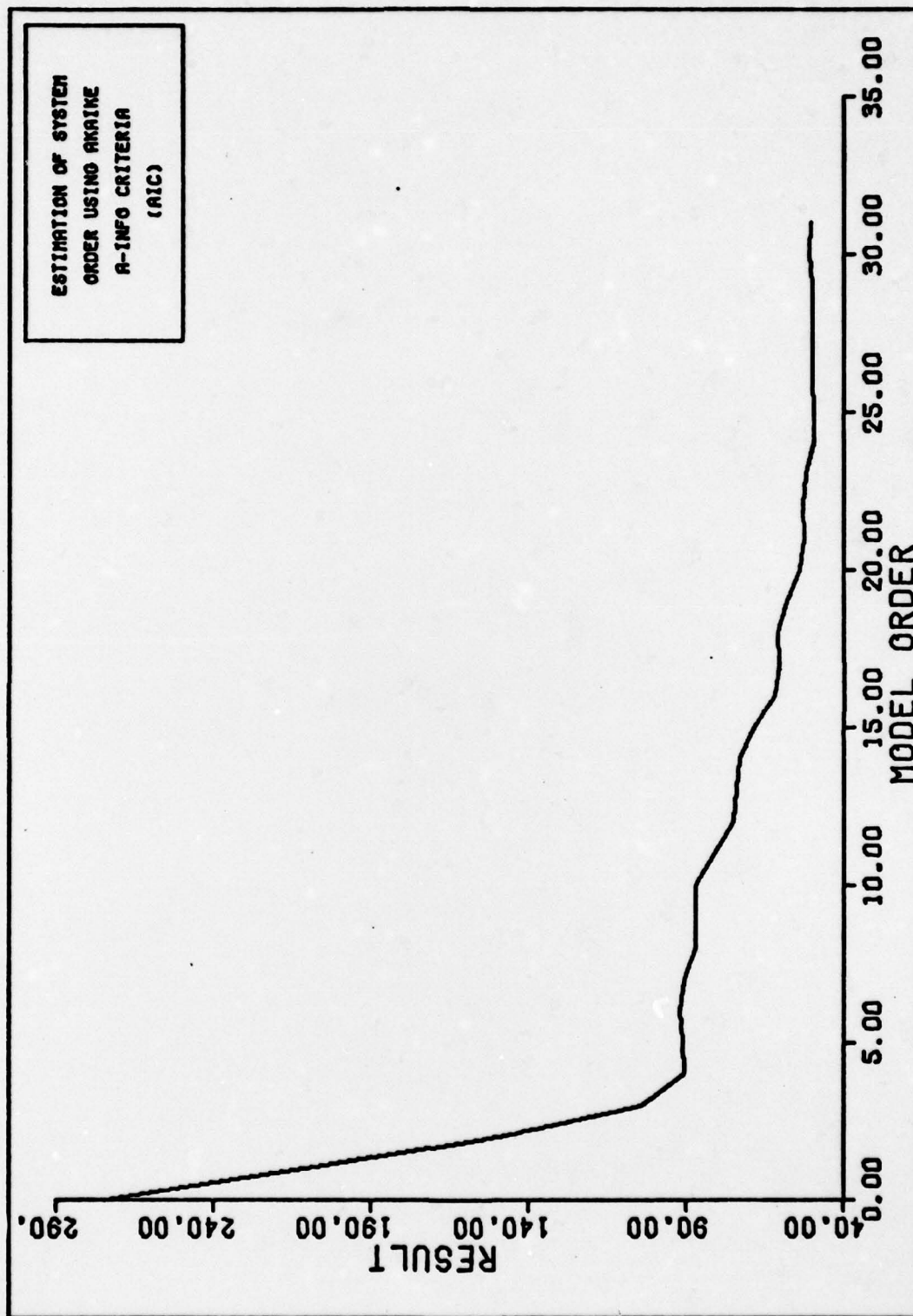


Figure 49. Amplitude of AIC as a Function of Model Order for
Sum of Sinusoids Input

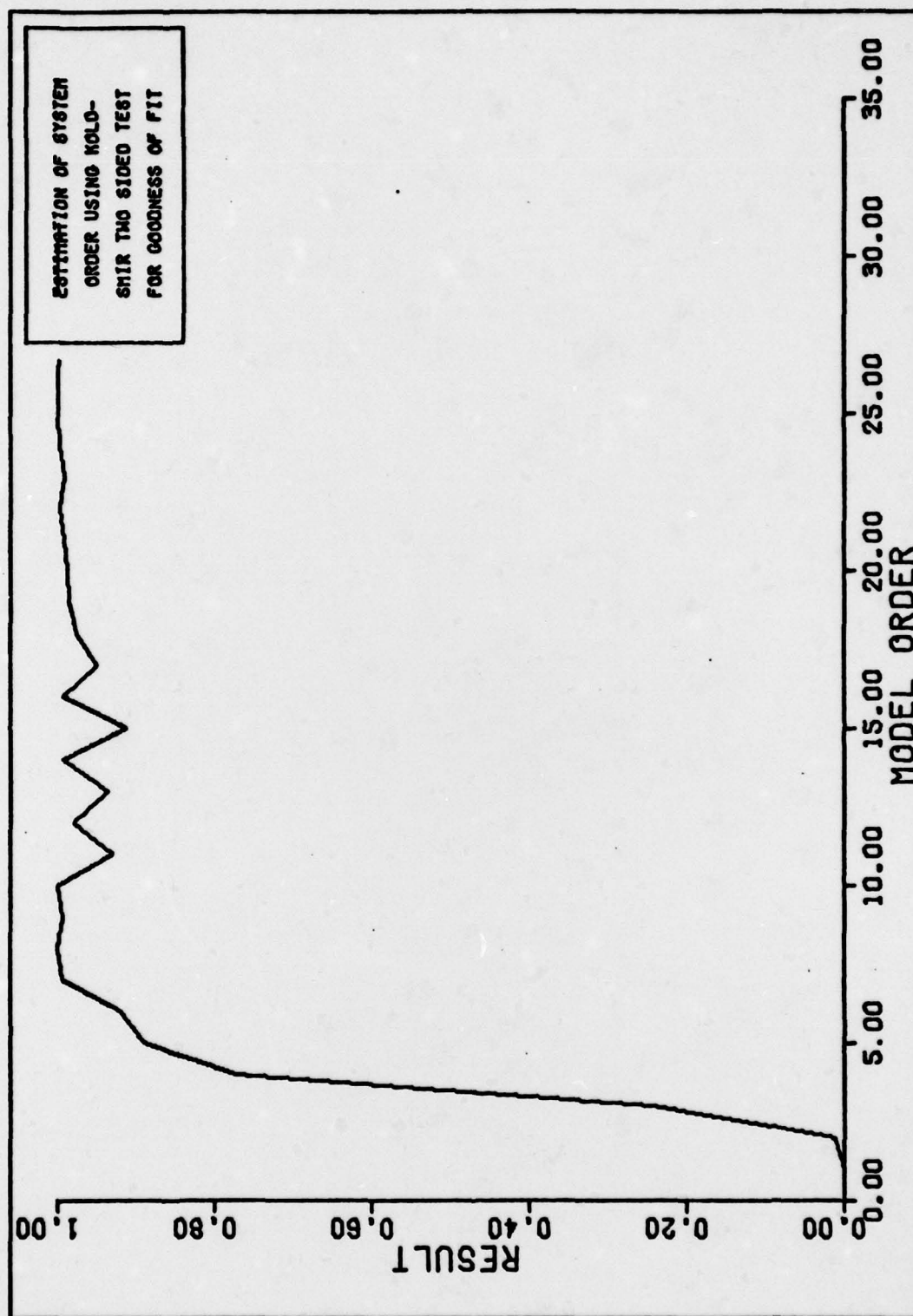


Figure 50. Probability of Kolmogorov-Smirnov Two Sided Test as
Function of Model Order for Sum of Sinusoids Input

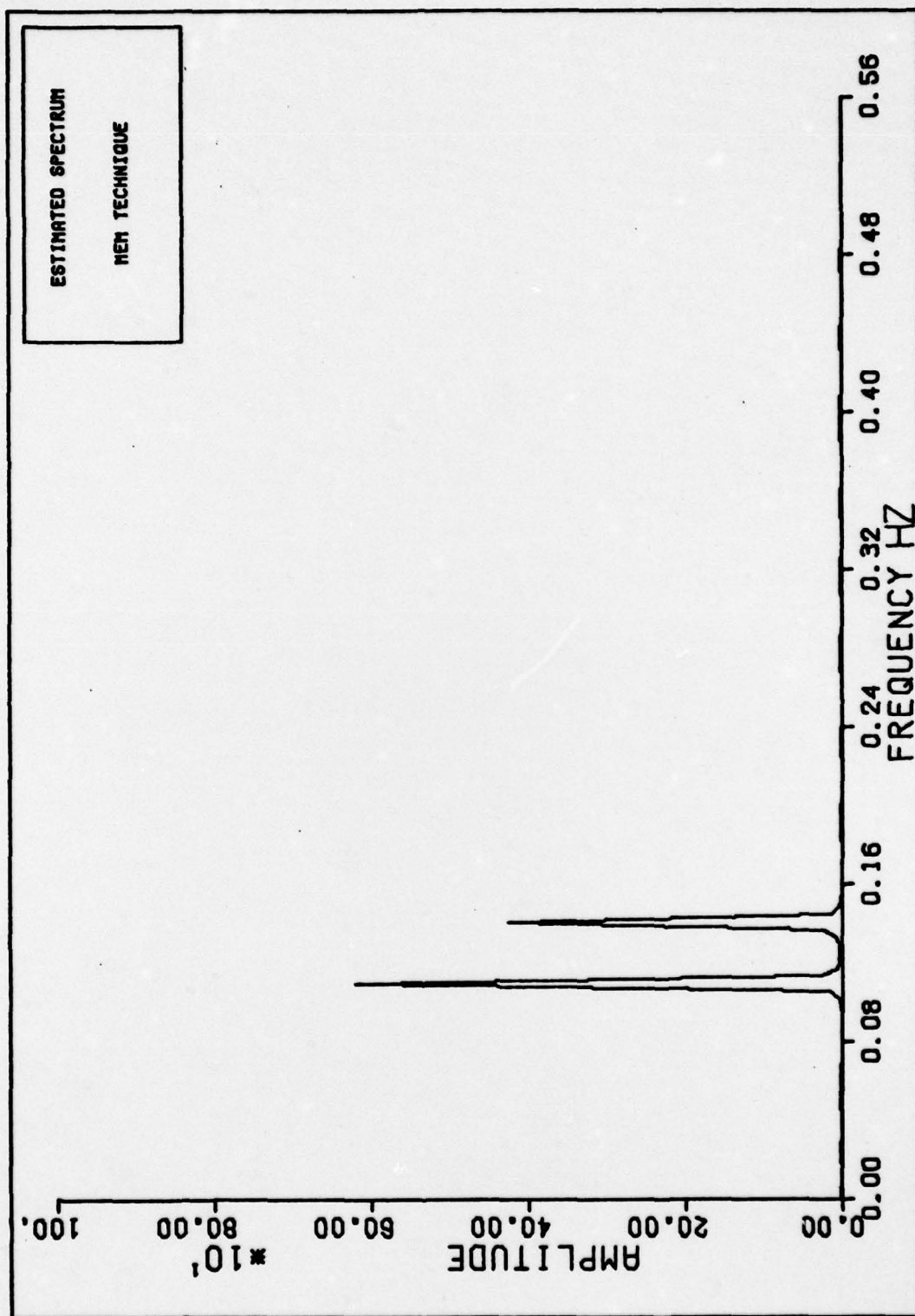


Figure 51. Estimated Mean of Estimated Spectrum Using the MEM Technique, Sum of Sinusoids Input

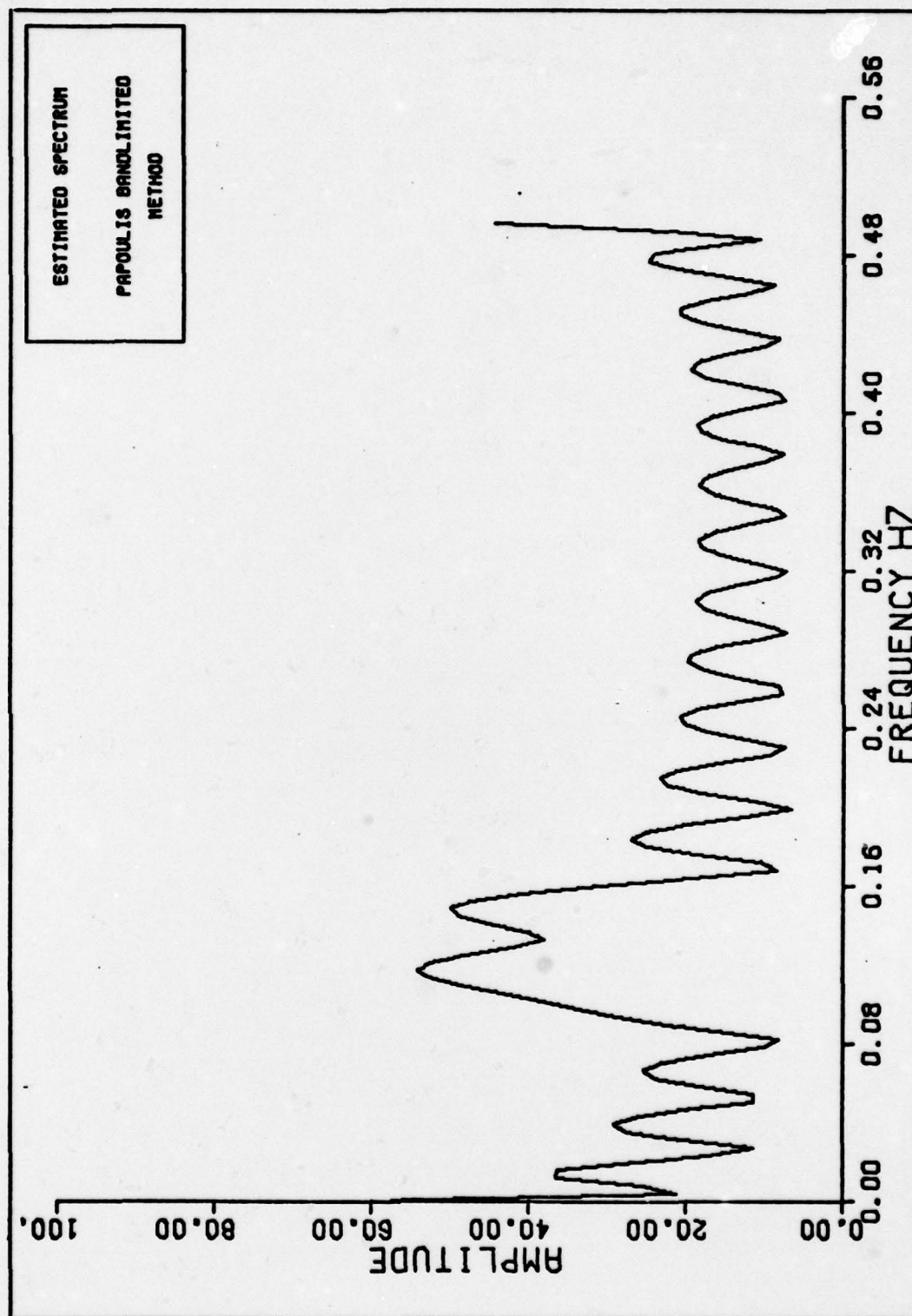


Figure 52. Estimated Mean of Estimated Spectrum Using the Papoulis Technique, Sum of Sinusoids Input

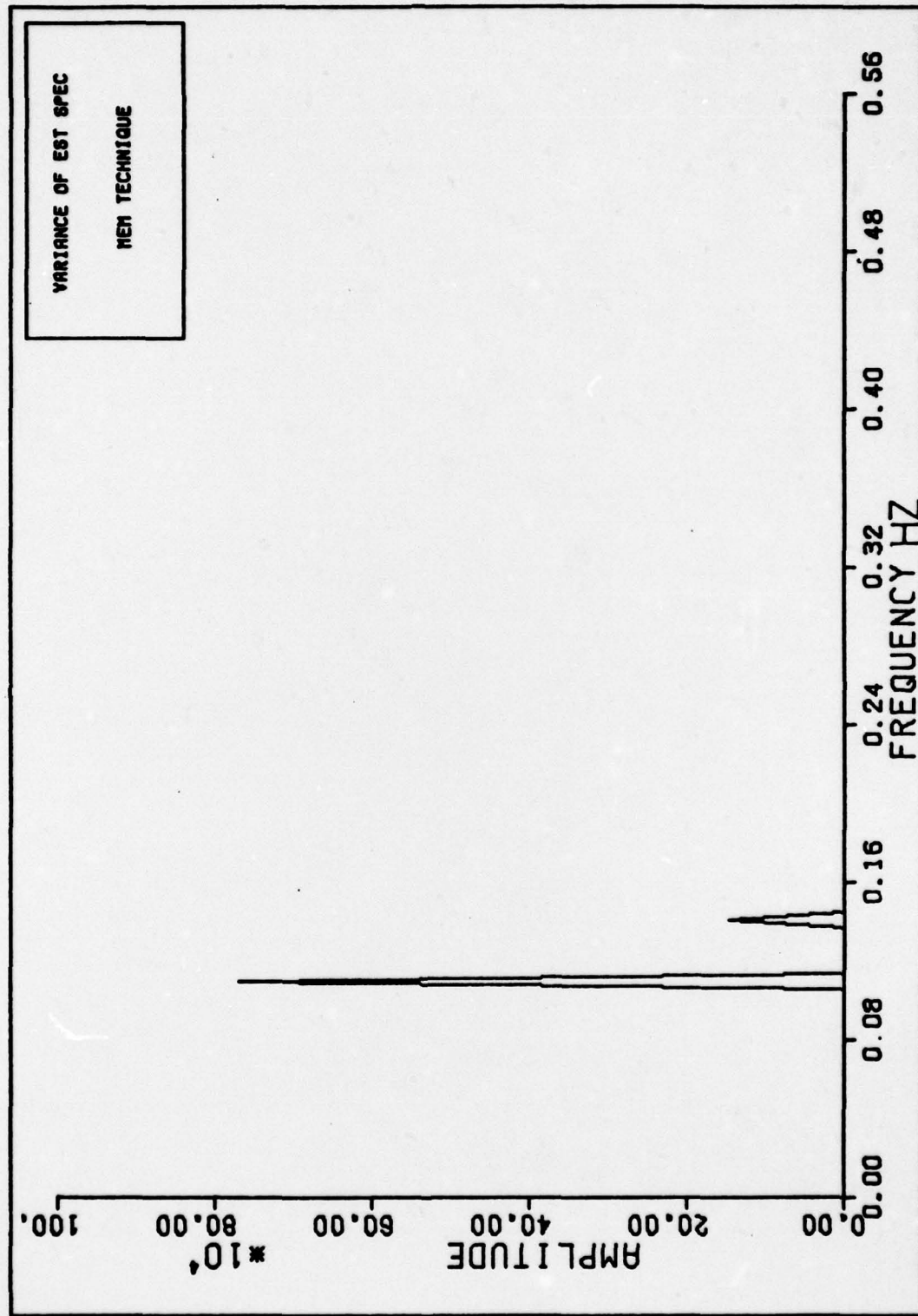


Figure 53. Estimated Variance of Estimated Spectrum Using the MEM Technique, Sum of Sinusoids Input

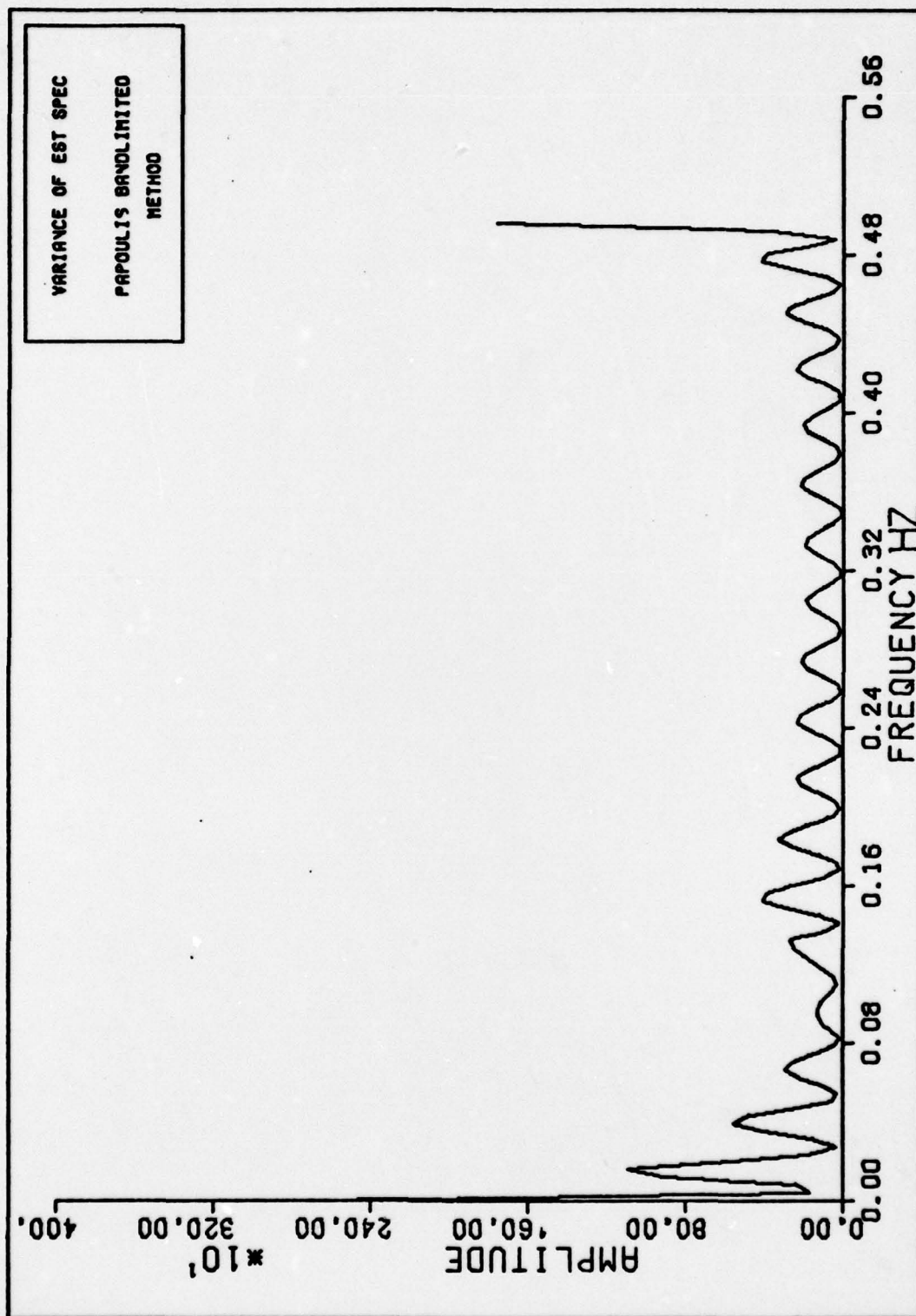


Figure 54. Estimated Variance of Estimated Spectrum Using the Papoulis Technique, Sum of Sinusoids Input

VITA

Paul B. Terry was born on 5 May 1943 in Provo, Utah. He enlisted in the Air Force in 1963. In 1975 he graduated from Colorado State University with a Bachelors degree in Electrical Engineering. After completing Officer Training School, he was commissioned and assigned to The Foreign Technology Division at Wright-Patterson AFB, where he was a space vehicle telemetry data analyst. Capt. Terry entered the School of Engineering, Air Force Institute of Technology, in June 1978.

Permanent address: 674 North 6th W.
Provo, Utah 84601

UNCLASSIFIED

SECURITY CLASSIFICATION OF THIS PAGE (When Data Entered)

| REPORT DOCUMENTATION PAGE | | READ INSTRUCTIONS BEFORE COMPLETING FORM |
|--|-----------------------|---|
| 1. REPORT NUMBER AFIT/GE/EE/79-38 | 2. GOVT ACCESSION NO. | 3. RECIPIENT'S CATALOG NUMBER |
| 4. TITLE (and Subtitle) SPECTRAL ANALYSIS OF SHORT RECORD TIME SERIES DATA | | 5. TYPE OF REPORT & PERIOD COVERED MS Thesis |
| | | 6. PERFORMING ORG. REPORT NUMBER |
| 7. AUTHOR(s) Paul B. Terry 1st Lt USAF | | 8. CONTRACT OR GRANT NUMBER(s) |
| 9. PERFORMING ORGANIZATION NAME AND ADDRESS Air Force Institute of Technology(AFIT/EN) Wright-Patterson AFB, Ohio 45433 | | 10. PROGRAM ELEMENT, PROJECT, TASK AREA & WORK UNIT NUMBERS |
| 11. CONTROLLING OFFICE NAME AND ADDRESS Rome Air Development Center/DCCL Griffiss AFB NY 13441 | | 12. REPORT DATE December 1979 |
| | | 13. NUMBER OF PAGES 133 |
| 14. MONITORING AGENCY NAME & ADDRESS(if different from Controlling Office) | | 15. SECURITY CLASS. (of this report) UNCLASSIFIED |
| 15a. DECLASSIFICATION/DOWNGRADING SCHEDULE | | |
| 16. DISTRIBUTION STATEMENT (of this Report) Approved for public release; distribution unlimited. | | |
| 17. DISTRIBUTION STATEMENT (of the abstract entered in Block 20, if different from Report) | | |
| 18. SUPPLEMENTARY NOTES Approved for public release; IAW AFR 190-17 Joseph P. Hipps, Maj, USAF Director of Public Affairs | | |
| 19. KEY WORDS (Continue on reverse side if necessary and identify by block number) Spectral Estimation Smoothed Periodogram Spectral Estimation Maximum Entropy spectral estimation Bandlimited extrapolation | | |
| 20. ABSTRACT (Continue on reverse side if necessary and identify by block number) Spectral estimation of data from some radar applications and seismological events is not accurate when short records are eval- uated using traditional techniques. A record of data is short if the number of samples from the process is more than an order of magnitude smaller than the reciprocal of the lowest frequency of interest. This analysis considers records of fewer than 128 sam- ples. Techniques that produce improved frequency and amplitude | | |

UNCLASSIFIED

SECURITY CLASSIFICATION OF THIS PAGE(When Data Entered)

resolution over smoothed periodograms and Fast Fourier Transform (FFT) are considered. Specifically, the Burg Maximum Entropy Method (MEM) and Papoulis Bandlimited Extrapolation are derived. These techniques are shown to produce estimates that become unbiased and consistent. Additionally, the effects of windowing, a problem inherent with periodograms, are not observed in these techniques.

Model order determination for the MEM technique is accomplished through implementation of two techniques developed by Akaike. These techniques are derived through the maximum likelihood estimation of the estimated power. Using Akaike's order techniques, MEM spectral estimation provides extremely good frequency resolution from very short input records.

Papoulis bandlimited extrapolation techniques provide accurate results when short records are evaluated. The technique is limited, in this research, to computational times commensurate with the MEM technique and does not produce resolution accuracy that is observed from MEM analysis. However, the estimated amplitudes are much closer than those generated from the MEM technique.

The report contains a 47 item bibliography.

SECURITY CLASSIFICATION OF THIS PAGE(When Data Entered)